ANALYSIS AND FIELD SIMULATION OF TWO ELECTRODES SPARK GAP SWITCH

A Thesis submitted to

Institute of science and technology

University of Turkish Aeronautical Association

By

Mohamed Ali Elweddad

Supervisor: Assist. Prof. Dr. Ibrahim Mahariq

In partial fulfillment of the requirement for the degree of Master of Science in

Electrical and Electronics Engineering

December, 2016

MOHAMED ALI ELWEDDAD, having student number 1303637003 and enrolled in the Master Program at the Institute of Science and Technology at the University of Turkish Aeronautical Association, after meeting all of the required conditions contained in the related regulations, has successfully accomplished, in front of the jury, the presentation of the thesis prepared with the title of: Analysis and field simulation of two electrodes spark gap switch.

".

Supervisor: **Assist. Prof. Dr. Ibrahim Mahariq**

The University of Turkish Aeronautical Association

Jury Members: **Assoc. Prof. Dr. Özgür KELEKÇİ**

The University of Turkish Aeronautical Association

Assist. Prof. Dr. Ozan Keysan

Middle East Technical University

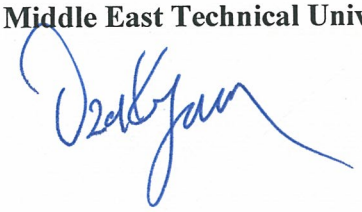

Thesis Defense Date: 23.12.2016

THE UNIVERSITY OF TURKISH AERONAUTICAL ASSOCIATION

INSTITUTE OF SCIENCE AND TECHNOLOGY

I hereby declare that all the information in this study I presented as my Master's Thesis, called: Analysis and Field Sımulatıon of Two Electrodes Spark Gap Switch, has been presented in accordance with the academic rules and ethical conduct. I also declare and certify with my honor that I have fully cited and referenced all the sources I made use of in this present study.

DECEMBER 2016

MOHAMED ALI ELWEDDAD

ACKNOWLEDGEMENTS

I would like to thank Assist. Prof. Dr. Ibrahim Mahariq for his supervision, special guidance, suggestions, and encouragement through the development of this thesis, I would like to thank all my family, my father, my mother, my wife, my brothers and sisters for their invaluable support. I would also like to express my special thanks to my country, which helped me and encourage me to be successful. I would also like to thank all of my colleagues in the university and all of the teachers I've had over the years.

Finally, I would like to thank my wife Manal for always having the time to listen to my hypothesis and theories, for reading my thesis.

DECEMBER 2016 **MOHAMED ALI ELWEDDAD**

TABLE OF CONTENTS

ACKNOLEDGMENTS..... ii

TABLE OF CONTENTS..... iii

LIST OF TAbLES..... vi

LIST OF FIGURES..... vii

LIST OF ABBRIVIATION..... ix

ABSTRACT..... xii

ÖZ..... xiii

CHAPTER ONE..... 1

1. INTRODUCTION..... 1

1.1 Background..... 1

1.2 Organization of the thesis..... 3

1.3 The objectives …….. 4

CHAPTER TWO..... 5

2. Electrical Breakdown of Gases..... 5

2.1 Ionization of Gases……. 6

2.2 Elementary Processes Related to Ionization of Gases….. 7

2.3 Townsend Mechanism…….. 8

2.4 Electron Avalanche…….. 9

2.5 Secondary Emission of Electrons……... 11

2.6 Streamer Mechanism…….. 13

2.6.1 The Panchen's law…… **15**

2.6.2 The limit of Panchen's law…….. **17**

2.7 Electric discharges ……. 17

2.7.1 Brush discharge……..... **18**

2.7.2 Dielectric barrier discharge …… **19**

2.7.3 Corona discharge……... **20**

2.7.4 Electric glow discharge……. **21**

2.7.5 Electrostatic discharge……... 22
2.7.6 Streamer discharge…….. …….. 23
2.7.7 Partial Discharge……. 24
2.7.8 Townsend discharge …….. 25
2.8 Types of DC discharges…….. 28
2.8.1 Dark Discharge……... 30
2.8.2 Glow discharge……... 31
2.8.3 Normal glow discharge…….. 31
CHAPTER THREE..... 33
3. Breakdown Voltage Of High Pressure Spark Gap……..... 33
3.1 The Principle of a closing switch…….. 33
3.2 Electrical breakdown in a gas gap switch……... 36
3.3 The time history of breakdown voltage behavior……... 37
3.4 The pulsed power switches…… 39
3.4.1 Pulsed Power Generation……. 39
3.4.2 The working pressure of high Power Switches……... 41
3.5 Spark gap switch electrical circuit……. ……. 42
3.5.1 Principle of work…… 43
3.6 The efficiency of spark gap switch…… 44
3.6.1 The charging method of a loss–free switch……. 45
3.6.2 The realistic spark gap switch model with losses…... 47
3.6.3 Single power supply circuit…… 47
3.6.4 DC voltage resonant charging circuit……. 52
3.7 The pulsed power forming network……. 55
3.8 The efficiency of pulsed plasmas switching…….. 57
3.9 The total efficiency of pulsed spark gap switch……... 58

CHAPTER FOUR..... 60
4. Modelling and Simulation of Spark Gap Switch…… 60
4.1 Different models for the conducting channel resistance…... 61
4.1.1 Toepler's model……. 63
4.1.2 Rompe and Weizel model with energy balance……... 65

4.1.3 Vlastos and Branginskii's model……. 67
4.1.4 Sorensen and Ristic model……... 69
4.2 An equivalent circuit model of spark gap switch…….. 70
4.2.1. The capacitance of spark switch under arc condition... 72
4.2.2 Peaking Capacitor…… 73
4.2.3 Spark gap Circuit simulation using Pspice software…. 74
4.3 Switch modeling and analysis using CST software……... 76
CHAPTER FIVE..... 81
5. RESULTS AND DISCUSSION……... 81
5.1 Breakdown Voltage analysis…… 81
5.2 The Electric field analysis…… 83
5.3 Resistive Phase Time calculations…….. 85
5.4 The Arc resistance calculations…….. 87
5.5 Analyzing Spark gap Circuit simulation…… 90
5.6 The E-Field modeling using CST…… 93
CHPTER SIX 100
6.1 Findings and the summary of work……... 98
6.2 The most important results…….. 98
6.3 The recommendation and future studies……. 106
6.4 Conclusion…… 106
REFERENCES……. 107

LIST OF TABLES

Table 1.1 Ionization energies and constants of some gases….. 10

Table 4.1 Arc-resistance models…… 62

Table 4.2 Model parameters for close/open switch…….. 75

Table 5.1 The values of calculated RLC circuit elements……. 92

Table 6.1 The calculated breakdown voltages……... 99

LIST OF FIGURES

Figure 2.1	Free path and mean free path of electrons……..	**9**
Figure 2.2	Electron generation according to the Townsend mechanism….	**12**
Figure 2.3	Townsend mechanism……	**12**
Figure 2.4	Distribution of electrons and positive ions in the avalanche…..	**14**
Figure 2.5	Distribution of ions and electrons due to positive streamer…...	**14**
Figure 2.6	Paschen curve for parallel electrode discharge……..	**16**
Figure 2.7	Brush discharge from an electrode…….	**19**
Figure 2.8	Basic dielectric-barrier discharge configurations……...	**20**
Figure 2.9	A typical point-to-plane corona geometry…….	**21**
Figure 2.10	The different glowing regions that make up a glow discharge..	**22**
Figure 2.11	Streamer properties in laboratory experiments…….	**24**
Figure 2.12	The possible locations of voids within the insulation system…	**25**
Figure 2.13	Schematic of simple gas breakdown test……	**26**
Figure 2.14	The electron Avalanche……..	**27**
Figure 2.15	Variation of current as a function of applied voltage…….	**28**
Figure 2.16	A simple circuit for electric discharge experiments……...	**28**
Figure 2.17	Voltage and current characteristics of the gas discharge……...	**29**
Figure 3.1	Voltage and current versus time in a spark gap closing switch	**35**
Figure 3.2	The self-breakdown gas gap time scales……	**38**
Figure 3.3	The pulsed power generation diagram……...	**40**
Figure 3.4	Simple capacitive storage discharge circuit……...	**40**
Figure 3.5	PFL circuit (b) output square pulse……	**41**
Figure 3.6	Ranges of gas pressure and operating voltages…….	**42**
Figure 3.7	The basic electric circuit of spark gap switch……	**43**
Figure 3.8	The electric circuit of static spark gap……...	**44**
Figure 3.9	A schematic of a charging circuit for a loss free switch.....	**46**
Figure 3.10	The equivalent circuit for the realistic spark gap switch……	**48**
Figure 3.11	The oscillation voltage and current across the capacitor ……...	**54**
Figure 3.12	The efficiency of resonant charging circuit ……...	**55**
Figure 3.13	A basic PFN generator circuit……	**57**

Figure 3.14	The output signals with a simple pulse forming line…….	**57**
Figure 4.1	Switch model with cone profile electrodes and the equivalent.. Circuit of spark gap switch.	**71**
Figure 4.2	The spark gap peaking switch……	**73**
Figure 4.3	The equivalent circuit simulation using Pspice……	**75**
Figure 4.4	The three dimensional switch model……	**78**
Figure 4.5	Electric field distribution using CST software…….	**80**
Figure 4.6	The input Gaussian pulse…….	**80**
Figure 5.1	The breakdown voltage values (Vb) as a function of the gas pressure times the inter-electrode distance (pd)	**82**
Figure 5.2	The breakdown voltage values (Vb in very small distances…. (mm)	**82**
Figure 5.3	Electric field with variation of (P*d)…….	**84**
Figure 5.4	The maximum electric field E versus the gap length…….	**84**
Figure 5.5	The calculated resistive phase for air gas at various pd values	**86**
Figure 5.6	The calculated resistive phase as function of electric field in three different gaps	**86**
Figure 5.7	The voltage drop across the gap……	**87**
Figure 5.8	The calculated arc-resistance for the air, at 7.74 atm and d = 0.5mm.	**88**
Figure 5.9	The calculated arc-resistance for the three different pressures..	**88**
Figure 5.10	The calculated arc-resistance for the three different pressures..	**89**
Figure 5.11	The calculated arc-resistance for the three different pressures	**90**
Figure 5.12	The output pulse from the spark gap switch, at p=5atm, …….	**91**
Figure 5.13	The output pulse from the spark gap switch, at p=5atm……..	**92**
Figure 5.14	The spark gap switch modeled by CST……..	**93**
Figure 5.15	The complete electric field distribution inside the gap switch	**94**
Figure 5.16	The input and output Gaussian signal at d = 1mm and rise….. time 10 ns	**95**
Figure 5.17	The input Gaussian signal at d = 1cm and rise time 10 ns……	**96**
Figure 5.18	Two output Gaussian signals at d = 1cm …….	**96**

Figure 5.19	The conical shape of spark gap switch…. ……	**97**
Figure 5.20	The cylinder and spherical shapes of spark gap switch…….	**97**
Figure 6.1	Spark gap equivalent RLC circuit……..	**103**
Figure 6.2	The circuit simulation by using Pspice……..	**104**
Figure 6.3	The output pulse from the spark gap switch, at p=5atm,……... d=2mm. r= 1cm	**105**

LIST OF ABBRIVIATION

A	Empirical coefficient for determining α
$A(x, t)$	Heating function
a	Coaxial transmission line inner conductor outer diameter
α	Townsend ionization coefficient
B	Empirical coefficient for determining α
β	Decay rate constant
C	α fit coefficient
D	Diffusion coefficient
d	Gap width
E	Electric field
$E0$	Applied or initial electric field
Er	Electric field at spherical avalanche front
e	Electron charge
ε_0	Permittivity of free space
ε_i	Ionization potential
η_{thrust}	Thrust efficiency
j_e	Electron current
K	Thermal conductivity
λ	Ionization mean-free-path
μ	Breakdown parameter
μ_0	Permeability of free space
$\mu_{e,+}$	Electron, ion mobility
p	pressure
ϕ	Electrostatic potential
Q	Capacitor charge
R	Plasma resistance
T	Temperature

Vb	Breakdown voltage
Zo	Characteristic impedance of a transmission line
POV	Peak Operating Voltage
SW	Short Wave
L	Inductor
S	Switch
GDT	gas discharge tube
γ	Secondary emission coefficient
k	Thermal diffusivity
t	Time

ABSTRACT

This thesis presents the results of gap switch to develop the study, a new electrodes shape of the spark-gap switch was suggested. The theoretical design parameters of the switch are discussed with analysis of the electrostatic and electromagnetic simulations of the discharge switch. The most important parameters such as the phase resistance, the time-dependent resistance, and the time-dependent inductance. Particularly the inductance of the spark gap largely effects rise time of the output pulses of pulsed power supply.

Based on the energy balance in the gap switch, some researchers simulated the inductance and resistance in terms of the time in the dissipation and formation of spark path. In this thesis, in order to avoid the complicated calculations of arc discharge parameters, a method was used for calculating the equivalent circuit parameters through the discharge phase. One of two objectives of this thesis is determining how to predict the arc resistance of voltage pulsed discharge and resistive phase time. To this end, two theoretical and empirical models of arc resistance equations were utilized. An important investigation was carried out by simulation to optimize the electrical circuits RLC and charging parameters. The program named P spice software was used for this purpose.

Based on the switch parameters an electrical circuit was modeled and established for the simulation arrangement. The second aim of this work is discussing the modeling and simulation of a peaking spark gap switch to investigate the decreasing in rising time for sub-nanosecond pulses. The modeling and simulation have been carried out using CST modeling software of the Computer Simulation Technology. By using this electrodynamic model, the switch breakdown region can be visualized in three dimensions by monitoring the E-field distribution.

Keywords: breakdown voltage, spark gap, electric fields (e-fields), inter-electrodes distance modeling, pulsed-power system.

ÖZET

Bu tezde boşluk anahtarı çalışmasının sonuçları sunulmaktadır. Çalışmayı geliştirmek amacıyla kıvılcım boşluk (aralık) anahtarının elektrotları için yeni bir biçim önerilmiştir. Anahtarın teorik tasarım parametreleri elektrostatik ve elektromanyetik anahtar deşarj stimülasyon analiziyle birlikte tartışılmıştır. En önemli parametreler (direnç fazı, zamana bağımlı direnç ve zamana bağımlı indüktans gibi), özellikle de kıvılcım boşluğu atımlı güç kaynağının çıktı atım zamanını büyük ölçüde etkilemektedir [2, 3, 5, 8].

Rompe ve Weizel boşluk anahtarının enerji dengesi açısından zaman bazında olduğu kadar akımla kıvılcım direnci arasında da bir ilişki bulunduğunu önerdi, bazı diğer araştırmacılar ise kıvılcım yolunun dağılması ve oluşumu süresi içinde indüktansı ve direnci simüle ettiler. İletken faz içinde boşluk anahtarını simüle etmek için eşdeğer RLC devresi kullanıldı. Bu tezde ark deşarj parametrelerinin karmaşık hesaplarından kaçınmak için deşarj fazı boyunca eşdeğer akım parametrelerinin hesaplanmasında yöntem [5] kullanıldı. Bu tezin iki amacından biri voltaj atımlı deşarjın ark direncinin ve direnç fazı süresinin kestiriminin nasıl olacağını tayin etmekti. Bu amaçla ark direnci eşitliklerinin iki teorik ve ampirik modeli kullanıldı. RLC elektrik devrelerini ve şarj parametrelerini optimize etmek için simülasyonla önemli bir araştırma yapıldı. Bu amaçla "P spice software" adlı program kullanıldı.

Anahtar parametrelerine dayanarak bir elektrik devresi modellendi ve simülasyonun düzenlenmesi amacıyla kuruldu. Bu çalışmanın ikinci amacı modellemenin ve nano-saniye altı atımlarda yükselme zamanının azaltılmasının araştırılması için pik yapan kıvılcımlı boşluk anahtarının simülasyonunun tartışılmasıdır. Modelleme ve simülasyon Computer Simulation Technology'nin CST modelleme yazılımı kullanılarak yapılmıştır. E-alanı dağılımının monitorize edilmesiyle anahtar kırılma bölgesi üç boyutlu olarak görselleştirilebilir.

Anahtar kelimeler: Kırılma voltajı, kıvılcım boşluğu (aralığı), elektrik alanları (e-alanları), elektrotlar arası mesafenin modellenmesi, atımlı güç sistemi. Eşdeğer RLC devresi, yükselme zamanı.

CHAPTER ONE

INTRODUCTION

1.1 Background

The breakdown voltage of gasses and turning it from the non-conducting state into high conducting state is an interesting phenomenon. It occurs as spark discharge in transmission lines and high–voltage circuits. The breakdown voltage in the pulsed power system is a new technological field. The main goal of a pulsed power system is converting input a low power and long–time into short– time and high power output pulses.

The nanosecond pulses are well known used for several applications such as electromagnetic (EM) forming, the power radar, medical electronics, diamond cutting, plasma ion implantation, sterilization, surface coating, food irradiation, defense application, waste water processing, ultra-wideband generation, etc. [1,7]. There are a lot of methods to generate high-voltage pulses, by using pulse transformer, pulse forming lines, Marx generator, high power switches and magnetic switching [8]. All previous devices give output high voltage pulses rise time in the nanosecond to microsecond ranges. Plasma gas switches such as pseudo sparks, spark gaps, and thyratrons use the ionized gasses to create high power pulses of few hundred megawatts at the load [1, 2, 4]. Pseudo sparks and thyratrons are low-pressure switches. Typically, they use pressures on the order of tens of bars. Pressurized spark gap switches are widely used to create output pulses with low rise times on the order of 100 ps.

Simply, the spark gap switch consists of two parallel electrodes, which are filled with an insulating gasses. When the applied high voltage across the gap electrodes increases sufficiently, the gas in the gap will be ionized, and an Avalanche discharge will take place. The gas inside the gap switch is heated to the high value of temperature and then, turn into a good conductor of electricity. By flowing high current through the ionized gas will keep it heated and preserve the conductive channel. Finally, the current will fall sufficiently and the gas in spark gap cools and becomes non-conducting. High-pressure gasses are beneficial in the operation of high speed and high power switches [1]. However, the rate of cooling and deionization of the used gas restrict the time of switching recovery. In avalanche process the spark gap switch starts to be conducted, this process is known as Breakdown and the voltage needed to launch this process is called Breakdown Voltage. (The breakdown voltage process is proportional to the gap distance between the switch electrodes. By applying the high voltage across the electrodes of the peaking switch, the plasma is created followed by an electric arc [9]. In [10], Hendriks et al. connected a wire in micrometer dimension to represent the arc discharge between the gap electrodes by using Computer Simulation Technology (CST) .during the conduction state the arc discharge between the electrodes is not a good conductor and there is a little resistance resisting the flowing current through it. The principle work of spark gap switch involves various parameters that can be adjusted depending on desired application.

Some important parameters of discharge channel should be considered such as breakdown voltage, inter-electrode distance, gas type, gas pressure, and the resistive losses. The last parameter includes the decreasing of the resistive phase time to develop the behavior of discharge channel. The switch is used for reduction the rise time of input pulse from the pulsed power generator. The energy of input pulse is stored in a peaking high voltage capacitor before transiting to the switch. In the peaking capacitor, the energy can be stored for very short time and discharge it quickly through the gap switch [3]. The peaking stage includes fast high-pressure spark gap switch along with high voltage peaking capacitor, which can effectively sharpen the rise time of output pulses. CST shows the electrostatic analysis of electric field © distribution in gap switch. Different inter-electrode distance is used and analyzed using (Pspice +CST software). These models enable us to understand the influence of non-uniformity in

the field distribution. Also, the simulation illustrates the electric field stress in various parts of the gap switch and electrodes. From the electrodes geometry, the spark gap switch is modeled as a combination of inductor and resistor connected in series and with a capacitor in parallel. For different pressure and distance values of the gap switch, some models were used analytically to obtain the desired electrode gap shape, gap distance and the output rise time. The two electrodes of the spark gap switch were selected in cone form, with electrodes diameter = 2cm and diameter of the entire cylindrical structure is 8cm. The breakdown voltage behavior depends on the nature of (non-uniformity/uniformity) of the electric field E in the inter-electrode gap of peaking switch. The results show that as the gap pressure increases the applied voltage withstand increases. It is also shown that we can decrease the output rise time of input pulses by reducing the inductance and inter-electrodes distance.

1.2 Organization of the thesis

The structure of this thesis is as following:

Chapter2: provides an overview of various mechanisms and factors related to breakdown voltage in glasses. Topics such as streamer and Townsend's mechanism, Panchen’s law, electric discharge types.

Chapter3: this chapter describes the fundamentals of closing switches and the principle of work of spark gap switch ıs explained ın details.in this chapter, we presented many Topics related to high-power switches such as The pulsed power forming a network, Pulsed Power Generation and electrical breakdown in a gas gap switch.

Chapter 4: illustrates the simulation of the spark gap switch by using some theoretical and empirical models to calculate important parameters such as arc resistance, resistive phase time, the inductance and the capacitance of the switch. The dynamic modeling of the spark gap switch is done using EM and Microwave Studio of CST package. CST shows the electrostatic analysis of electric field © distribution inside the gap switch.

Furthermore, in this chapter, the switch was modeled as a combination of inductor and resistor connected in series and with a capacitor in parallel.

Chapter (5) presents observed results, including calculated breakdown voltages, wav eforms, the output rise times and pulse durations. Moreover, we showed the calculate d arc-resistance, resistive phase time and the electrostatic analysis of electric field (E) distribution in the gap.

Chapter 6 provides summary of previous sections and presents concluding remarks.

1.3 The objectives

The main three objectives of this thesis are as following

- study the most important switch parameters which determine the conducting channel and the closure time such as (the resistive phase time, the arc resistance, breakdown voltage and the switch inductance) .
- The effect of switch geometry (inductance, and inter-electrode distance) on the output pulses rise time by modeling the equivalent circuit of the switch using (P spice).
- The static modeling of the E-field by using Microwave Studio CST package to visualize the field distribution in three dimensions.

CHAPTER TWO

ELECTRICAL BREAKDOWN OF GASES

Gasses are perfect dielectric under normal conditions. However, when the adequate high voltage is applied between two conductors separated by a gaseous medium, electric discharge may occur. During the discharge, the gas medium loses its insulating properties and an ionized channel is created conducting a large current and leading voltage to collapse. The maximum applied voltage between the electrodes at the moment of voltage collapse is called breakdown voltage.

Discharges in gasses are fundamental of two types: non-sustaining discharge and self-sustaining discharge. The first type, consisting of local or corona discharge, occurs around conductors with sufficiently high potentials, but not enough to extend to an opposite potential electrode to create a conducting path. The second type passes from a non-sustaining discharge to a self-sustaining discharge forming an electrical breakdown in the gaseous media between electrodes.

Due to numerous existing factors, there are many types of electrical discharges in gasses. There are various conditions that determine the initial state of the gas (for example, pressure and composition), the numerous external effects that impact the gas, the materials, different shapes, arrangements of electrodes, and the different geometry of the electric field growing in the gas. Moreover, the laws applying to these discharges are more complex than the laws governing the passing of current through electrolytes and metals. The electric discharge in gasses follows Ohm's law only in cases where the externally applied voltage is quite small. Consequently, the electric discharges properties in gasses are usually represented by a volt-ampere characteristic [1, 2].

2.1 Ionization of gasses

The electrostatic fields in Electrical dielectrics materials can continue almost indefinitely. These materials offer a very high resistance to the passing of direct currents. However, they cannot resist an infinitely high voltage.

When the voltage across the insulation exceeds a critical value the insulation will be damaged. The dielectrics perhaps gaseous, liquid or solid in form. Gaseous insulation in practice is not free of electrically charged particles, including free electrons. The dielectrics perhaps gaseous, liquid or solid in form. Gaseous insulation in practice is not free of electrically charged particles, it is including free electrons. The electrons, which may be created by field emission or irradiation can initiate the breakdown process. These free electrons are accelerated from the cathode to the anode by the electric stress applying a force on them. They gain a kinetic energy (½ mu2) as they are moving through the field. The energy is usually expressed as a voltage (in electron volt, eV, where e is the charge on an electron) as the energy involved is extremely small. [The energy Ei = e Vi is expressed in electron volt. 1 e V = 1.6 x 10-19 J]. These free electrons, moving towards the anode collide with the gas molecules existent between the electrodes. In these collisions, part of the kinetic energy of the electrons is lost and the other part is transmitted to the neutral molecule. If molecules gain sufficient energy (extra than the energy Ei necessary for ionization to occur), it may be ionized by the collision.

The electron avalanche is set up by accelerating the newly liberated electron and impinging electrons in the field. Moreover, increase in voltage results in additional ionizing processes. The Ionization increases quickly with voltage once these secondary processes occur until ultimately breakdown takes place. In uniform fields, at voltages below breakdown point the ionization present normally too small to impact engineering applications. In non-uniform fields, however, great ionization may be existing in the region of high stress, at voltages well below breakdown, shaping the corona discharge [1, 2].

2.2 Elementary Processes Related to Ionization of Gases

In this part, the theory of ionization of gasses is presented. Ionization is a process of releasing an electron from the molecule of the gas with the simultaneous production of a positive ion. Ionization may occur by photo-ionization, collision, and secondary processes.

When ionization occurs by collision, a neutral gas molecule has a collision with free electrons, and new electrons and positive ions are released. The energy of the charged particles rely on its mass m and velocity vd. The kinetic energy produced from the charged particles due to the electric potential V is given by [2]:

$$E\nu = \frac{1}{2} m v^2 \qquad 2.1$$

The most important process leading to the breakdown of gasses is the Ionization by electron impact for higher field strength. The activity of ionization by electron collision depends on the energy that each electron can gain along the mean free path in direction of the field. The energy eV that can be gained by moving the particle a distance r0 in the direction of the field is given by equation [1, 2]:

$$e\nu = \int_0^{r0} e\vec{E}(r)\, d\vec{r} \qquad 2.2$$

To make an ionization, the energy achieved between collisions needs to overtake the necessary energy to release an electron from its atomic shell.

$$A + e^- \rightarrow e^- + A^+ + e^- \qquad 2.3$$

Where A represents molecule or a neutral atom in the gas, A+ is the Positive ion and e– is the electron generated in the ionization process. The gas atoms can excite to higher states after the collision by Electrons of lower energy (eVi). To return from the excited state the atoms radiate a return of energy of a photon (hv), which ionize another atom whose ionization energy is equal to or less than the photon energy[1, 2].

$$A + h\nu \rightarrow e^- + A^+ \qquad 2.4$$

Where A represents molecule or a neutral atom in the gas, A+ are the positive ion and hv is the photon energy. This process known as photo-ionization includes an interaction of radiation with particles and happens when the amount of radiation energy absorbed by a molecule or an atom exceeds its ionization energy level, generating a photon to eject one or more electrons. To remain discharge processes, the secondary electron is produced by additional ionization mechanisms (secondary processes). These mechanisms include positive ions may liberate electrons from the cathode when they are hitting on it. The excited molecules or atoms in avalanches may emit photons, leading to the releasing of electrons due to photoemission. Thermal ionization may take place due to the high temperatures in the plasma channel [1].

The ionization process is influenced by many factors such as gas properties, pressure, temperature, electrode topology and material, among others. Two theories are generally accepted for explaining the breakdown mechanism under different conditions. Townsend's theory and Streamer theory. The ionization process is affected by many factors such as pressure, gas properties, electrode topology, temperature, and materials, among others. Two theories are accepted for explaining the breakdown mechanism under different conditions: Townsend's theory and Streamer theory [2].

2.3 Townsend Mechanism

The Townsend discharge is a process of gas ionization where liberated electrons are accelerated by applying an electric field, collide with gas molecules, and consequently, released more electrons. Those electrons are in turn accelerated and release extra electrons. The result is an avalanche multiplication that allows electrical conduction through the gas. The discharge needs a source of free electrons and a sufficient electric field; without both, the phenomenon does not occur. Ionization can happen if the amount of energy caused by electromagnetic radiation, collision or secondary processes exceeds the ionization energy. The ionization condition can be expressed in terms of electric field strength E and releasing free pat λE, which is the average distance a particle cross between collisions under the effect of electric powered field E.as shown in figure (2.1)[2].

$$eE\lambda_E \triangleright W_i = eV_i \qquad 2.5$$

Where W_i the ionization energy, e is the charge of the electron and V_i is ionization potential.

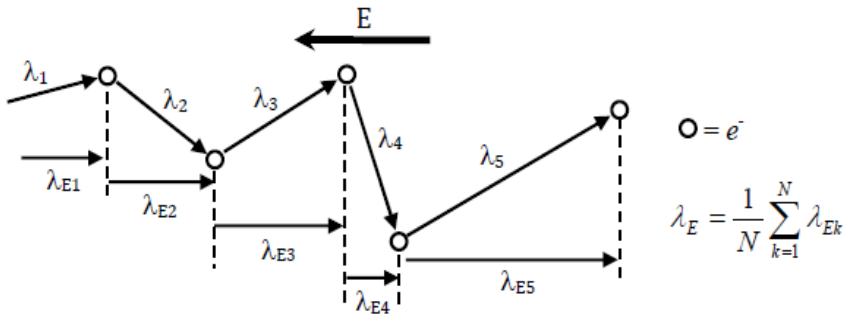

Figure 2.1 Free path and mean free path of electron

2.4 Electron Avalanche

When a high voltage is applied to the electrodes, liberated electrons will accelerate and collide with molecules of gas. The process in which free electrons in a transit medium are subjected to strong acceleration by an electric field and collide with other atoms of the medium. This releases extra electrons, which accelerate and collide with further atoms. This liberates additional electrons, which accelerate and collide with another atom, releasing more electrons. In gasses, this causes the affected region to become an electrically conductive plasma. Depending on field strength, the number of new electron's dn created over the distance dx is expressed as [1].

$$dn = \alpha n(\mathrm{x})\,\mathrm{dx} \qquad 2.6$$

Where αn the number of electrons generated by an electron as it travels a unit distance in the direction of the field, α is the ionization coefficient of electrons, coefficient α is also known Townsend's first ionization coefficient. Homogeneous fields, where α is constant, the result of the integration over a distance d from the cathode to anode is given by equation [1].

$$n- = n_0 e^{ad} \qquad 2.7$$

Where n_0 the number of essential electrons produced at the cathode. This exponential rise of the electrons number is called an electron avalanche and can be expressed in terms of current, with I0 the current leaving the cathode.

$$I = I_0 e^{ad} \tag{2.8}$$

I is the current flowing in the device, I_0 is the photoelectric current generated at the cathode surface, e is Euler's number and αn is the first Townsend ionization coefficient, expressing the number of ion pairs generated per unit length (e.g. meter) by a negative ion (anion) moving from cathode to anode, where d represents the distance between the plates.

For a given gas at a constant temperature, the energy distribution depends on the value E/p (pressure and electric field). In addition, for a given energy distribution, the probability of that ionization occurs will depend on the pressure of the gas.

$$\frac{\alpha}{p} = f(\frac{E}{p}) \tag{2. 9}$$

The coefficient α can be represented by an equation as following

$$\frac{\alpha}{p} = Ae^{-[B/(E/p)]} \tag{2. 10}$$

Where B and A stay relatively constants for a specific gas over a range of fields and pressures. Equation (9) proves that α/p depends on E/p, which has been confirmed experimentally within certain ranges of E/p. Therefore, for different gasses the constants B and A have been experimentally determined. Some of these values for some gasses are listed in Table 1.1.

Table 1.1 Ionization Energies and Constants of Some Gases[1]

Gas	N_2	Ar	SF_6	Air
A (1/mm_kPa)	9.0	10.5	-	11.2
B (V/mm_kPa)	256.5	135.0	-	273.7
E/p range (V/mm_kPa)	75 – 450	75 – 450	-	75 – 600
Ionization Energy W_i (eV)	15.6	15.9	15.9	-

2.5. Secondary Emission of Electrons

According to equation (2.8), for a specific pressure a logarithmic graph of (I) vs inter-electrode distance should yield a direct line of slope α. However, Townsend Noticed that at higher voltages the current increasing at a faster rate than given by equation 2.8. To explain that difference, Townsend supposed that the current should be affected by the second mechanism.

There are many secondary processes, which play an important role for calculating the exponential growth of the current (equation 8). , due to the collision of electrons and molecules, The acceleration of positive ions in the electric field leads to emission of secondary electrons from the cathode, in addition, other processes, such as the arrival of photons, neutral and metastable particles. Electrons created by these processes are called secondary electrons[2, 3].

The secondary ionization coefficient γ is described as the number of secondary electrons generated per happening of positive ion, photon, excited or metastable particle. The total values of γ corresponds to the sum of individual coefficients due to the secondary processes and is known "Townsend's second ionization coefficient" The Townsend model is based on the assumption that an avalanche starts near to the cathode due to n0 (Figure 2), and travel across the space then produces $n_0(e^{ad}-1)$ ions. On hitting the cathode, these ions release $\gamma n_0(e^{ad}-1)$ secondary electrons through secondary emission[3].

Supposing (n)as the number of electrons reaching the anode per second, (n0)as the number of electrons released from cathode by u v. illumination,(n+) as the number of electrons released from cathode by positive ion bombardment, and γ as the number of electrons liberated from cathode per incident positive ion, then

$$n = (n_0 + n_+)\, e^{ad} \qquad 2.11$$

Where: $n_+ = \gamma\left[n - (n_0 + n_+)\right]$ 2.12

Replacing equation (1.12) into equation (1.11) gives

$$n = n_0 \frac{e^{ad}}{1-\gamma(e^{ad}-1)} \qquad 2.13$$

Or expressed in terms of current $I = I_0 \frac{e^{ad}}{1-\gamma(e^{ad}-1)}$ 2.14

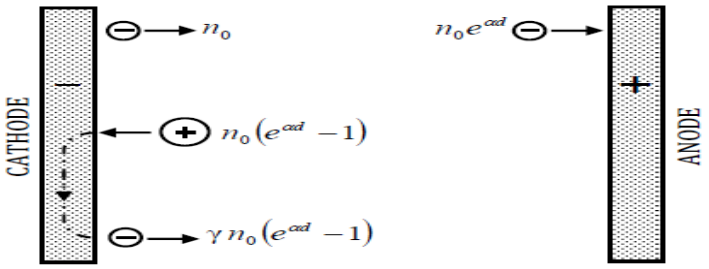

Figure 2.2 Electron generation according to the Townsend mechanism[4]

The values for γ can be determined experimentally from equation (1.12) for specific values of E, p, α and inter-electrode distance. The Values of γ are dependent on the cathode surface. Low work function material will produce greater emissions. Values of γ are small at low values of E/p and higher at greater value of E/p. these values are expected since at high values of E/p the number of positive ions and photons is large with energy high enough to eject electrons from the cathode[4].

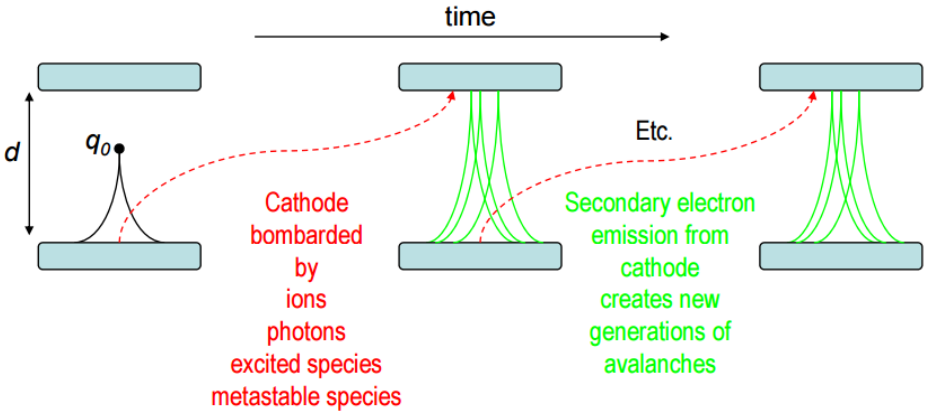

Figure 2.3 Townsend mechanism

2.6 Streamer Mechanism

The growth of charge carriers in an avalanche in uniform electric fields is described as e^{ad}. Meek and Loeb explained that the exponential growth of an avalanche cannot be increased since the avalanche becomes unstable at a critical length. The growth is valid only if the electric field produced by space charges and can be neglected compared to the original uniform field E0. According to Townsend theory, the breakdown voltage depends on the gas density and electrode spacing. There is an empirical evidence, which appeared to be inconsistent with the Townsend mechanism. In spark gaps, for example at atmospheric pressure with electrode distance ~1 cm, the delay time was too short to have involved a series of avalanches produced by ions hitting the cathode. In this case, the breakdown voltage is independent on the material of the cathode. Which an evidence of difference from the Townsend breakdown. The mechanism of the breakdown voltage, in this case, is dependent of the concept of streamer– a thin ionized channel, fast growing between electrodes[4].

Neither the streamer nor the Townsend mechanisms alone can explain the behavior of the breakdown over the full range of pressures. In streamer mechanism, the secondary electrons produced at the cathode is neglected and the Townsend mechanism ignores field distortion by space charge. A more realistic description of the breakdown process is a buildup of space charge in a sequence of avalanches until the field distortion expedite the collapse of the gap. This is achieved when two conditions are met, applied field above a critical field, E_{cr} and a critical distance d_{cr} in electrode gaps. The critical field in ambient air is nearly $3*10^6$ V / m. The beginning of ionization process of breakdown voltage is represented in figure 2.5 and figure 2.6. The streamer theory of the spark for the positive streamer was proposed by Loeb and Meek and independently the streamer theory for the negative streamer by Raether[2].

As long as the net charge is not enough to deform the field, the avalanche moves with the electron drift velocity suitable to the applied field. The electron density developed in the avalanche combine both the drift and diffusion. As result, there is an expansion of electron cloud behind, which is left with the trail of positive ions. When the electron avalanche head increases to a size such that the space charge distribution due to ions and electrons protect itself from the applied field, the propagation and increasing of

the avalanche change significantly, and the streamer phase follows. The necessary conditions for streamer propagation are: the high-energy photons must be generated in the avalanche, the photons should be absorbed to produce sufficient electrons at the tip. The field of space charge at the behind of the avalanche tip should be enough to generate a sufficient secondary avalanche in the enhanced field. Veldhuizen mentioned a range for streamer velocity from [2, 4].

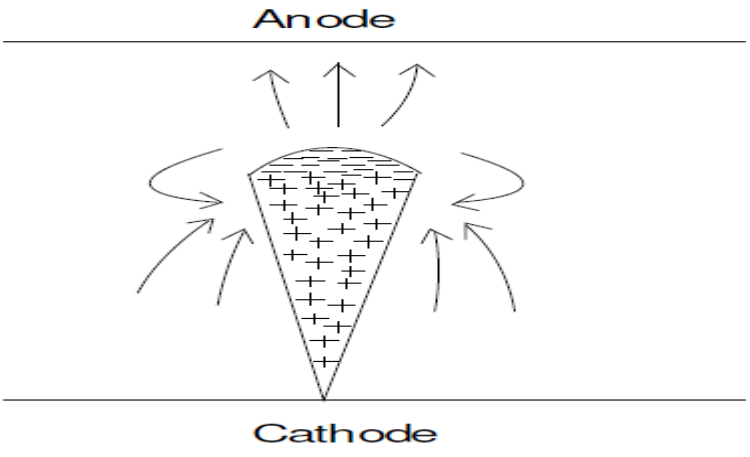

Figure 2. 4 Distribution of electrons and positive ions

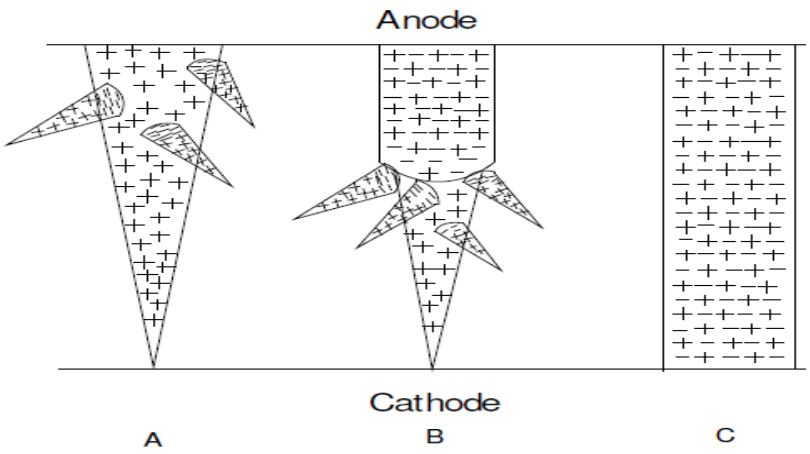

Figure 2. 5 Distribution of ions and electrons due to positive streamer by Meek[3]

2.6 .1 The Panchen's law

The law basically states that, at higher pressures (up to a few torr) the breakdown voltage of a gap is a function (not linear) of the gas pressure and the gap length, generally written as V= f (pd), where p is the pressure and d is the gap distance [4].

The Paschen law is only working at higher pressures (p>several Torr) and distances of more than several mm, the result (p d) is a measuring the number of electrons collision during crossing the gap. The pressure should be exchanged by gas density, which is influenced by the temperature and pressure of the gas. Many other factors affecting the breakdown voltage of the gap, such as particles (dust), radiation, surface irregularities and electrode shape. Paschen's law applies the Townsend breakdown mechanism in gasses. Those are groups of secondary electrons in the gap[4]. This fact was at first noticed experimentally by De La Rue and Muller, and was later widely studied by Paschen [2.4]. Combining the following equations

$$\alpha = Ap\exp\left(-\frac{ViAp}{E}\right) = Ap\exp\left(-\frac{Bp}{E}\right) \qquad 2.15$$

And

$$\alpha d = \ln\left(1+\frac{1}{\gamma}\right) \qquad 2.16$$

Resulting in

$$Apd\exp\left(-\frac{Bp}{E}\right) = in\left(1+\frac{1}{\gamma}\right) \qquad 2.17$$

From the above equations, the breakdown voltage b V is gained as

$$V_b = \frac{Bpd}{\ln(\mathrm{pd})+\mathrm{C}} \qquad 2.18$$

Where $C = \ln\left[\frac{A}{\ln\left(1+\frac{1}{\gamma}\right)}\right]$ 2.19

The equation 2.18 is the Panchen law for planar electrodes. Typically, the Townsend's mechanism and its extension and the Panchen's law, apply at specific range of p d product.

Moreover, modifications for highly electronegative gases are necessary because they re-combine the secondary electrons very fast. In general, the simple equation that define the relationship between V_b and (p d) is draw in figure 2.7. The breakdown voltage V_b in the equation 2.18 explains that at large Pd value (high-pressure insulation) V_b increases because there are a lot of collisions (large distance or high pressure). At low p d value (vacuum insulation), also V_b increases because of a small number of collisions (small distance or low pressure)[2]. Hence, there are a minimum values of V_b which are found from $\frac{dV_b}{d(\mathrm{pd})} = 0$ 2.20

$$(\mathrm{pd})_{\min} = \frac{2.72}{A}\ln(1+\frac{1}{\gamma}) \quad 2.21$$

$$(\mathrm{V}_b)_{\min} = B(\mathrm{pd})_{\min} \quad 2.23$$

Where the values of (B and A) are gas dependent coefficients.

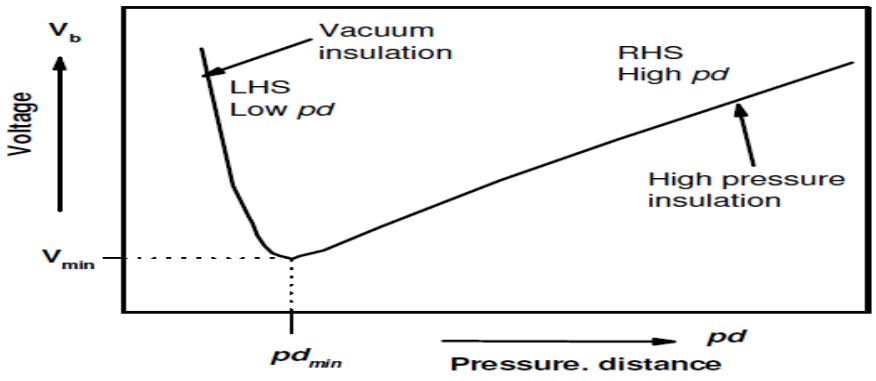

Figure 2.6 Paschen curve for parallel electrode discharge

2.6.2. The limit of Panchen's law

A number of empirical investigations have been conducted to prove Panchen's Law. The empirical results agreed with equation2. 18. for different values of p d up to a few atmosphere pressures. At high values of pressures, additional effects due to differences in the cathode surface should be taken into consideration. These differences cause the field to be intensified leading to breakdown at values of voltages lower than those found from equation2. 18. Otherwise, in small gaps (~ 100 μm) when the surface roughness is not negligible, changing the pressures has a different effect than changing the distance between the electrodes. The discharge is not understood enough at these distances[5, 6]. It is stated that at these small distances, the quality of the electrode surface shape has great influence[6].

At high values of the product p d, a critical size of an electron avalanche distorts the field by the space charges of positive ions and electrons. The formation of space charge initiates the gas breakdown by a streamer. The streamer is explained in the above section. Under small values of Pd, the streamer breakdown is replaced by the Townsend breakdown. More decrease of (p d) value leading to vacuum breakdown. However, the limits of (p d) for these mechanisms are not very sharp[2, 6].

2.7. Electric discharges

Electric discharge describes any flow of electric charge through a gas, liquid or solid. Electric discharges include the following:

- Brush discharge
- Dielectric barrier discharge
- Corona discharge
- Electric glow discharge
- Electrostatic discharge
- Streamer discharge
- Partial discharge
- Townsend discharge

2.7.1 Brush discharge

When the electric field near an electrode with a radius or curvature between about 5 mm and 50 mm is sufficiently large (about 500 kV/m), irregular multiple discharge paths are seen that have the look of a brush. This brush-like shape is shown in figure 2.8. If the electrode is too sharp, a corona discharge will usually occur instead of a brush discharge. Typically, a brush discharge is an electrical breakdown between a grounded conducting electrode and no conducting surface. Unlike a spark discharge, where a large percentage of the maximum possible stored energy is released per discharge, a much smaller percentage of the maximum energy is released per brush discharge. As with corona discharge, this breakdown is referred to as a one-electrode discharge (even though it can also occur between two electrodes)[7].

Also, two characteristics of a brush discharge are an acoustical crack and a burst of current. The energy density is larger than a corona discharge and is thought capable of igniting some flammable gas vapors but not flammable suspended polymer dust. Common hydro- carbons, however, are easily ignited. Sulfur dust in an oxygen-enriched atmosphere can occasionally be ignited. About I to 3.6 mJ energy is released during a brush discharge, and the surface charge is greater than about 3 it has been shown that greater positive surface charge is required to ignite certain gases, such as hydrogen, than negative surface charge via a brush discharge.

For some situations such as with a mixture of propane and air, positive surface charge could not even ignite the material while 7.4 pC/m2 of negative surface charge could. As the area of the charged surface increases, the strength of the brush discharge generally increases. When a metal tool or human finger, for example, is brought near charged insulating objects, such as bags or tubes, a brush discharge can occur. It can also occur when conducting objects are inserted into a charged region, such as a bin of charged powder. The electric field to initiate a brush discharge can be generated by charge on the electrode or on a nearby insulating surface. Static eliminators can be used to reduce or neutralize excessive charge on insulating surfaces[2, 7].

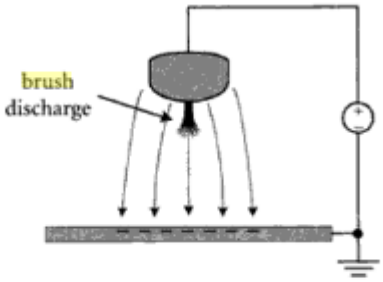

Figure 2.7 Brush discharge from an electrode

2.7.2 Dielectric barrier discharge

Typical planar DBD configurations are sketched in Fig. 2.9 as a consequence of the presence of at least one dielectric barrier. These discharges require alternating voltages for their operation. The insulator cannot pass a dc current. Its dielectric constant and thickness in combination with the time derivative of the applied voltage, dU /dt, determine the amount of displacement current that can be passed through the dielectric(s). To transport current in the discharge gap the electric field has to be high enough to cause breakdown in the gas.

In most applications, the dielectric limits the average current density in the gas space. It thus acts as a ballast which, in the ideal case, does not consume energy[8].

Preferred materials for the dielectric barrier are glass or silica glass, in special cases also ceramic materials, and thin enamel or polymer layers. In some applications, additional protective or functional coatings are applied. At very high frequencies the current limitation by the dielectric becomes less effective. For this reason, DBDs are normally operated at line frequency and about 10 MHz when the electric field in the discharge gap is high enough to cause the breakdown. In most gasses, a large number of micro -discharges are observed when the pressure is on the order of 105 Pa. This is a preferred pressure range for ozone generation, excimer formation, as well as for flue gas treatment and pollution control. Figure 2.9 shows micro discharges in a 1-mm gap containing atmospheric-pressure air, photographed through a transparent electrode[8]

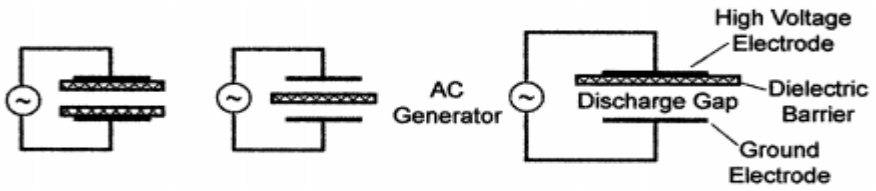

Fig. 2.8 Basic dielectric-barrier discharge configurations

2.7.3 Corona discharge

Corona discharge is a gas discharge where the geometry confines the gas ionizing processes to the high-field ionization region(s) around the active electrode(s). The corona geometry is named positive, negative, bipolar, AC, or HF, according to the polarity of the active electrode(s), while the current conduction in any corona region is called unipolar or bipolar dependent on whether one or both ion polarities is importance. Figure 2.10 shows a typical positive point-to-plane corona, with some commonly used terms.

However, all discharge forms have ionization regions, and thus the really distinguishing feature of coronas is the existence of a low field drift region connecting the ionization region(s) with the eventual low field, passive electrodes. In this drift region, ions and electrons drift and react with neutrals, but with low energy to ionize and low density to react with other ionized particles. In unipolar conduction coronas, the drifting ions/electrons will always be of the corona polarity, and their space -charge field will be the dominating factor in determining both the corona current/voltage characteristic and the current density distribution in the discharge gap. Electrically, the drift region then behaves as a large non-linear resistor in series in the ionization region, often making external stabilizing resistances superfluous.

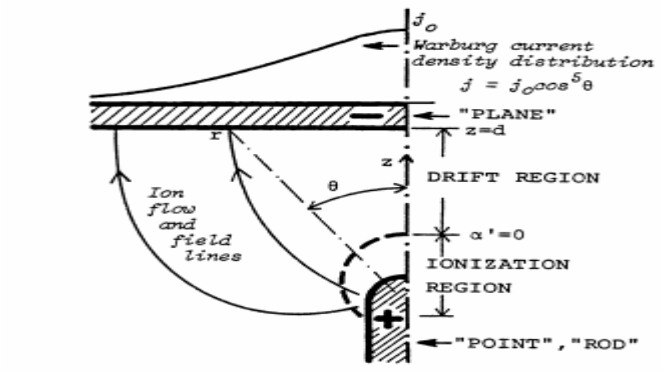

Fig. 2.9 a typical point-to-plane corona geometry [9]

2.7.4 Electric glow discharge

The glow discharge is the forming of a plasma by the electrical breakdown of gases. In general, the gases are insulators, when you apply a high voltage across two electrodes filled with gas, these electrons will be accelerated in the electric field © between the two electrodes. If the mean free path of electrons is long sufficiently that over that distance, they obtain enough energy to ionize the gas molecules, this process releases more electrons, which, then will ionize more and more gas molecules. Thus the formed ions can also expel electrons when they collide with the cathode (negative electrode).

The different collisions among the electrons, ions, and neutral gas molecules result in breakdown voltage, and the current is sustained between the anode and cathode of the discharge tube. The formed plasma thus is an electrically neutral mixture of positive ions, electrons, and electronically excited neutral gas molecules. The emission of excited molecules leading to lower energy states that we can notice as the glow. [5]

As above would point out, there is a strong relationship between the gas pressure and distance between the gap electrodes, and minimum voltage at which the breakdown voltage occurs. The breakdown voltage Vs is a function of (p) the pressure, and (d) the distance between the two electrodes. The accurate shape of this function differ somewhat according to the specific gas, but its main characteristic stays the same.

The voltage ranges from about one to a few thousands of volts, at a pd on the order of one torr-cm. To the either side of this minimum, (Vs) rises.

This curve reflects the behavior for a given pressure. For some applied voltage above the minimum, there is a zone of electrode distances over which the breakdown occurs, but if one electrode moves too far apart or very close together the voltage is not enough to cause breakdown voltage. Basically, this is because when the two electrodes are very close to each other, the mean free path of the electron is too long relative to the gap distance, and there is not enough electrons collisions occur to make breakdown voltage. When the electrodes are too far from each other, however, the gap is too longer than the electron mean free path, and the electrons suffer so many collisions and they never arrive at the anode. The law explains the relationship between Vs, p and d is called Panchen's law, and the curve is a Panchen curve [5]

The electric discharge for a given gas depends on the voltage across the electrodes, pressure and the current through the gap. Fig 2.16 illustrates the different glowing regions that make up a glow discharge and a diagram giving their names [5].

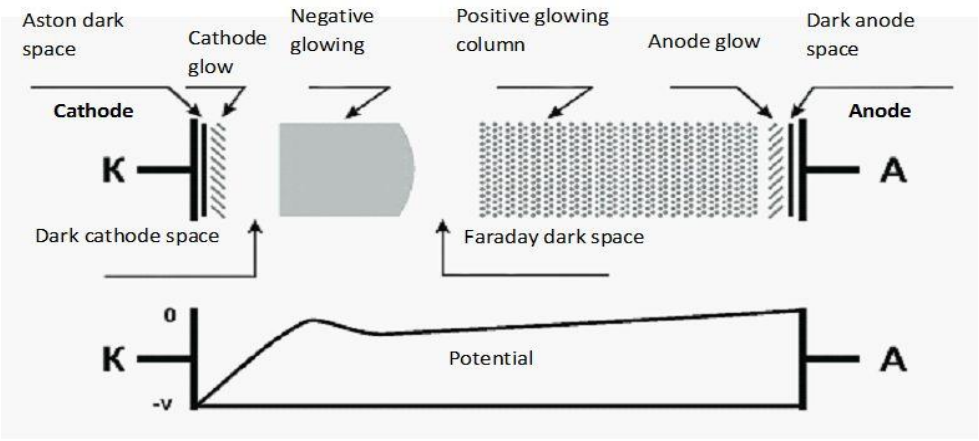

Fig 2.10 The different glowing regions that make up a glow discharge

2.7.5 Electrostatic discharge

It is the flowing of electricity between two charged objects suddenly caused by contact, an electrical short, or dielectric breakdown. A setting up of Static electricity can be created by electrostatic induction or by tribe charging. The ESD take place when different charged objects are placed close together or when the insulator between them breaks down, oftentimes creating a visible spark [6].

ESD can generate the spectacular electric spark (light with the sound of thunder). Electric sparks request a field strength more than approximately 40 kV/cm in the air, as notably happens in the lightning strike. Other types of ESD include the brush discharge from blunt electrodes and corona discharges from the sharp electrodes. A range of harmful effects can be caused by ESD in the industry, including coal dust explosions and gas and fuel vapor, and the failure of solid state electronics elements such as very small integrated circuits .These can be damaged when exposed to high voltages. Therefore, electronics manufacturers establish electrostatic protective regions free of static, using new methods to prevent charging, such as grounding human workers to remove static, avoid high charging materials, using antistatic devices and controlling humidity[7,4, 6].

2.7.6 Streamer discharge

A streamer discharge is a kind of transient electrical discharge. Streamer discharges can be formed when an insulating medium (an example air) is exposed to high potential difference. When an electric field generated by applying sufficiently high voltage, then accelerated electrons will strike the air molecules with enough energy to hit other electrons off them, ionizing them, and free electrons continue to strike more and more molecules in a chain reaction. These electron avalanches (Townsend discharges) produce electrically and ionized conductive zones in the air close to the electrode generating the electric field. The space charges produced by the electron avalanches provide rising to an additional electric field. The growth of new avalanche can be enhanced by the field in a particular direction.

Then the ionized regions increase fast in that direction, and forming discharge called a streamer [8]. Fig 2.12shows the streamer properties in laboratory experiments. The segment length (L) represents the length of a single segment of a streamer. D min is the minimum diameter, represents the lower segment diameter as streamer can reach. The energy per length represents the amount of energy which dissipated per length of single segment [9].

Streamers exist only for a short time and filamentary, and they are different from corona discharges. They are widely used in many applications such as air purification, plasma medicine, and ozone production, Streamer paves for generating arcs and lightning leaders, the ionized paths generated by streamer are heated by the large currents. Streamers can be noticed as a sprite in the upper atmosphere. Because of low pressure, sprite is much larger than streamer at ground pressure [8, 10].

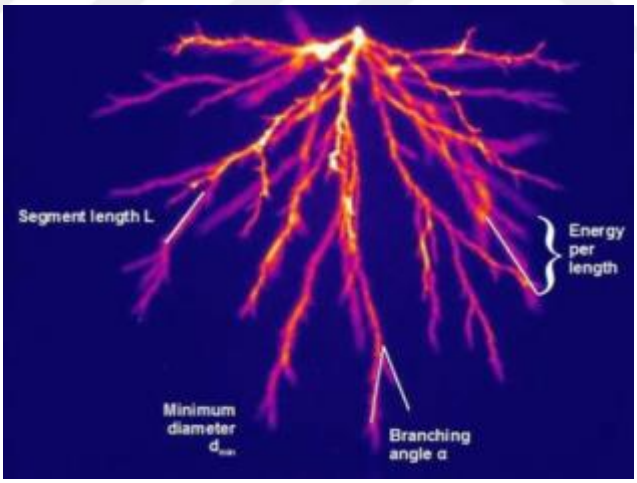

Fig 2.11 Streamer properties in laboratory experiments as used in[10]

2.7.7 Partial Discharge

Partial Discharge can be described as an electrical pulse or discharge in a gas-filled void or on a dielectric surface of a solid or liquid insulation system. This pulse or discharge only partially bridges the gap between phase insulation to ground, and phase

to phase insulation. These discharges might occur in any void between the copper conductor and the grounded motor frame reference. The voids may be located between the copper conductor and insulation wall or internal to the insulation itself, between the outer insulation wall and the grounded frame or along the surface of the insulation.

The pulses occur at high frequencies, therefore they attenuate quickly as they pass to ground. The discharges are effectively small arcs occurring within the insulation system, therefore deteriorating the insulation, and can result in eventual complete insulation failure. The possible locations of voids within the insulation system are illustrated in Figure 2.13[11].

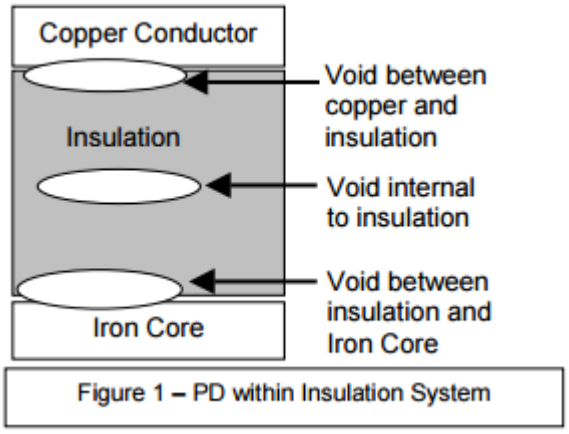

Figure 2.12 The possible locations of voids within the insulation system[11]

2.7.8 Townsend discharge

A simple gas breakdown test system is illustrated in Figure 2.14. It consists of a pair of parallel plates enclosed in a gas chamber and separated by a distance d. The electric field between the electrodes is assumed to be uniformly distributed when a high voltage is applied between the two electrodes. When free electrons are emitted from the cathode by any means, they are accelerated toward the anode under the strong applied electric field. If the electrons acquire enough energy, they can ionize the gas

molecules through collisions. The generated new electrons propagate along the field as the primary ones and then ionize other gas molecules. The primary avalanche ends after the ions enter the cathode region. If the amplification and electron avalanche is increased, more electrons are liberated in the gap by secondary ionization from positive ions, excited atoms, photons, and mat stables. These secondary electrons initiate new avalanches, resulting in a space charge formation in the gap[12].

The space charge formation enhances the electric field somewhere between the electrodes, with a subsequent fast current increase will lead to the breakdown of the gas ultimately. This is the classical Townsend mechanism [4].

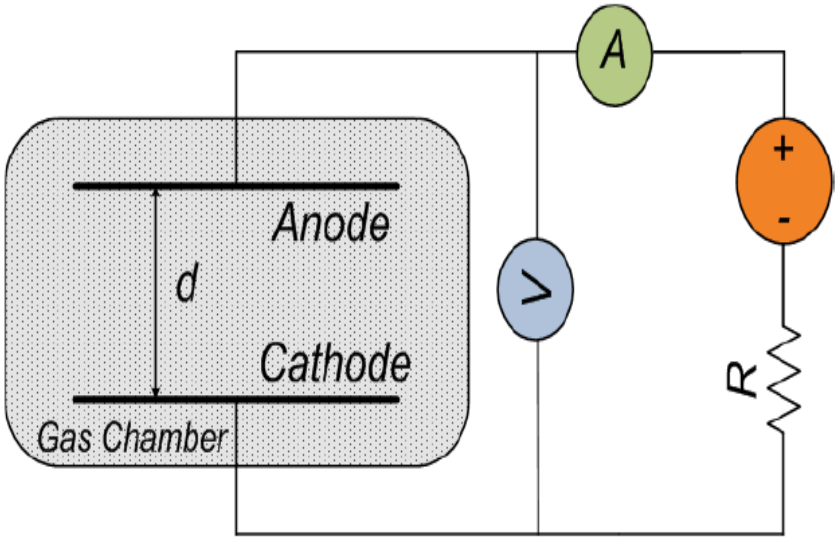

Figure 2.13 Schematic of simple gas breakdown test[12]

Suppose a free electron exists (caused by some external effect such as radio-activity or cosmic radiation) in a gas where an electric field exists. If the field strength is sufficiently high, then it is likely to ionize the gas molecule by simple collision resulting in two free electrons and a positive ion. These two electrons will be able to cause further ionization by collision leading in general to 4 electrons and 3 positive ions. The process is cumulative, and the number of free electrons will go on increasing as they continue to move under the action of the electric field.

The swarm of electrons and positive ions produced in this way is called an electron avalanche. In the space of a few millimeters, it may grow until it contains many millions of electrons. This is shown in figure 2.15 [2, 12].

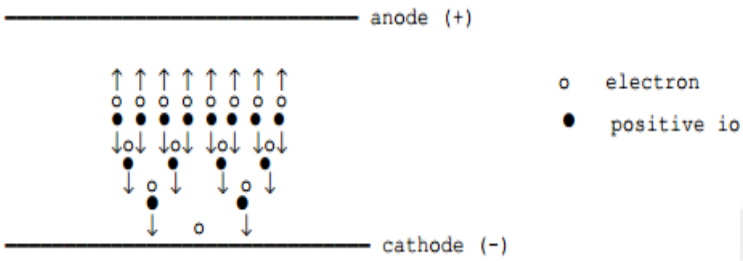

Figure 2.14 Electron Avalanche

The relationship between the current and applied voltage was explained by Townsend as shown in Figure 2.16[2]. He determined that the current at first increases proportionally as the voltage increases, and then reaches a saturation current I_0 and remains steady for a while. The current I_0 results through photoelectric effect produced at the cathode by external irradiation. If the (Vo) breakdown voltage of the gap. In the steady state, the circuit current is given by[12, 13].

$$I = \frac{I_0 e^{\alpha d}}{1-\gamma(\mathrm{e}^{\alpha d}-1)} \qquad 2.24$$

where α is Townsend first ionization coefficient, γ is Townsend secondary ionization coefficient, d is the distance between electrodes, I0 is saturation current, I is current flowing in the circuit[13].

The internal resistance of power supply will be neglected, the current becomes infinite if

$$\gamma(\mathrm{e}^{\alpha d}-1) = 1 \qquad 2.25$$

Normally, $e\alpha d$ >> 1, and Equation 1.2 is simply expressed as

$$\gamma e^{\alpha d} = 1 \qquad 2.26$$

Equation (1.2) defines the onset condition of spark and is known as the Townsend criterion for spark breakdown[13].

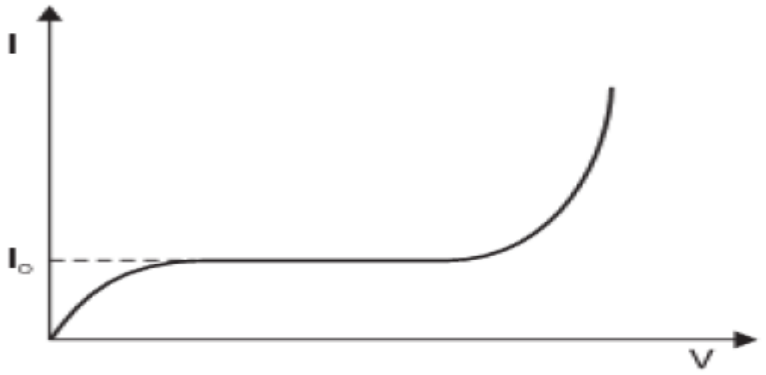

Figure 2.15 Variation of current as a function of applied voltage

2.8 Types of DC discharges

To make the gasses electrically conducting, an adequate number of charge carriers should be generated. Although there are already a particular number of charge carriers existent at room temperature (typically, 106 electrons/m3 in atmospheric air). This number is too small to create electrical conductivity. The small number of charge carriers is responsible for the breakdown of the gas gap. In the circuit shown in Figure. When the voltage is applied to the circuit, the gap voltage V can be calculated [2, 3]as

$$V_{gap} = V_0 - IR_c \qquad 2.27$$

V_0 Is the applied voltage, R_c is the load line resistor, and I is the circuit current. Rc is ballast resistor, R_{gap} spark gap resistance, I the current meter.

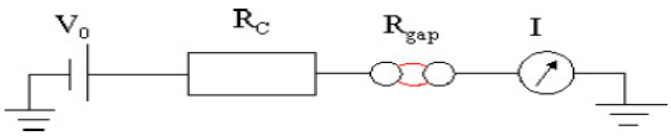

Figure 2- 16 A simple circuit for electric discharge experiments

Breakdown of the non–conducting gasses set up a conducting path between the electrodes. Transit of electric current through the electrodes gap leads to phenomena known as gaseous discharge. In the gaseous discharge process, an electrically conducting plasma is created, which contains a mixture of ions, electrons, and neutral particles. The structure and distribution of plasma between two electrodes is a function of discharge method and other discharge parameters. Figure 1 shows the basic physical structure of an electric discharge. All the component of the structure shown are not always found in any given discharge, but the discharge depends on pressures, voltages, and dimensions of the electrodes[3, 14].

The Panchen's Law, between the gap distance between electrodes, the pressure, and the applied voltage that must be met in order to set up the discharge. Changes in any of above variables, or the type of used gas, will change the appearance of the discharge. Once the electric discharge has occurred,, a couple of electrons will get in into the discharge gap from the cathode. One electron is accelerated toward the anode and the other recombines with an approaching + ion. The different types of discharge in the electrode gap through the V – I characteristic with fixed voltage source V 0. After the occurrence of the collapse, the value of the current I will be determined by the sum of the ballast and gap resistances C gap R + R. when the voltage decreases leading to the current increases along the load line[3, 14].

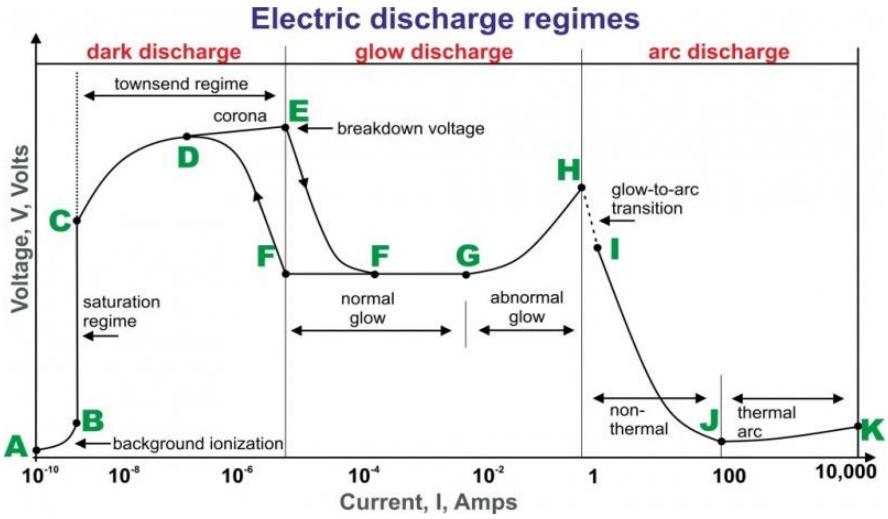

Figure 2- 17 voltage and current characteristics of the gas discharge[15]

Depending on the (I – V) characteristic, the applied voltage V0 on the electrodes and the load line C R may cross the curve at several points. Then the discharge in the gap is unstable and changes randomly[3, 14].The above figure2.16 is an ideal V/I curve of a glow discharge. The main properties of the breakdown voltage, the characteristic of voltage – current and the structure of the discharge process depend on the applied voltage, geometry of the electrodes, the type of the gas, the gas pressure and the electrode material[15].

2.8.1. Dark Discharge (dark current)

The region between A and E on the voltage-current characteristic is described a dark discharge due to except both corona discharges and the breakdown itself and the discharge remains invisible

- **A – B** During the ionization stage of the breakdown process, the applied electric field along the discharge tube sweeps out the ions and electrons which created by ionization from radioactive minerals , background radiation ,Background radiation from cosmic rays, or other sources, produces a measurable degree of ionization in the air at atmospheric pressure. The ions and electrons travel to the electrodes in the applied electric field leading to

produce a weak electric current. The Increasing of voltage sweeping out causing to increase the fraction of these ions and electrons[15, 16].

- **B – C** by increasing the voltage between the electrodes all the electrons and ions are swept away, and the current will be saturated. In the saturation zone, the voltage is increasing while the current remain constant. This current rely on linearly on the radiation source strength[15].
- **C – E** by increasing the voltage across the discharge tube beyond point C, the current will increase exponentially. Now the electric field is high enough so at first the electrons present in the gas can gain enough energy before arriving at the anode to ionize neutral atoms. As the electric field becomes stronger, the secondary electron may also ionize another atom leading to an avalanche of electrons and ions production. The region of increasing current is known as the Townsend discharge[15, 16].

- **D – E** Corona discharge occurs in Townsend dark discharge in the region of a high electric field near the sharp points, edges, or wires in gasses before the electrical breakdown. If the corona current is high enough, corona discharge can be technically "glow discharge", visible to the eye. In low currents, the whole corona is dark, as suitable for the dark discharges. Related phenomena contain the silent electrical discharge, filamentary discharge, the brush discharge, and a luminous discharge in a non-uniform electric field where corona discharges are active at the same time and create streamers through the gas[15, 16].
- **E-** When the electrical breakdown occurs in Townsend region, the cathode then emits secondary electrons due to ion or photon impact. At breakdown or sparking potential VB, the current may increase by a factor of 104 to 108, and it is limited by the internal resistance of the power supply. If the resistance is very high, the discharge tube cannot get enough current to break down the gas, and the tube will remain in the corona region with small points or brush discharges on the electrodes. If the internal resistance of the power supply is low, then the gas will be ionized at the voltage Vb, and shift into the normal glow discharge regime. The electric breakdown voltage for a specific gas and

electrode material depends on the pressure and the space between the electrodes, pad, as expressed in Panchen's law[15, 17].

2.8.2 Glow discharge

The main difference between glow discharge and the dark discharge is the non-uniform distribution of the potential difference applied across the electrodes gap. The glow discharge can be divided into three parts: subnormal, normal, and abnormal. The transition from the dark to glow discharge region corresponds to subnormal. There is no significant change of the current, and the cathode thickness layer for the self–sustained discharge is greater than the normal regime[18] [19].

2.8.3. Normal glow discharge

It is also called glow discharge zone due to the plasma is shining. The gas glows due to the energy of the electrons and density number are high enough to generate visible lights by collisions. The applications of glow discharge process including the fluorescent lights, magnetron discharges which used for depositing thin films, dc voltage parallel plate plasma systems and electro bombardment plasma generators. The F–G, part of the V – I curve, corresponds to normal the normal discharge.

The characteristic of normal discharge phenomenon is the current density near the cathode stay constant as the discharge current carry on to be varied. When decreases or increases the radiant current spots on the surface of cathode expands or contracts. Figure 2- 16 shows an ideal glow discharge zone, which by itself is non-uniform in the nature. In a glow discharge, the electrons are emitted from the cold cathode due to secondary emission particularly by positive ion bombardment[19].

The normal glow discharge region unlike the Townsend or arc discharges, It is characterized by distinguished region with large variation in the intensity of the light, electric field, plasma potential, and distribution of charge densities (electrons and ions).A special feature of this discharge is a large layer of the positive space charge at the cathode, with an intensive field at the surface and large potential drop of a few hundreds of volts. This region is called as the cathode fall. The cathode fall cannot be defined by only light emission but also by the characteristic of the electric field distribution. By high electric field, the cathode fall accelerates the electrons to high

energies to create ionization and subsequent avalanche. If the inter -electrode distance is large enough, an electrically neutral plasma with weak field is created between the anode and the cathode layer. Its comparatively homogeneous part called positive column. It is practically separated from the anode by the anode fall[19].

The anode fall is known as the voltage between the anode and the extrapolated value of the linear potential gradient of the positive column to the anode. Due to the traveling of electrons from the positive column to the anode, a negative space charge formed at the anode fall. The electric field of this region higher than the positive column and hence pulls out the electrons of it. The multiplication of the electrons is three orders of magnitude smaller than the number of electrons generated in the cathode layer. Consequently, the cathode fall is much higher than the anode fall. The voltage of the anode fall increases with the increasing of the current, and decreases with the increasing of pressure.

CHAPTER THREE

BREAKDOWN VOLTAGE OF A HIGH PRESSURE SPARK GAP

The experimental study of spark discharge in spark gap has a long history .The basic information in the past several years have been the systematic acquisition of the relevant fundamental process and results in the understanding of discharge phenomena. We choice the spark gap as the FSD is because of its amazing performance in high power switches. The study includes a self-breakdown gas gap with an arrangement of two electrodes separated by an insulating gas medium. The voltage breakdown of the gas, brought about by several processes of ionization and other discharges in a gaseous medium. In this chapter, we will discuss some of the basic physical processes, which considerably aided our understanding of gaseous spark gap and their properties in breakdown processes [18, 20, 21].

Some of the terminologies specified to spark gap switches and their basic mechanisms responsible for the breakdown and re–breakdown voltage of the electrode gap are described here. Apart from these, we discuss several theoretical models, which agree with many experimental data. They consider the closure phase (‘resistive phase’ in spark gap terminology) of the switch as a function of time[2, 3, 7].

3.1 The Principle of a closing switch

The secondary electron emissions from the cathode and the Ionization processes in the inter–electrode space cause a fast increasing of the current. This fast transformation of the current creates a non–self–sustaining discharge to some forms of self–sustaining discharge. This is known as an electrical breakdown. Electrical breakdown in the gasses is a fast sequence of irreversible events, which quickly leading to the transformation of the gas from its insulating state (conductivity ~ 10-14 W-1m-1) to good conducting state. Gas filled spark gaps use a high or low- pressure gasses such as, nitrogen, air, hydrogen, and SF6.

The capabilities of the voltage standoff of the switch are determined by the breakdown characteristics of the insulator and the field emissions characteristics of the electrodes. For high pressure gas switches, the breakdown of the bulk dielectric medium is usually close, but before the field emission from the electrodes becomes a problem[11].

One of the desired operating characteristics such as current and voltage relationship related to a closing switch is shown in Figure 3- 1. The effective operation of closing switch demands a gaseous medium with a high breakdown strength v_b , small voltage drop or low conduction voltage V_F , and a short formative time lag $\tau_f = (\tau_c - \tau_b)$. The switch is at first opened (non–conducting), at the time $\tau \succ \tau_b$. At this stage, the applied voltage b V between the electrodes of the gap is high in the ambient temperature (T). When the switch is closed (start conducting) at the time $\tau = \tau_b$ then the voltage V (t) drops and causing an increase in the current i(t) . This is can be as the breakdown phase or closure phase or turn–on time.

The voltage V_F across the electrodes through the conducting stage is much lower than V_b depending on the degree of ionization. The temperature of the gas is very high during this stage. It is desirable that such switches should close quickly and with a minimum losing of the energy. The efficiency E_{ff} of such a switch has presented by Christo porous[11].

$$E_{ff} = (1 - v_F / v_b)^2 \qquad 3.1$$

To develop the efficiency of the switch, the voltage drop v_b or the breakdown strength should be large, the forward voltage drop V_F or resistivity of the gap during the conduction interval must be small, and τ_f of very short duration [11].

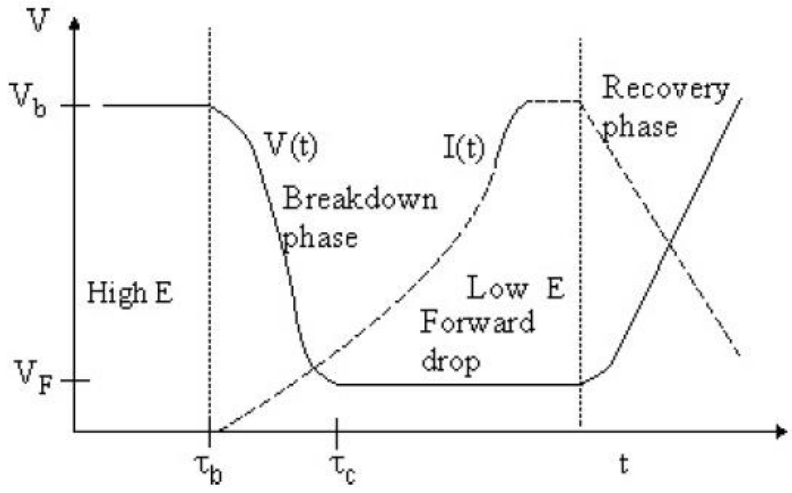

Figure 3- 1 Voltage and current versus time in a spark gap closing switch

The energy must be enough to accelerate the charge carriers inside the gap to establish and sustain conduction and ionization. When the resistance of conducting gap (s) becomes sufficiently low, the impedance of the switch start to be dominated by the inductance of the geometry of the swıtch and the dimension of the conducting channel (s). This is called the inductive phase and can affect the rate of switch closure dI / dt. The switch voltage in the "on" state (forward drop) is very important to determıne overall switch efficiency. For most switches, complex kinetic processes rather than determine the time of the forward conduction voltage. In general, the formative time can be determined by the pre–breakdown period of the insulating gas, where dI / dt is determined by many factors including the geometry of the switch, the dynamics of the final conducting state, and prospective external constraints. A suitable selection of the gaseous medium is desired for optimal performance of the spark gap switch with the following properties[3].

3.2 Large hold–off voltage b V during open condition

- To prevent early breakdown and leakage current at high E, large attachment rate constant k_a (ε) or cross section σ (ε) are required, where (ε) means a function of energy.

- At low gas temperature a strong electron attachment is highly required, i.e., large k_a (ε) or σ (ε) at low-temperature T.

Low forward voltage drop F V during conduction

- In this Conducting stage, a high electron drift velocity v_d is required at low E, it means maxima in conductivity.
- AT low © should be no electron attachment. That means ignore k_a (ε) or σ (ε) at a high temperature of the gas. This stage demands a large rate of ionization.

Short τ_f during change

- A bıg change in the effective of ionization coefficient a is required with respect to change in E. Whenever there is an increase in change the better it is. Because the lower would be τ_f and the faster is a transition to the arc.

3.2 Electrical breakdown in a gas gap

The recovery time generally refers to the time for the recovery of insulation properties of the spark gap, then the applied voltage can be reapplied to the gap at some rate (dV / dt). The re–breakdown voltage at the gap is referred to be the recovery voltage. The recovery voltages of spark gaps that are operated at the high PRR have been less than the DC hold off voltage. Most plasma switches require the idea of attachment and recombination of electrons in the recovery processes.

The recovery processes inside the gaps are functions of plasma kinetic characteristics of the conducting ambiance Temperature, charge density, attachment, mobility, recombination and other cross sections, mean free paths, external applied fields, etc. Only after a limited delay, the recovery phase will go ahead to a point that a particular voltage can be withstood. This leads to the recovery characteristic that limits the PRR of the gap switch operation. If a certain rate of applying voltage is exceeded, thereafter there is a high probability that a conducting channel will be re-established[3].

In many cases, recombination and attachment may happen speedily but the ionized gas is then left in a heated state. Therefore, the regions of low gas density may persist. It means that the mean free path of stray charges is higher and sudden reapplying voltage may initiate an avalanche. Thus, the gas should be deionized, cooled and homogenized to allow full voltage recovery. This is the main reason why gas flow is used in many situations. Some gap switches may require a little or no gas flow if the electrodes gap geometry or operating conditions result in enough cooling and reduced energy deposition. At very high levels of pressures, the recovery processes are such that the recovery time may reduce safely because in part, of intense cooling of the arc plasma.

3.3 The time history of the breakdown voltage behavior

The self-breakdown characteristics of spark gap depend on many parameters including, the duration, which the electrodes have been exposed to the applied voltage. The time intervals related to pulse charged spark gap are illustrated in figure 3- 2[2].

- The required time to raise the applying gap voltage to the self-breakdown voltage V_{sb} is the charging time τ_c .
- 2) In spark gap the time between the self–breakdown voltage V_{sb} and the application of the voltage V_{ov} for the release of an appropriately located initiatory electron in the electrically stressed systems is known the statistical delay time τ_{sd} .
- 3) After the statistical delay time, the important time interval to the starting of breakdown voltage is related to the streamer formation τ_{sf} .
- 4) This time needed for the spark gap closure through heating of the electrons, known a column heating time τ_{ch} .

The working principle of the spark gap includes many parameters that should be optimum for particular applications. Some of those parameters include(the breakdown voltage for a given pressure and electrodes distance, gas type, gas pressure, decreasing the resistive phase time or the time of conducting channel formation τ_{ch} , minimize

the electrodes erosion for reliable operation and decreasing the spark gap inductance for the low rise time of output pulses). Two general operational types require different design for a self-breakdown gas spark gap. For a gas gaps which are required to turn on at a relatively constant applied voltage without breaking down, until an overvoltage takes place, the Paschen low curve is the criterion of the operation. The gaps of the electrodes that are required to breakdown voltage at a specified time/or voltage during the voltage transient,, the criteria of operation depends on spacing and geometry[3].

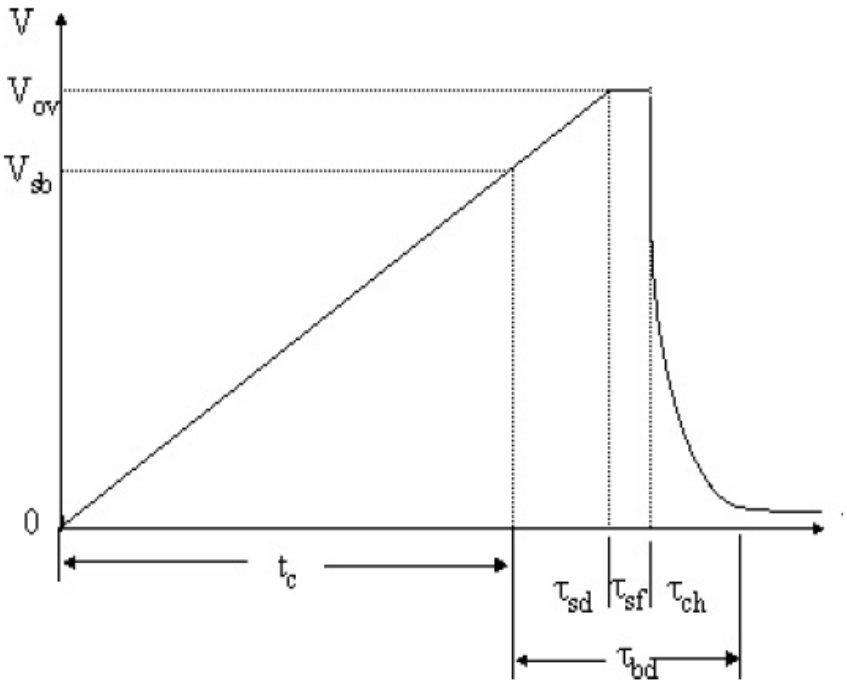

Figure 3- 2 The self-breakdown gas gap time scales[2]

The design of high power switches requests a wide range of characteristics. The characteristics can be arranged into those relating to the electrical capabilities of the spark gap switch and those relating to its operational, physical and other features. For instance, carrying a large amount of charge transfer or high current, to resist very high voltage, to supply very reliable and very long life operation, maintainability, ease of structure, weight and volume, and the cost of the switch, dominate the choice of switches and determine the good design[3].

The switch can carry a very High current and great amount of charge transfer by forcing the discharge to move along the electrodes surface while decreasing the electrodes erosion by spreading the arc heat over a large electrode area. Uniform fields geometries can be made to be very strong and long-lived, but the low electrıc field enhancement establish slower closure tıme and usually the repeatability ıs unacceptable in terms of closure time. The gap closure time of a point plane gap is rapid, but with undesirable voltage hold–off, which means that a pre– breakdown voltage behavior is very likely[3].

3.4 The pulsed power switches

The pulsed power engineering is the technology to store the energy in capacitive or inductive form over long periods of time (usually seconds to minutes) and then discharging it to the load over too much shorter time (usually nanoseconds to microseconds) as an energy by closing or opening the power switches. Power switches, power generation, pulse forming network, and the load are the main components of the pulsed power system[3].

3.4.1 Pulsed Power Generation

Many types of high power and nanosecond pulse generators are available currently. However, the performance of high voltage generators varies generally and they should be selected according to the load requirements, such as a rise time, output voltage, pulse width, repetition rate, and peak power. The main objective of all pulsed power generators is to convert a long-time input, a low-power into a high-power short-time output. A general pulsed power generation diagram is shown as figure 3.3[22].

The high voltage power supply which fed from ac power by rectifiers is the power source to the pulsed power generator. It determines the spend time to charge the energy storage section, which normally start from microseconds to minutes, The pulse energy can be stored in the energy storage side for an amount of times which depends on the output requirements. Which rely on the application. All of these stages usually requires power switch. The impedance match part, for instance, transmission line, is necessary to transfer the maximum power to the load with the minimum losses.

The final part before the discharge load, the initial power switch, delivers all pulses of power into the load. In general, all pulsed power generation circuits are classified capacitive or inductive storage. There are two methods to generate short pulses such as capacitive storage discharge circuit and pulse forming line (PFL). Other pulsed power generators such as Blumlein PFL and Marx generator are generally adapted from them.

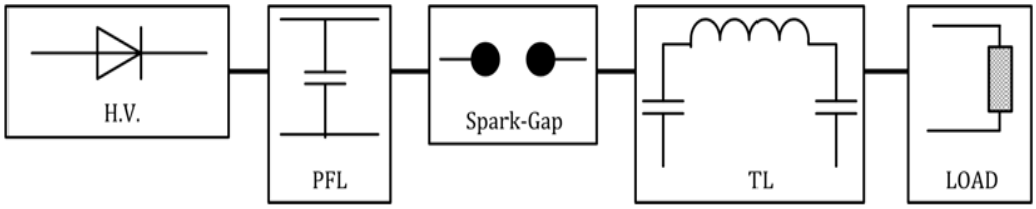

Figure 3.3 The pulsed power generation diagram

The simple RC circuit shown in Figure 3.4 can be easily used for generation double-exponential very high voltage pulses by charging the high voltage capacitor C and then discharging its energy to the load by closing the switch S1 [22].

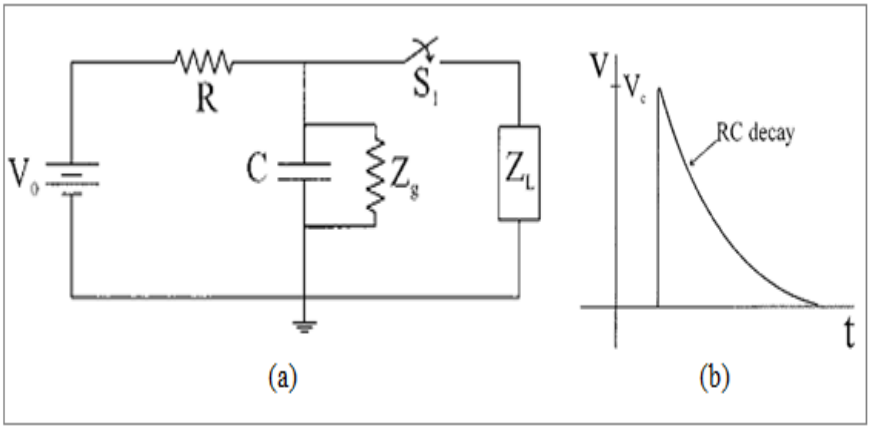

Figure 3.4 Simple capacitive storage discharge circuit

PFL or transmission line in figure 3.5 is another alternative way to generate high voltage square pulses. When the switch S_1 is closed at t = t_0 , a pulse of amplitude (–V0/2) propagates down the line across the line length d. Then it reflects at (d) and returns back to the switch and the load R.

$$t = t_0 + \frac{2d\sqrt{\varepsilon_r}}{c}(\text{sec}) \qquad 3.2$$

Where d is the length of the transmission line in meters, ε_r is the relative permittivity of the transmission line, c is the speed of light.

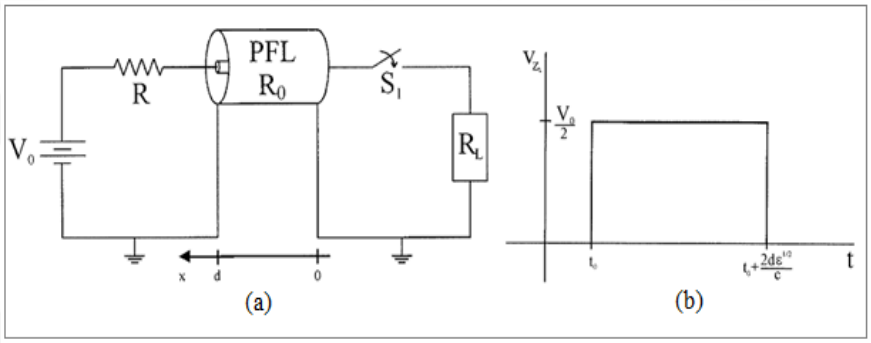

Figure 3.5 PFL circuit (b) output square pulse [22]

3.4.2 The working pressure and operating voltages of high Power Switches

High Power switches, between the storage devices as capacitors and the loads, play a major role in the generation of pulsed power. The rise time, shape, and magnitude of the output pulse depend highly on the properties of the high power switches. Moreover, the maximum capacity and density of the power that the switches could handle also the effect on the performance of pulse generators. Switches are in general classified into closing switches for storage capacitive devices and opening switches for discharge inductive devices. Semiconductor switches and filled gas switches are two common kinds of closing switches. Gas switches play very important role in high power pulse generators. These switches are easy to use and can handle a large amount of currents, and we can trigger it accurately. Several types of gas switches such as thyratron ignitron, krytron, pseudo spark switch, and spark gap are reported in literature [23]. Their working gas pressure and hold-off voltages ranges are shown in figure 3.6.

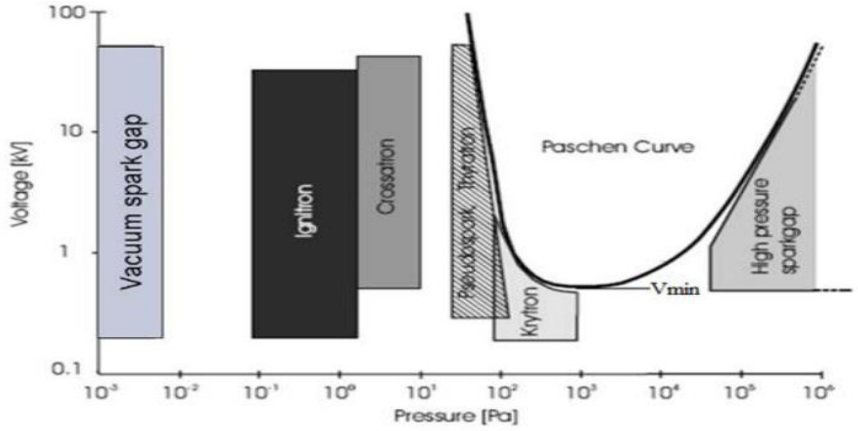

Figure 3.6 Ranges of gas pressure and operating voltages [23]

3.5 Spark gap switch electrical circuit

A spark gap swıtch includes of an arrangement of two or more conducting electrodes separated by a gap (dıstance) usually filled with a gas such as air, Nitrogen and SF6, is designed to allow high an electric spark to pass between the conductors. Figure 3- 3 illustrates the basic electric circuit of spark gap switch. When the applied voltage difference between the electrodes, then it will initiate the breakdown voltage of the gas inside the gap, an electric spark forms, ionizing the gas and quickly reducing its electrical resistance. An electric current flows through the gap until broken the path of ionized gas or reduces the current below the minimum value called the holding current. This usually take place when the applied voltage drops, but in some cases happens when the heat of the gas rises, extend and subsequently breaking the filament of ionized gas. Usually, the process of ionizing the gas is disruptive and violent, often it leads to sound (a spark plug or thunder for a lightning discharge), light and heat.

The spark gap switch was used in early electrical equipment, such as electrostatic machines, spark gap radio transmitters, and X-ray machines. The most use of spark gaps today is to ignite the fuel in internal combustion engines by using spark plugs , and they are also frequently used in lightning arresters and other devices for protection the electrical equipment's from high-voltage[24-26].

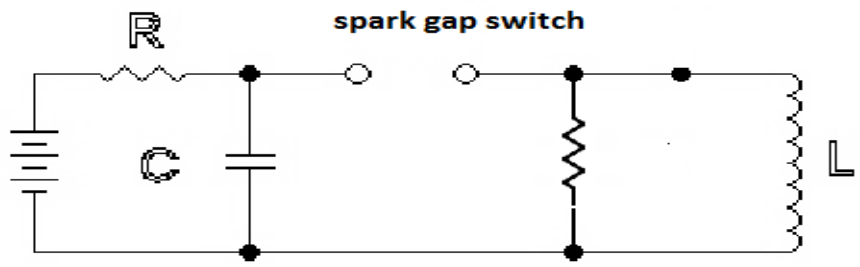

Figure 3- 7 The basic electric circuit of spark gap switch [3]

3.5.1 Principle of work

When the voltage across the spark gap electrodes becomes sufficiently high, the gas in the gap ionizes, and an Avalanche effect take place. The air inside the gap is heated to a very high temperature and turn into a very good conductor of electricity. High current flowing through the ionized gas keeps it heated and creates the conductive channel. Eventually the flowing current will fall sufficiently that the gas in the spark gap switch cools and turn to non-conducting.

The process of the avalanche when the spark gap switch starts to conduct is known as firing or breakdown, and the applied voltage which required to initiate the avalanche process is called the breakdown voltage. The breakdown voltage depends on the dist ance and the pressure between the electrodes. During conduction, the arc between the electrodes is not a perfect conductor and a little resistance withstands the flowing of current through it. The dissipation of power because of the arc resistance in the gap is known as conduction loss and the power is lost as heating, so that keeps the arc very hot and conductive[27].

The necessary current to conserve the arc conductive is usually called the holding current. When temperatures of the arc drops and the arc stops conducting, it is known as quenching. The important facts of a static spark gaps are that they are “turned-on” by enough high voltage, remains on due to initial current flow, and after that “turns-off” when the current falls down too low. The electrodes of a static spark gap are always aligned. If a high voltage triggered it the static gaps it will fire at any time when the applied voltage goes above its breakdown voltage point. This property is useful for

two reasons: It prevents the initial voltage from getting too high. The static gap switches efficiently limits the initial voltage by firing whenever its value of breakdown voltage is exceeded. Figure 3.8 shows the circuit schematic of static spark gap[27].

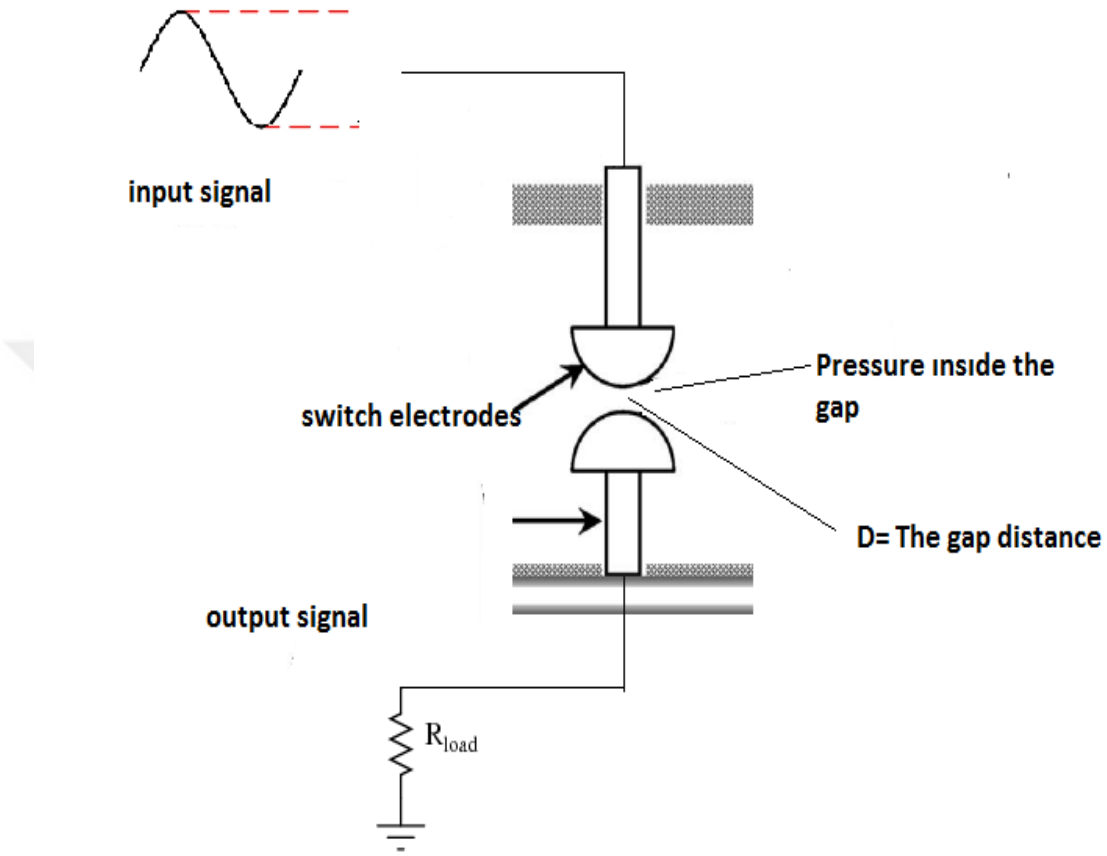

Figure 3.8 The electric circuit of static spark gap

3.6 The efficiency of spark gap switch

The traditional spark gaps or plasma-closing switches have a various losses of power in their repetitive operations such as the consumption of power in the resistive circuit elements and in switch gap. Instantly after the extinction of a discharge, the electrodes gap stay reinforced in residual charges. To keep the switch in conduction would depends on many factors particular how quickly the discharge process goes into the non-conducting medium and the rate how can the applied voltage builds up across the electrodes gap . Since pulsed plasmas switches generate an output power pulses at the load, the efficiency of the switch is very important considering the design of the

charging circuit and electrodes gap geometry. For simplicity's sake, an equivalent electrical circuit model of the spark gap switch is explained for studying the physical behavior of pulsed plasma switches depending on different electrical circuit's schemes in repetitive mode. This contain a resonant charging circuit, which improves the recovery time of the gap switch highly[27].

3.6.1 The charging method of a loss–free switch

The capacitor charging circuit, as shown schematically in Figure 3.9, includes a high voltage source, a charging element, a load, and the pulse-forming network (e.g., a capacitor). Since the charging circuit effects the characteristics of output pulse waveforms at the high PRR, the circuit design and the selection of the circuit components are of most important for the overall pulse efficiency and operation. To design the circuit of the switch the following important considerations should be taken[28].

• For each output pulses the same amount of input energy must be stored

• The power supply must isolated from the switch by the charging element during delivering the pulse and immediately after the pulse delivered

After the pulse delivered to the load, the instantly isolation is necessary to allow the ionized gas to deionize and return back to its non-conducting state. A constant voltage V0 is applied to the spark gap closing switch through a charging resistance C R that limits the increasing of current and decouples the switch from the power supply.

While the gap switch keeps open, V_0 charges the high voltage capacitor C. When the applied voltage across the capacitor V_c overtake the threshold breakdown voltage, the gap switch closes and the stored capacitor discharges quickly through the load. The output load is represented by L and R are connected in series with C[28].

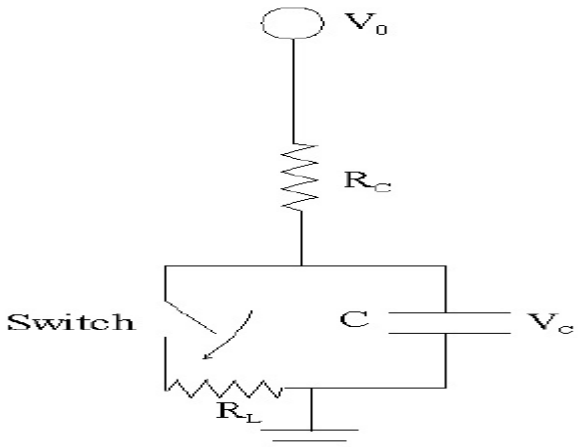

Figure 3.9 A schematic of a charging circuit for a loss free switch.

The development of time of applied voltage $_{C}V$ across the gap switch is given as [28]

$$V_c = V_0\left[1-\exp(-\frac{t}{\tau})\right] \quad 3.3$$

Where the time constant for the charging circuit is $\tau = (\mathrm{R}_c+\mathrm{R}_L)\mathrm{C}$. V_0 is the applied voltage from the supply. If the gap switch closes at a certain time T after the last firing, then the average output power assuming the loss free switch is acquired as

$$P_{out} = \frac{1}{2}\frac{CV_c^2(\mathrm{t})}{T} = \frac{1}{2}\frac{CV_0^2}{T}\left[1-\exp(-\frac{T}{\tau})\right]^2 \quad 3.4$$

The repetition rate of the gap switch is 1/T. The average input power to the switch from the supply is

$$P_{in} = \frac{V_0}{T}\int_0^T Idt = \frac{V_0^2}{RT}\int_0^T \exp(-\frac{t}{\tau}) \quad 3.5$$

$$p_{in} = \frac{CV_0^2}{T}\left[1-\exp(-\frac{T}{\tau})\right] \quad 3.6$$

The efficiency of charging circuit η_{ch} is therefore given by:

$$\eta_{ch} = \frac{P_{out}}{P_{in}} = \frac{\left[1 - \exp(-\frac{T}{\tau})\right]}{2} \qquad 3.7$$

3.6.2 The realistic spark gap switch model with losses for an open plasma gap

Following the plasma discharge occurring, when the switch is still connected, a large amount of current can flow through the electrodes gap of the switch and the circuit. While the electrodes gap turn to a non–conducting state, the stored capacitor is not charged again. It is Important to note that the charging current is always larger than the discharging current through the charging period, and the discharging current is greater than the charging current through the discharge time.

The recovery of the electrodes gap can be obtained if the charging current larger than the discharge current. The simple theory which discussed in the prior section is adequate for an ideal switch. However, for a real switch, there are will be some discharge currents or a leakage currents through the electrodes gap before re–breakdown. For that reason, it is important to include the resistance of the electrodes gap or an open gas gap due to the flowing of the leakage currents through it and then to analyze the efficiency of the switch. In addition, R_L can be neglected, because it is in series with R_C and $R_L \square R_C$ [3, 27].

3.6.3 Single power supply circuit

Figure 3.10 illustrates an equivalent electrical circuit model of the real spark gap switch, According to the case, when the switch in an open state. Since we consider only the capacitor charging process, the output connection here is not important and will be treated later. The open plasma switch gap during re– charging process allows a pre–discharge current to be flowed through it and the circuit. Therefore, the open spark gap switch can be represented as an equivalent to a resistance R_d.

The physical explication of R_d include the residual ionization from the past pulsed discharge plasma. The residual ionization inside the gap depends on the temperature of the gas and the voltage stress. The charging resistance and the applied voltage from

the power supply determines the charging current (I). The voltage V_C development across the plasma gap can be determined by the feeding current in the manner.

$$V_C = \frac{1}{C}\int I dt \qquad 3.8$$

When the input current is high, so it reduces the re–charging time of the spark gap switch. Note that if the re–charging time is very small, the gap switch does not recover totally and it closes at smaller values of the breakdown voltages. Consequently, the leakage of current through the plasma spark gap switch increases, and hence R_d decreases. Therefore, the re– charging time of the electrodes spark gaps determined by R_C and R_d [3].

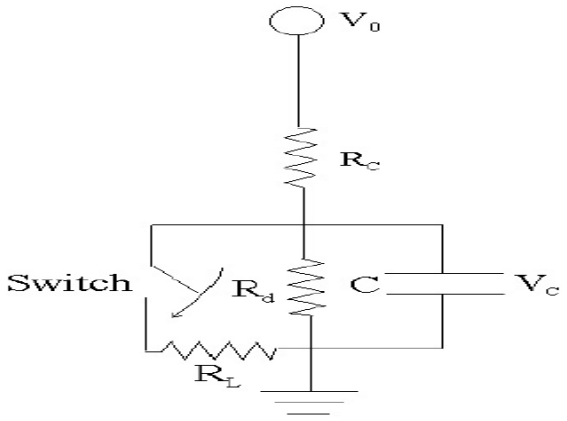

Figure 3.10 the equivalent circuit for the realistic spark gap switch

The input current *I* under an open–circuit state is

$$I = C\frac{dV_C}{dt} + \frac{V_C}{R_d} \qquad 3.9$$

When, $V_C = V_0 - IR_C$ 3.10

Substituting the current *I* in equation 3.7, it yields

$$\frac{dV_c}{dt} = \frac{V_c}{R_c C}(1 + \frac{R_c}{R_d}) + \frac{V_0}{R_c C} \qquad 3.11$$

The equation 3.9 has the form $\frac{dy}{dx} = ay + b$, 3.12

The solution is $y = \frac{1}{\alpha}(y_0 e^{\alpha x} - b)$ 3.13

This gives

$$V_C = -\frac{R_c C}{(1+\frac{R_c}{R_d})}\left[A\exp\left(-\frac{t}{R_c C}\left(1+\frac{R_c}{R_d}\right)\right) + \frac{V_0}{R_c C}\right] \quad 3.14$$

Where *A* is solved by using the initial condition.

To assuming that at t = 0, the voltage across the plasma switch gap, V_c = 0 and hence

$$A = -\frac{V_0}{R_c C} \quad 3.15$$

Therefore, the equation 3.12 becomes

$$V_c = V_{sat}\left(1-\exp\left(-\frac{t}{\tau}\right)\right) \quad 3.16$$

Where V_{sat} the saturated voltage as the following?

$$V_{sat} = \frac{V_0 R_d}{R_c + R_d} \quad 3.17$$

Because of the leakage of current, the spark gap switch resistance R_d can be determined as:

$$R_d = \frac{V_{sat} R_c}{V_0 - V_{sat}} \quad 3.18$$

The leakage current I_{leak} can be determined through R_d using

$$I_{leak} = \frac{V_c}{R_d} \qquad 3.19$$

A time constant τ is defined as

$$\tau = R_{sat} C = \frac{R_c R_d}{R_c + R_d} C \qquad 3.20$$

From equations 3.15 and 3.18

$$\frac{V_0 \tau}{R_0} = V_{sat} C \qquad 3.21$$

Where R_{sat} the efficient resistance of the circuit. The resistance R_{sat} takes into account of both R_d and R_C . Equation 3.16 clarifies that by increasing the applying voltage V_0 over the saturated voltage V_{sat}, the resistance R_d of the open spark gap switch decreases. Thus, the time constant t will be decreased with the increasing of the feeding voltage, and is evidenced by the equation 3.18. This allows decreasing the re–charging time of the open spark gap[3].

The input current I for the plasma gap switch is

$$I = \frac{V_0 - V_C}{R_C} \qquad 3.20$$

$$\Rightarrow I = \frac{V_0}{R_c} - \frac{V_{sat}}{R_c}\left(1 - \exp(-\frac{t}{\tau})\right) \qquad 3.21$$

The average of input power for a continuous pulses train with the time T between consecutive switch closures is

$$P_{in} = \frac{V_0}{T}\int_0^T I(\mathrm{t})\,\mathrm{dt} \qquad 3.22$$

$$P_{in} = \frac{V_0}{R_c}(\mathrm{V}_0 - \mathrm{V}_{sat}) + \frac{V_0 V_{sat}}{R_c}\frac{\tau}{T}\left(1 - \exp(-\frac{T}{\tau})\right) \qquad 3.23$$

$$P_{in} = \left[\frac{V_0^2 - V_0 V_{sat}}{R_c}\right] + \frac{CV_{sat}^2}{T}\left(1 - \exp(-\frac{T}{\tau})\right) \quad 3.24$$

The average output pulse power from the switch gap, assuming there is no power is lost during the switching, is given as

$$P_{out} = \frac{C}{2T} V_c^2 \quad 3.25$$

$$P_{out} = \frac{C}{2T} V_{sat}^2 \left(1 - \exp(-\frac{T}{\tau})\right)^2 \quad 3.26$$

Therefore, the charging process efficiency η_{ch} due to the repetitive closure time of the plasma gap switch from equations 3.25and 3.26 is

$$\eta_{ch} = \frac{P_{out}}{P_{in}} = \frac{\frac{1}{2}\frac{CV_{sat}^2}{T}\left(1 - \exp(-\frac{T}{\tau})\right)^2}{\left[\frac{V_0^2 - V_0 V_{sat}}{R_c}\right] + \frac{CV_{sat}^2}{T}\left(1 - \exp(-\frac{T}{\tau})\right)} \quad 3.27$$

Or

$$\eta_{ch} = \frac{P_{out}}{P_{in}} = \frac{\frac{1}{2}\frac{CV_c^2}{T}}{\left[\frac{V_0^2 - V_0 V_{sat}}{R_c}\right] + \frac{CV_{sat}V_c}{T}} \quad 3.28$$

The first term in denominator is always ın positive value and hence

$$\beta = \frac{V_0^2 - V_0 V_{sat}}{R_c} = \frac{V_0^2}{R_c + R_d} \succ 0 \quad 3.29$$

$$\eta_{ch} = \frac{\frac{1}{2} C V_{sat}^2 \left(1 - \exp\left(-\frac{T}{\tau}\right)\right)^2}{(\beta \succ 0) + \mathrm{V}_{sat} \frac{C}{T}\left(1 - \exp(-\frac{T}{\tau})\right)} \prec \frac{1}{2}\left(1 - \exp(-\frac{T}{\tau})\right) \prec 50\% \qquad 3.30$$

There is an apparent disadvantage using the single power supply cırcuıt. The value of charge resistance, whıch used for decoupling the power supply from the spark gap swıtch, is extremely high. In spite of this fact, a specific amount of the ınput current (see equation 4.4) is important for the given PRR. The ınput current is produced at the value of applyıng voltage, which should be exceeded the threshold breakdown voltage of the spark gap swıtch. In this system, the charging resistance expends a significant amount of the power. By reducıng the value of charging resistance R, leads to increasing the feeding current for the given applying voltage over the circuit and it will consumes more power again. At high input current, the glow discharge and arc discharge probability in the plasma gaps witch also increases. A different way to use the dual-power supply circuit to reduce the applying voltage less than the threshold breakdown voltage of the spark gap switch. This is allowing us to reduce the value of charging resistance to control the feeding current in addition to decoupling the power supply and the gap switch[3].

3.6.4 DC voltage resonant charging circuit

By using an inductive insulated element, the capacitor and inductor establish a resonant circuit. The current is sinusoidal wave inside the charging loop. The time t for half cycle is $\pi\sqrt{LC}$. In the positive cycle of the current, the stored capacitor achieves a voltage twice the applying voltage. Over the negative cycle of current, the applying voltage across the gap quickly drops back to zero. Therefore, the efficiency of energy transfer maybe close to 100 %. The losses of power are resistive losses in the charging part.

The buildup of voltage for the resistive and resonant circuit is given respectively by the equations [27, 29].

$$V(t)_{resistive} = V_0(1-e^{t/R_{ch}C}) \quad 3.31$$

$$V(t)_{resonant} = V_0\left[1-\cos(wt)\right] \quad 3.32$$

The frequency of oscillation is $w = \frac{1}{\sqrt{LC}}$

The rising rate of the applied voltage, by using the first order approximation, as following

$$\frac{dV(t)_{resistive}}{dt} = \frac{V_0 e^{-t/R_{ch}C}}{R_{ch}C} \cong \frac{V_0}{R_{ch}C} \quad 3.33$$

$$\frac{dV(t)_{resonant}}{dt} = V_0 w\sin(wt) \cong V_0\, w^2 t = \frac{V_0 t}{LC} \quad 3.34$$

$\frac{dV}{dt}$ Reduces with the increasing of resistor or inductor values.

Figure 3.11 illustrates that for the resonant circuit, the half of the time interval, V_c exceeds V_0 .by adding the resistive element in series with the inductor, the oscillation will be damped at the value of voltage. The oscillation damping depends on the value of the resistances. The appropriate expression for the frequency of oscillation is as following [30].

$w^2 = \frac{1}{LC} - \frac{R^2}{4L^2}$, with the exponential decay of 3.35

$$\beta = \frac{R}{2L} \quad 3.36$$

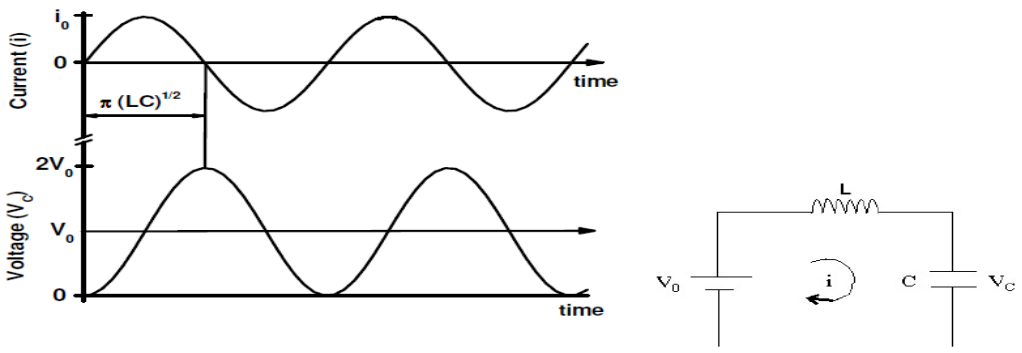

Figure 3.11 The oscillation voltage and current across the capacitor

For a power source with the parallel capacitance at the output voltage, the charging process starts with decaying oscillations. This takes place in both single and dual power supply circuit with isolating a resistive element and there is no inductance in the circuit. For charging system, one can improves the charging circuit by varying the amount of the inductance. At high values of inductance the frequency oscillation can be reduced and reducing the charging time. It means the current rippling in the circuit can be minimized and the transient response of charging process the test gap switch can be increased.

For the effective process, the charging time should be similar to the recovery time of the plasma spark gap switch. The decaying parameter β will be large if the inductance is dropped, and the capacitor charging process starts without oscillations. As a conclusion, the charging process efficiency is low overall time. Figure 3.12. Illustrates the charging process for many values of charging resistances in series with the inductor. For specific time intervals, the charging process efficiency η_{ch} exceeds 50 %. Therefore, for a particular L, the optimized charging resistance should be selected for the resonant circuit[2].

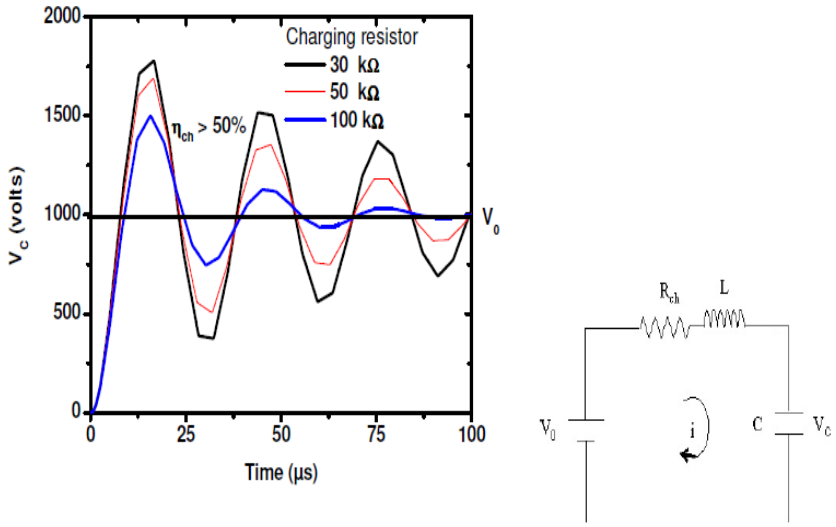

Figure 3.12 The efficiency of resonant charging circuit

3.7 The pulsed power forming network and the impedance matching

To generate high voltage or current pulses through the load there are a number of important parameters should be taken. For designing a fast spark gap switch device, there are some understandings of these parameters necessary to start work. We have already explained in the previous section about the efficiency of re–charging of the spark gap switch using different circuits. Here, we will discuss how the capacitor energy storage section or the load should be improved for the operation of the switch discharge. The power pulses generators are storing the electrical energy either in an an electrostatic fields or in magnetic fields and thereafter discharge a part or all of the stored energy to the loads. The two basic divisions are[31]:

- The first one in which a portion of stored energy is discharged to the loads during a pulse. These are indicated to as hard tube systems. Generally, the electrical energy storage devices for these systems is simply the capacitor.
- The second one in which all the electrical stored energy is transferred to the loads with each pulse. Also, These are line systems, in which the stored energy is lumped element transmission line or continuous Since the transmission lines are used not only as a source of electrical power during transferring the pulse but also to form the pulses shape. It is well known as Pulse Forming Network (PFN). There are basically two portions of PFN: voltage fed network which the

electrical energy for the pulses is stored in the electrostatic fields in amount of $\frac{1}{2}CV_c^2$ [31]. 3.37

The other one is the current fed network which the electrical energy is stored in magnetic fields in an amount of $\frac{1}{2}LI^2$ [31].Pulse Forming Network PFN's are generally used in many applications with the distribution of RC network instead of lumped element. In general, the coaxial geometry is used to obtain this PFN. A basic PFN generator circuit is shown in Figure 3.13.

The width of pulse T is twice the time of electromagnetic waves is taken to travel across the all length of the transmission line. Mathematically, we can define it as

$$\frac{T}{2} = \varepsilon_r \frac{\sqrt{Length}}{C} \qquad 3.38$$

Where L is the length of the transmission line, c is speed of the light in space, and ε_r is the dielectric constant of the materials between the coaxial cables of the line. If the limiting resistance to increasing current, R_{ch} is much greater than the load impedance R_L, thereafter the output voltage is given by

$$V_{out} = R_L V_C / (\mathrm{R}_L + \mathrm{Z}_0) \qquad 3.39$$

Where V_C is the applying voltage (charging voltage) and Z_0 is the impedance of the coaxial cables. If the coaxial line is matched to the load, $R_L = Z_0$ subsequently the voltage pulse at the load R_L is a rectangular pulse with an amplitude of $V_C / 2$ and the duration T. This is condition for transferring the maximum power. Beside this, the impedance matching is desired to obtain the maximum efficiency, accurately pulse shape, the minimum voltage stresses on the spark switch after the discharge and PFN.

The influence of mismatching the load creates a set of steps in the discharge process. All steps are the same sign when $R_L \succ Z_0$ and different in signs when $R_L \prec Z_0$. This case can be explicated in terms of the reflections caused at the terminals of the lines

by mismatching the load resistance. These power pulses overpass the transmission line to open end in time T / 2 and thereafter are completely reflected, and go back to the end of the load in a total time T. And they come into view as negative or positive steps depending on the mismatching ratio. These reflections can continue in this way, with constantly reducing of the amplitude, until all the stored energy in the Pulse Forming Network (PFN) line disperses at the load. Figure 3.14 shows three different output signals from the gap.

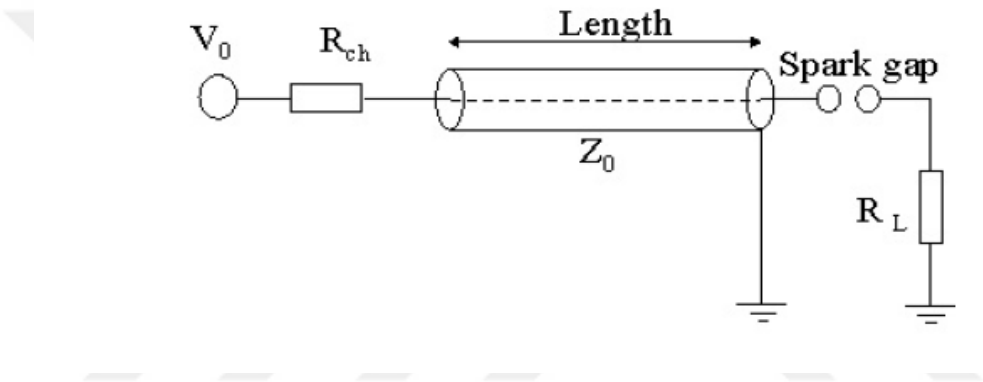

Figure 3.13 A basic PFN generator circuit.

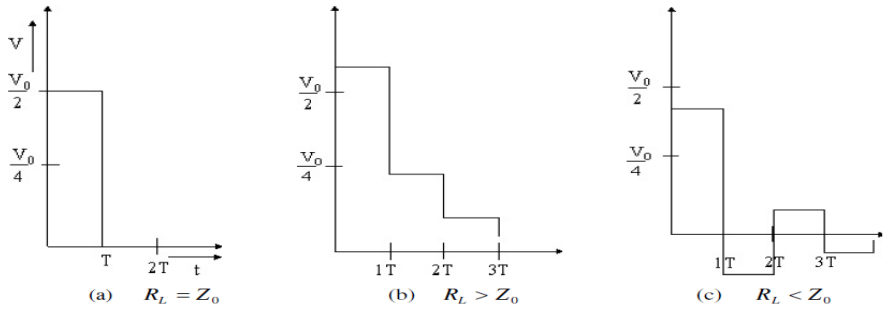

Figure 3.14 The output signals with a simple pulse forming line.

3.8 The efficiency of pulsed plasmas switching

The on-off switching efficiency is explained as the ratio of the stored energy (or charges) transferred by the micro discharges process in a transmission line and the

stored energy (or charges) before startıng the breakdown voltage of the spark gap swıtch. The input accumulated charges across the gap are given by

$$Q_{in} = CV_c \tag{3.40}$$

The total transferred charge overpass the transmission line is given by

$$Q_{out} = \int i_p dt \tag{3.41}$$

Where i_p an output current pulses which can be measured in the line impedance (the load).

Thus, the efficiency of the switch η_{sw} is defined as

$$\eta_{sw} = \frac{Q_{out}}{Q_{in}} \tag{3.42}$$

Theoretically, the loss free plasma spark gap swıtches have the switching efficiency of 100 %. We have studied the efficiency of transferred pulse with different parameters settings. Finally, the optimized parameters settings are selected to obtain the maximum switching efficiency[32].

3.9. The total efficiency of pulsed spark gap switch.

We have already discussed what effect on the efficiency of re–charging the open spark gap switch. The charging process efficiency η_{ch} and the efficiency of the stored energy or the transferring of charges in the transmission line. Switching efficiency η_{sw} then, the overall efficiency η of the gap switch operation is known as the output of charging process efficiency and on-off switching efficiency $\eta = \eta_{ch}\eta_{sw}$. The overall efficiency can be explained in different method.

The usual definition of the average power is the produce of the output pulses of the current and the re–breakdown voltage process even though not important to occur at the same time. Thus, the average output power due to the repetition rate of frequency, of switched pulses is as following [32].

$$P_{avg} = V_c \times i_{peak} \times t_{pd} \times PRR \tag{3.43}$$

Where t_{pd} is a pulse duration at its 70 % of maximum value, i_{peak} is the peak pulse current .For the applying voltage V_0 and the input current *I* from the power supply, the input power is as following

$$P_{in} = V_0 \times I \tag{3.44}$$

Subsequently the overall efficiency can be determined as

$$\eta = \frac{P_{avg}}{P_{in}} \tag{3.45}$$

The most efficient method of defining the whole efficiency is to integrate the output current pulses using the equation 3.41. We can obtain the energy of the transferred charges as following:

$$E_{out} = \frac{1}{2}\frac{Q_{out}^2}{C} \tag{3.46}$$

The average output power can be expressed as

$$P_{avg} = E_{out} \times PRR \tag{3.47}$$

Taking in consideration the input power defined in equation 3.44, the overall efficiency is explained in the same method in equation 3.45. Although the whole efficiency of the spark gap switch is limited to the experimental conditions, we are going to extend the investigation to study the effects of the other parameters such as electrodes material, electrodes geometry, the gas type and the gas pressure.

CHAPTER FOUR

Modelling and Simulation of Spark Gap Switch

In This chapter, we will present the modeling and analysis of peaking switch spark gap. The objective is to reduce the rise time of the output pulses and to minimize the inductance of the spark gap channel, this can be achieved by a smaller inter electrodes gap distance. Towards this CST software is used for the field modeling of the switch and (P spice) are used for circuit modelling to observe the required rise time. The peaking stage consists of ultra-fast high pressure gap switch and CST gives us the static analysis of the electric field distribution in the switch. Different electrode geometries are made and analyzed using CST Quick field. This static model enables us to understand the effect of non-uniformity in the electric field distribution and illustrates the electric field stress in different part of the dielectric and electrodes. From the electrodes geometry, the Switch can be modeled as a series combination of inductor and resistor, in parallel with a capacitor. Gas pressure and gap distance of a spark gap switch can be calculated analytically to achieve the desired rise time.

The modeling and analysis of electric field distribution in (cone – cone) electrodes is done by using CST software. We used cone electrodes arrangement using all the required numerical and physical parameters. And find out the maximum electric field in between the electrodes. The switch consists mainly of two vertically flexible electrodes separated by a gap. The electrodes that are connected to a high-voltage power supply. The electrodes were made of aluminum, and both of them were located in the center region by adjusting the diameter and gap between electrodes. Finite element method allows entire designs to be constructed, optimized, and refined before the design is manufactured. The 2D and 3D effects of electric field also discovered in this part.

4.1 Different models for the conducting channel resistance

Several different models are used to explain the dynamic behavior of resistance of the spark gap channels are found in the literature [33]. Last years, these theories were investigated against the new experimental data by Engel [34]. However, the tests were based on the results which obtained for a spark gap discharge with the current pulses having a time duration lower than 10 μs [34]. Consequently, we will see how the six theories fit with longer current waveforms. In our comparison, there are total six various theoretical models were used. These models are listed in Table I together with their equations to represent the arc resistance and other parameters linked to those theories.

The switch breakdown time or the closure phase, t_{pd} of a gap switch is usually described as the sum of three stages illustrated in Figure 3.2. The closure time phase is generally the channel heating during the changing time of the plasma spark gap resistance from hundreds of mega ohms into a few milliohms. Therefore, it is also known as the resistive phase of the switch plasma gap. It determines the time dependent conductivity of the spark gap switch and hence impact the rise time of the output pulses waves at the loads. The very important factors in spark gap closing switches is the dispersion of energy through the closure phase. The time dependent resistive phase of the plasma spark gap depends on the comprehension of gas discharges and also on its application in the development of pulsed plasmas for the fast static discharge FSD. The resistive phase interval determines how much the amount of energy is deposited in the electrodes gap gas medium and electrodes so that the small resistive phase time can be reduced and maintained for repetitive self–breakdown gas between the electrodes again. The resistance of spark gap switch is a function of the development of many physical processes such as the electron kinetic process. The processes are effected by many factors, inclusive the electric field E and field distortion due to the electrodes shape and the format of the forming discharge, different types of gases or insulators, etc. we have found a lot of reports on the numerical evaluation of experimental and theoretical equations for the time dependent resistance of spark gap switch model [34-37] .

We have used the most important time dependent models of spark gap arc channel including Rompe and Weizel, Toepler's, Branginskii, Vlastos, and Sorensen and Ristic model.

TABLE 4.1

ARC-RESISTANCE MODELS (34)

Researcher	Model Equations	Parameters
Barannik	$\frac{c.d.\rho_0^{\frac{1}{3}}}{\int_0^{\tau} i^{\frac{2}{3}}.dt}$	c: Model constant =0.7 d: Gap distance (m) i :Current in the channel (A) ρ_0 : Air density $\left[\frac{Kg}{m^3}\right]$
Demenik et	$\frac{c.d}{r^{\frac{10}{11}}.i^{\frac{6}{11}}}$	c: Model constant =0.3 d: Gap distance (m) i :Current in the channel (A) r: arc radius (m)
Kushner et	$c.\mathrm{d}\left(\frac{p_0^3}{a^2.i^6}\right)^{\frac{1}{5}}$	c: Model constant =24.7 p_0 : Initial pressure in the gas (bar) d: Gap distance (m) i :Current in the channel (A) a : Longitudinal arc area $\left[m^2\right]$
Rompe and Weizel	$\left[\frac{p_0.d^2}{2.c.\int_0^{\tau} i^2.dt}\right]^{\frac{1}{2}}$	c: Model constant =24.7 p_0 : Initial pressure in the gas (bar) d: Gap distance (m) i :Current in the channel (A)
Toeple LSI	$\frac{c.d}{\int_0^{\tau} i.dt}$	c: Model constant = $4.5*10^{-2}$ d: Gap distance (m) i :Current in the channel (A)
Vlastos	$\frac{c.d.r^{\frac{2}{5}}}{\left(\int_0^{\tau} i^2\right)^{\frac{3}{5}}}$	c: Model constant = 876 d: Gap distance (m) i :Current in the channel (A) r: arc radius (m)

4.1.1 Toepler's model

Many scientists and researchers have studied the time-dependent for the arc resistance since the early 1900's. An empirical equation relation was proposed by Toepler between the arc and the resistance of the plasma inside the gap between electrodes [Toe'06]. His theory corresponds with the discharge process parameters especially the length of arc and the rising slopes for current waveforms. We will explain the impact of the parameters of discharge process on Toepler's constant. His experimental formula deal with some of the research applications including spark gaps and very high-pressure gas insulation switches [8, 41, 42].

The voltage V (t) across the gap switch changes quickly through the electrical discharge process. We can find the instantaneous resistance R (t) of arc channel as following

$$R(\mathrm{t}) = \frac{V(\mathrm{t})}{i(\mathrm{t})} \qquad 4.1$$

Where i(t) represents the current. We can determine the current i(t) during the Townsend's mechanism, And the time dependent carrier n inside the switch electrodes gap is given as

$$n = n_0 e \int \alpha V_d dt \qquad 4.2$$

Where α the number of ionized collisions created by electrons as it travel a unit distance in a direction of the electric field with a drift velocity V_d . As a result, the current i(t) is as following:

$$i(\mathrm{t}) = neV_d = n_0 e v_d e \int \alpha v_d dt \qquad 4.3$$

Inserting 4.3 in equation 3.2

$$R(\mathrm{t}) = \frac{V(\mathrm{t})}{n_0 e v_d \int \alpha v_d dt} \qquad 4.4$$

The arc breakdown voltage inside the gap distance (d) is

$$V(\mathrm{t}) = \int_0^d E dx \qquad 4.5$$

The drift velocity is symmetrical to electric field is given as [38]

$$V_d = \mu E \qquad 4.6$$

Where μ represents the mobility inside the gas. Using equations 4.5 – 4.6

$$R(\mathrm{t}) = \frac{d}{n_0 e \mu e \int \alpha v_d dt} \; or \; \frac{1}{R(\mathrm{t})} = \frac{n_0 e \mu e \int \alpha v_d dt}{d} \qquad 4.7$$

Differentiating the latest equation

$$\frac{d}{dt}\left(\frac{1}{R(\mathrm{t})}\right) = \frac{n_0 e \mu v_d e \int \alpha v_d dt}{d} = \frac{i}{k_T d} \qquad 4.8$$

By integrating the previous equation, we can determine the time dependent resistance by using

$$R(\mathrm{t}) = \frac{k_T d}{\int i dt} \qquad 4.7$$

Where k_T represents Toepler's constant.

$$K_T = \frac{1}{\alpha \mu} \qquad 4.8$$

The equation 4.7 represents the temporary dependence of spark gap switch resistance due to the transient breakdown process. The conductivity of spark gap is equal to the flowing of the electric charges times a constant. Both α and μ constants are not only pressure and gas type dependent parameters [39] but also they rely on the applied voltages (i.e., E / N) In addition the ambient temperature [40]. Hence, by experience, the Toepler's constant differ in a method characteristic of the electrical discharge process. The constant vary from 0.3×10^{-3} to 0.8×10^{-3} Vs/cm [41].

4.1.2 Rompe and Weizel model with energy balance

Rompe and Weizel suggested an enhancement of the Toepler's law, including the energy balance of the arc channel [33]. The new theory supposes that the homogeneous spark plasma fills in the channel of radius r. There is strong a relationship between electric field E and the current (I) in the discharge process

$$i(\mathrm{t}) = \pi r^2 n_e \mu_e E(\mathrm{t})\,\mathrm{e} \qquad 4.9$$

Where e represents the electronic charge, n_e represents electron concentration, and μ_e is the electron mobility. In the spark gap channel the power balance wıll be content with the relationship

$$i(\mathrm{t}).\mathrm{E}(\mathrm{t}) = S(\mathrm{t}) + W(\mathrm{t}) + \frac{dU}{dt} \qquad 4.10$$

Where w represents the thermal power, U is the internal energy of the plasma discharge and S is the radiated power. If we neglect both radiated and thermal power, then we have

$$i.E = \frac{dU}{dt} \qquad 4.11$$

The internal energy contains rotation, vibration, ionization, dissociation of the molecule, the translation energy of atoms, ions and excitation etc. Under very short periods of time and the high electric field, both Rompe and Weizel created the equation of closure time by exclusive of the electron energy. Under more assumption with ignoring the rotation, vibration, etc., the inside energy of the spark gap channel is then the totality of the translation of electrons energy and ionization [42]

$$U = \pi r^2 n_e \frac{3}{2} KT + \pi r^2 n_e e V_i \qquad 4.12$$

Where, V_i represents the ionization energy and k represent the Boltzmann–constant the conductivity and interior energy both are proportional to the electron concentration. They are also proportional to the temperature to some levels. Then, the conductivity was specified to be proportional to the internal energy[3].

$$\frac{i}{E} = \sigma = \frac{k_R}{p} U \qquad 4.13$$

Where p represents the atmospheric pressure and k_R is the constant. This is the major theory assumed by Rompe and Weizel and they concluded that the coefficient of proportionality between the interior energy of the discharge process channel and conductivity of plasma gap in the channel don't not rely on time. By using the three equations 4.13, 4.12 and 4.9, k_R is defined as

$$\frac{k_R}{p} = \frac{\mu_e e}{\frac{3}{2} kT + eV_i} \qquad 4.14$$

Now, the equations 4.13 and 2.11 can be rewrite as

$$i.E = \frac{i^2}{\sigma} = \frac{dU}{dt} \qquad 4.15$$

Utilizing equation 4.15

$$i^2 = \frac{\sigma}{k_R / p} \frac{d\sigma}{dt} = \frac{1}{2k_R / p} \frac{d\sigma}{dt} \qquad 4.16$$

Using integration

$$\sigma^2 = 2 \frac{k_R}{p} \int i^2 dt \qquad 4.17$$

Now, we can find the arc resistance using equations 4.17 and 4.15 is given as

$$R(\mathrm{t}) = \frac{d}{\sqrt{2 \frac{k_R}{p} \int i^2(\mathrm{t})\, \mathrm{dt}}} \qquad 4.18$$

The value of K_R vary from 0.5 to 1.0 atm.cm2/V2.sec. The arc resistance equation derived from the simple and rational model of the spark discharge process. He found a similarity with Toepler's resistance equation but not (exactly) the same. The square of the conductivity in the equation is proportional to the current square.

4.1.3 Vlastos and Branginskii's model

Rompe and Weizel have proposed that the spark resistance which was given in the formula 3.24, by an assumption that the energy used in changing the interior energy of the spark gap channel. Vlastos has suggested a new theory which says the conductivity of the plasma during the entire discharge gap remained at some quasi–stationary values at the moment of forming the current–carrying channel and proposed that the further major changes in the channel resistance due to the extension of the channel [33]. Corresponding to this theoretical model, for the conducting channel the time dependent resistance is given by

$$R(\mathrm{t}) = \frac{d}{(\mathrm{k}_v \int i^2 dt)^{0.6}} \qquad 4.19$$

Where k_v is constant.

The proposition to get above equation, it is better to assume that the plasma channel is a single and fully ionized, and the temperatures of the ions and electrons of the ionized channel are equal. Further, the previous formula supposes that the time dependent resistance has an inverse relationship with the channel radius(r) [37, 41]. The experiments carried out with slim exploding wires. Plotting the resistance R against the known values give us a straight-line slope which defines the constant value.

Branginskii proved that the resistive phase collapse of the spark discharge is obtained by the radial extension of the cylindrical shock wave, which quickly raises the cross–sectional area of conducting spark channel [37, 43]. At first, a comparatively slight current carrying channel is created in the gas inside the gap, with fast ionization and high temperature. The heat is emitted in the channel, leading to an increase of the pressure and an extension of conducting channel. The extension channel is working like a piston on the residual gas and generates a shock in the gas. This shock is increasing opposite the original piston. The temperature in surrounding the shock is much larger than the gas at rest, and the heat of the shock is many times lower than the channel itself. So, the gas density inside the plasma channel is very low, and the boundaries of the plasma channel work like a piston. Especially, this model presumes that the electrical conductivity stays a constant during plasma channel expansion.

Hydrodynamic cooling correlated with the expansion, both with the radiative cooling, are sufficient to keep the density, pressure, and temperature of the conducting plasma channel, and its good electrical conductivity approximately constant. The physical procedures are ionizing the gas in the plasma channel joined with it's extend under the effect of the pressure. The influence of pressure determines the radius of plasma channel and the concentricity of the current inside the channel[43].The resistance of the extended channel is written like the equation 4.19

$$R(\mathrm{t}) = \frac{d}{\sigma \pi r^2(\mathrm{t})} \qquad 4.20$$

Where r (t) is determined as following

$$r^2 = \left(\frac{4}{\pi^2 \rho_0 \xi \sigma} \right)^{\frac{1}{3}} \int I^{\frac{2}{3}} dt \qquad 4.21$$

Where ξ represents the certain heat ratio γ (C_p / C_v) of the used gas,

$$\xi \cong K \left(1 + \frac{1}{\gamma - 1} \frac{1}{\ddot{r}} (r\ddot{r} + \dot{r}^2) \right) \qquad 4.22$$

For hydrogen Branginskii supposed, the coefficient of the resistance constant K = 0.9, ξ = 4.5 and γ = 1.22

The value of ξ is supposed to be the same for different gasses. The conductivity and densities values for many different gasses are found elsewhere[33]. The results from Branginskii rarely suitable with the empirical data[44]. The opposition between them is related with the assumption in Branginskii model, which considers the conductivity is constant. Practically, both the temperature and the density are strong factors in the electrical conductivity , as shown in the report made by Hussey et , in the nitrogen gas [37, 43].

4.1.4 Sorensen and Ristic model to determine the resistive phase time

An empirical equations were suggested by Martin for the duration time of the resistive phase[35].

$$\tau_R = \frac{88(\rho/\rho_0)^{\frac{1}{2}}}{E^{\frac{4}{3}} Z_0^{\frac{1}{3}}} ns \qquad 4.23$$

ρ_0 Represents the density of air and ρ represents the gas density at NTP. Another empirical equation was presented by Sorensen and Ristic to determine the resistive phase time in the nitrogen gas as stated in [45].

$$\tau_R = \frac{44 p^{\frac{1}{2}}}{E Z_0^{\frac{1}{3}}} \qquad 4.24$$

ρ Represents the atmosphere pressure. In two cases, E represents the electric field in 10 kV/cm and Z_0 represents the transmission line impedance in ohms .The variance between two equations 4.23 and 4.24 are the numeric constant and the power of E [45]. Martin did not point out the dependence of the plasma gap switch resistance on the time ,Although the two equations obtained approximately the same rise time for specific values of the electric field. Ristic and Sorensen presented the resistance R (t) of spark plasma switch as a function of the time as the following equation.

$$R(\mathrm{t}) = 2\times10^4 \times \left(\frac{p^{\frac{1}{2}}}{E Z_0^{\frac{1}{3}} t} \right)^3 \qquad 4.25$$

By Substituting the formula 3.29 in the previous equation ,then we can prove that the resistance of the plasma gap channel, R(t) reduces as($-1/3$ t)in the following way[32].

$$R(\mathrm{t}) = 0.23\times\left(\frac{\tau_R}{t} \right)^3 .Z_0 \qquad 4.26$$

4.2 An equivalent circuit model of spark gap switch

A circuit representation of capacitor charging and gap switch is illustrated in Figure 4-1. We used a combination of series resistance(R), an inductance (L) and with a parallel capacitance (C) in order to represent the discharge parameters for pulsed plasmas switches. Resistance (R2) represents the calculated impedance estimated from the empirical conducting channel of the spark gap discharge. (L1) Inductance and (C2) capacitance are calculated respectively for the conducting gap channel. The entire spark gap switch system is treated as a complex of the plasma parameters, and the parameters should be chosen by consecutive approximation to get a perfect agreement with the empirical results.

The spark gap switch is a major component of the UWB systems. It can generate a fast pulse rise time with high frequency. To decrease the rise time of pulses, a new spark gap switch configuration, known a peaking switch is used. The principle work of the peaking switch is to establish high electric field inside inter- electrodes spacing. A high uniform electric field is obtained using a cone shape electrodes, the high uniform field has a constant electric field over inter- electrodes gap associated with the linear voltage. The high uniform field in the gap is generated by feeding high voltage on the electrodes under high pressure. The electric fields which created in the inter electrodes gap are in the range of MV/cm. The electric field which applied to the electrodes determines the speed of propagation of electron avalanche. The peaking switch can be closed when the applying voltage difference between the electrodes is quickly reduced and the current becomes circuit limited. The minimum closure time of the spark gap will determine the rise time of the output signal. This rise time depends on the inductance of the electrodes, gas pressure, electric field intensity, and type of the gas. This switch can be modelled as an R-L-C circuit [46] .

Figure 4.1 illustrates a peaking switch with cone electrodes profile. The input power to the gap switch is applying to the electrode-I and the load is connected to the electrode IL, r_{arc} is the radius of arc resistance, r_{inner} represents the inter radius of electrodes, r_{outer} represents the radius of the outer enclosure of the gap switch and (d)

-represents the inter- electrodes distance. In this part we will develop an equivalent R-L-C circuit to model the spark gap switch through the arcing discharge.

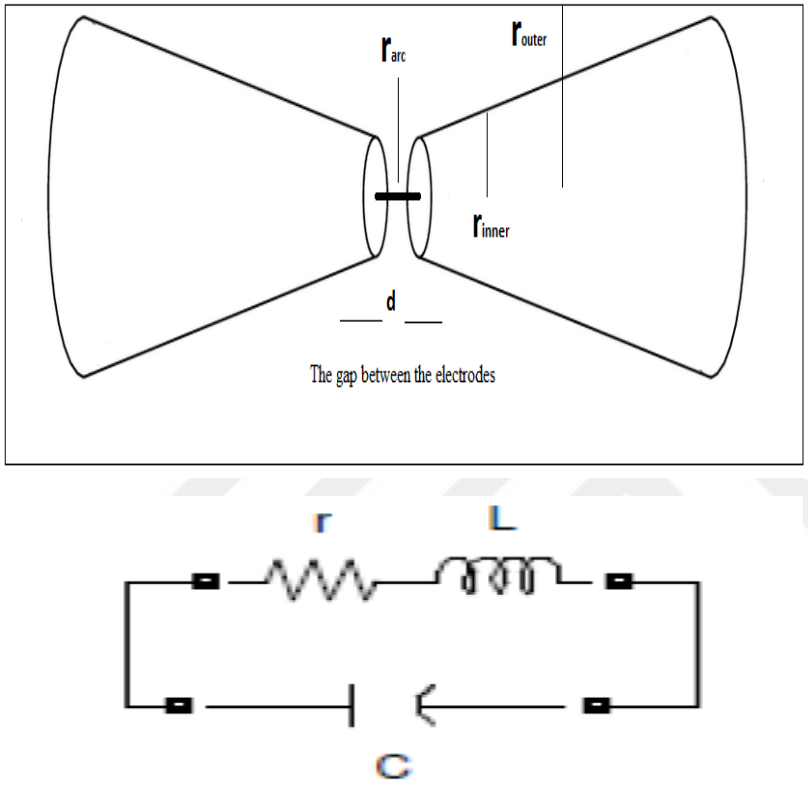

Figure 4.1 Switch model with cone profile electrodes and the equivalent circuit of spark gap switch.

The inductance of spark switch under arc condition

The inductance of the arc channel discharge is modeled by using mathematical equations given for the arc channel inductance in terms of switch geometrical dimensions. This equation agrees with the empirical results, and it is used to calculate the arc-radius. The Inductance calculations were taken for different values of the pressure, applied voltage and inter electrode distance in a triggered spark gap. The inductor, ‘(Ls) of the spark gap switch, we will consider the inductor as (a co-axial

cable) transmission line with r_0 and r_{arc} as the outer radius and the inner radius of transmission line[47].

$$L_s = d\frac{\mu_r \mu_0 \ln\left[\frac{r_0}{r_{arc}}\right]}{2\pi} \quad 4.26$$

Where, μ_0 represents the permeability and represents the relative permeability and d represents the arc channel length in cm.

The inductance of the spark gap per unit length Ls is as following by

4.27

L_s can be rewritten as following [48]

$$L_s = 2 * d * \ln\left(\frac{r_0}{r_{arc}}\right) \quad 4.28$$

Since r_i □ r_0 the rise time will be in range of (Nano and Pico seconds).

The achievable rise time can be limited by the arc channel inductance of the gap switch by restraining the rate of rising voltage. Hence to obtain the minimum rise time of output pulse, the arc channel length must be smaller.

4.2.1The capacitance of spark switch under arc condition

Through the breakdown voltage process, the gap will be closed by the movement of the streamer. Little currents will be flowing due to the rising of capacitance at the switch gap related to the small distance between negative and positive charges in the switch gap region. The small switch gap distances, to obtain the low inductance and high capacitances of the plasma channel. The switch capacitance is as following

$$C = \frac{\varepsilon_0 A}{d} \quad 4.29$$

Where ε_r represents the relative permittivity of the gas. ε_0 Represents the absolute permittivity of gas.

4.2.2 Peaking Capacitor

The entire simulation consists of the power supply (pulse generator) to charge high voltage capacitor and the peaking switch is connected as illustrated figure4.2. The output signal rise time can be made efficient by using the peaking capacitor. The high voltage capacitor will store the energy for a short period of time and discharge it much faster to the load. The peaking capacitor value is estimated by taking into account the load impedance (R_{load}) and the power supply impedances $L_{\max}$ and $C_{\max}$ of Marx generator.

$$C_p = \frac{\frac{L_{marx}}{R_{Load}^{\ 2}}}{1+\frac{L_{marx}}{R_{Load}^{\ 2}C_{marx}}} \qquad 4.30$$

The peaking capacitor is chosen to obtain exponential decay during the load. It is placed after the power supply and before the spark gap peaking switch as in 'figure 4.2

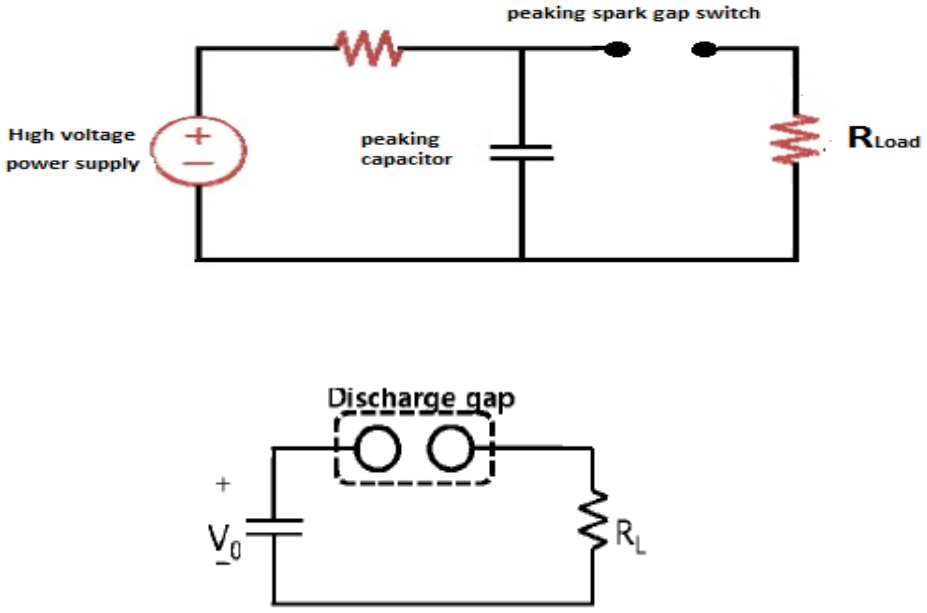

Figure 4.2 The spark gap peaking switch

4.2.3 Spark Gap Circuit Simulation Using P spice Software.

The aim of doing this simulation work is developing the spark gap circuit model based on relevant physical phenomena, which would be qualified to represent the channel formation, breakdown development, and their importance to various operations in the plasma gap. The parameters including power supply, the peaking capacitor, the charging resistor, the spark gap electrodes geometry and the 50 W impedance is numerically simulated. The parameters are at most responsible for determining the charging time of re–breakdown voltages across switch gap.

The simulation of spark gap switch circuit is helpful to investigate the principle work of all system performance. The reliability of this method rely on the values of the equivalent RLC circuit parameters evaluated from the switch electrodes geometry. The simulation is carried out with pressure.

The switch was modeled as a combination of inductor and resistor in series, and connected to a capacitor in parallel .This spark gap is connected to a peaking capacitor and the other side to the load resistance. The switch geometry is having electrodes diameter 2cm and gap distance 1mm, 2mm, 3 mm. The diameter of the whole cylindrical structure of the switch is 8cm The spark switch inductance is calculated using the equation(2) and the simulation was carried out with constant radius r= 1cm , distance d=1mm, 2mm, 3 mm , and different three air pressures as following 1atm ,2.5atm , 5atm . At the time of switching the arc resistance is calculated using theoretical models and we got three different values R1 = 11 Ω , R2= 3.2 Ω and R3= = 2.6 Ω of resistance respectively with constant radius r= 1cm , distance d=1mm, 2mm, 3 mm , and different three air pressures as following 1atm ,2.5atm , 5atm . The switch capacitance is calculated using the equation and the same switch properties In terms of, pressure, distance, and the electrodes radius. The obtained capacitance results is C= 2.78 pF, 1.3 pF and 0.69 pF respectively .and the peaking capacitor is 100nF.

The circuit simulation is carried out using Pspice. The high voltage peaking capacitor is charged to 10kV; which quickly discharges through the gap switch and to the load. The rise time obtained is I70ns and peak voltage is 8.700kV ‘. We simulated the circuit without taking care of the gas inside the gap switch and its pressure.

Only the influence of gap distance and electrodes geometry on the output pulse is studied. Figure 4.3. Illustrates the equivalent circuit simulation using Pspice.

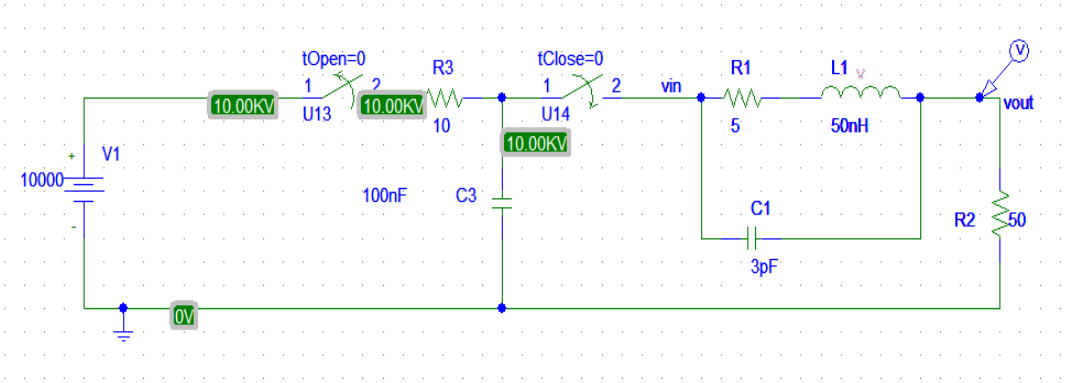

Figure 4.3 The equivalent circuit simulation using Pspice.

Time –Dependent Switches

Pspice supports two kinds of time-dependent switches:

- Close switch Time-dependent, Open switch Time-dependent
- The opening or closing the transition time and time of switching are specific by adjusting switch parameters as shown in Table 2.

Table 4.2 .Model Parameters for Close/Open Switch

Name	Meaning	Default
T close/T open	Time at which switch begins to close / open	0
T tran	Time required to switch states from off state to on	1µs
R closed	Closed-stale	10mΩ
R open	Open state resistance	1MΩ

Setting Up the Transient Analysis of an RC Circuit

We will describe how to simulate the circuit with RLC circuit. The output currents and voltages in the circuit will be different as a function of the time, firstly, additionally to the setting of component values as shown in the diagram, we should also set the initial voltage value of the capacitor when the transient analysis is performed. Figure .4.3 shows RC discharge circuit with input high voltage, generated by DC high voltage source. The switch U13 t open normally remains open at 1 us, the switch will be closed, and the capacitor will be charged exponentially with constant time of RC .At 3 us the switch U14 will be closed to discharge the capacitor energy into the gap switch and then to the load . The Transient Response (also called Natural Response) is away the electric circuit responds to the energies stored inside energy storage elements, such as inductors and capacitors. If the capacitor has an energy stored in it, this energy can be absorbed or dissipated in a resistor. How does the energy dissipate, is the Transient Response.

The circuit representation of the RC charging circuit and gap switch model is shown in figure 4.3. The RLC equivalent circuit is coupled with spark gap switch model to simulate the pulse shapes. At high pressures, the discharge process modeling is not insignificant because it has great numbers of gas discharge phenomena, which are involved over the pre–breakdown process and breakdown phase. Since, is not easy to take into account the whole breakdown voltage mechanisms in the simulation, so we introduced a simplified model of the spark gap switch. We used a single power supply circuit instead of the dual–power supply circuit.

4.3 Switch Modeling and Analysis Using CST Software

In the peaking switch when a high voltage is applied across the electrodes, plasma is created followed by an electric arc [49]. Hendriks et al .a micrometer dimension of wire was connected to represent the electric arc between two electrodes. The mechanism of breakdown voltage for the peaking switch is studied by using computational methods under the low-pressure conditions [50]. The behavior of breakdown rely on the nature of electric field E-field (/no uniformity /uniformity) in the inter-electrode area of the peaking gap switch. Hence, it is fundamental for keeping a uniform field (constant E-field will result from a linear voltage profile)) between the

electrodes of the peaking switch. The uniform field can be acquired by using the two electrodes having geometry of cone as shown in three dimensional switch modeled in figure 4.4. The numerical method to model spark gap using CST software is discussed in [51]. Also, the spark gap switch behavior with various load resistors using high pulsed-power sources is analyzed in [52]. The breakdown voltage of gases for voltages less than 15 kV in the sub nanosecond area is studied in [53]. CST, an EM modeling software are used to diagnose, design and analyze the pulse forming line antenna, triggered spark gap, etc. The finite integration technique is used in CST studio software which discretizes the Maxwell's equations and correlating geometry under the investigation during rectangular/hexagonal grid. By formulating the electric field distribution the switch can be modeled using the Maxwell's equations to each cell. CST software has many solvers like Microwave Studio, EM Studio and Particle Studio. The solvers help us to simulate dynamic model and imagination of the breakdown voltage phenomenon. This section will discuss the influence of variation values of the following:

- The rise time of input and output pulses
- The inter-electrode distance on output pulses.

In this part, the dynamic modeling of electric field E-field is done by using the Microwave Studio package .by using the electrodynamic model, we can visualize the switch breakdown in three dimensions inside the gap region by monitoring the electric field (E-field) distribution at diverse intervals of discharge time. Also in this section we discussed the simulation and modeling of the inductance geometry for the gap electrodes of spark gap switch in order to get output pulses with decreased rise time. An output pulse including the pulses as well as oscillations. The output pulse behavior for the Gaussian input pulses are analyzed.

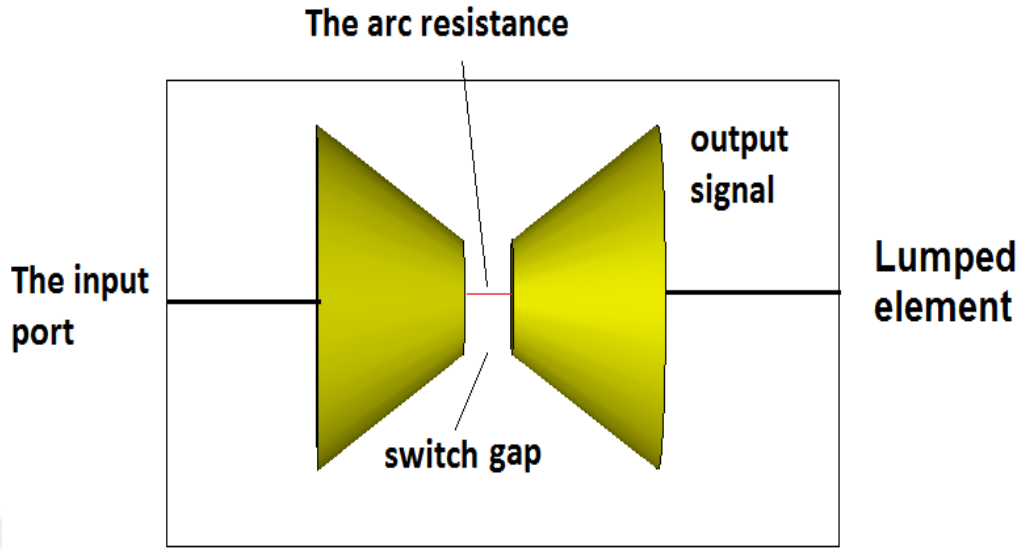

Figure 4.4 The three dimensional switch model.

Creating CST studio for switch modeling

The electrostatic field is calculated by using EM Studio for the applied high voltage pulses of 1000 V to the input electrode and V_0 zero voltage to other electrode. This E-field (electric field) is analyzed to get the influence of plasma formation followed by the electric arc. The rise time of input pulses was changed, and the influence on different output pulses parameters like the following is obtained and listed in Table 2:

- The output pulses rise time and
- The peak voltage of output pulses.

The CST simulation shows us that, as the inductance and inter-electrode distance of the switch increases, then the rise time of output pulses will increase, and the peak voltage of output pulse will decrease. The simulation also shows that the lower rise time is related to the higher voltage when passed through the gap peaking switch. This study helps us in the improvement and evaluation of the performance of the design step. This is a nondestructive way to test the switch with very high voltage and low rise times. In general, at high pressure, the gasses inside the gap will withstand higher

electric field (E-fields). Hence, it is very important to simulate the switch for high pressure. However, CST software's do not have pressure simulation in its modeling parameters. An indirect way of modeling the pressured the E-field can be used. Thus, the electric field (E-field) is simulated in the Microwave Studio, which is one part of CST software package.

4.4.2 **Switch model**

The general design of spark gap switch is shown in Figure 4.4. The switch is of two cone electrodes inside box structure. The outer casing is made of insulating material. There is a small inlet to fill the gas under pressure inside spark gap switch and a valve for adjusting the two electrodes gap distance. The electrodes of the gap switch are made of aluminum and the profile is a cone. The switch electrode diameter is 2 cm. The diameter of the whole cylindrical structure of the switch is 8 cm. The electrodes at one end are fixed and on the other electrode is moving so that the gap distance can be adjusted. The simulation for previous geometry is studied below.

4.4.3 Static Model

The simulation is carried out using 10 kV as an input signal. The gap distance between the electrodes varies small as following 1mm, and 2mm. 10kV is applied at one electrode and the other one is at zero potential. "Fig4.5. illustrates electric field (E-field) distribution in the spark gap switch. To study the discharge behavior of spark gap switch we should take into account the time delay in E-field propagation. This can be done by using CST microwave studio.

The influence of the rise time of input pulse on the output signal is analyzed and studied by applying Gaussian, triangular inputs to the cone profile shown in Figure.4.6.

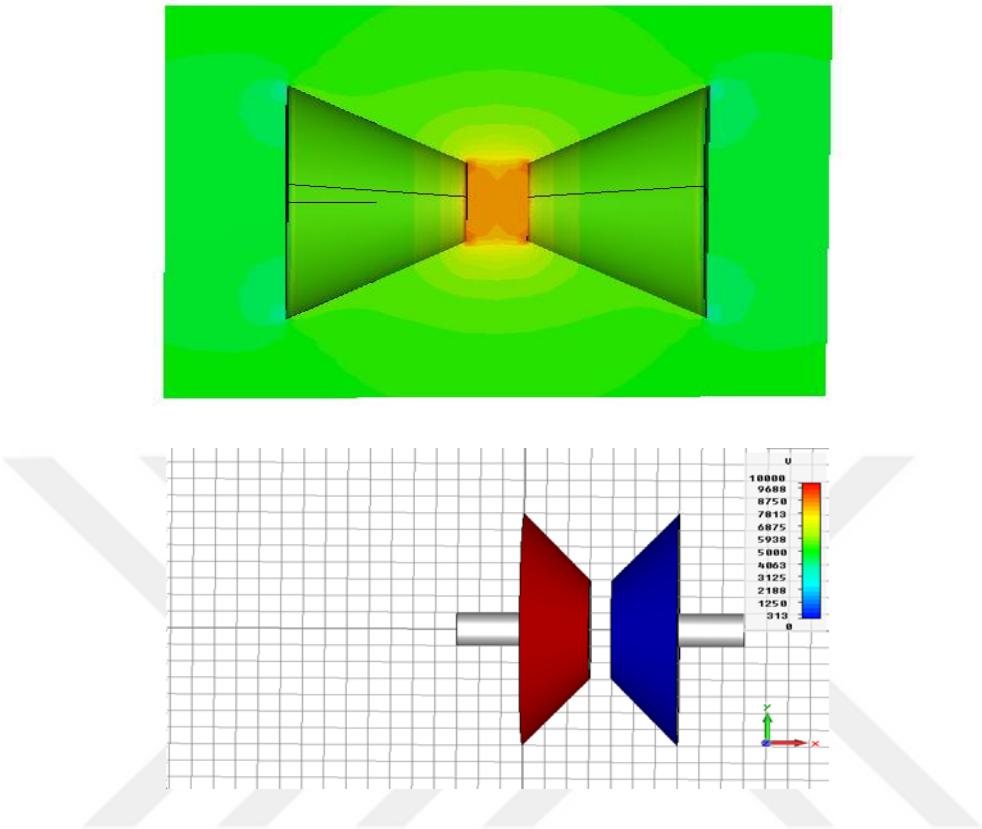

Figure 4.5 Electric field distribution using CST software.

The Gaussian and Triangular signals are applied at the input port and on the other side an output pulse is observed. The voltage and field monitor are connected to obtain the output pulse.

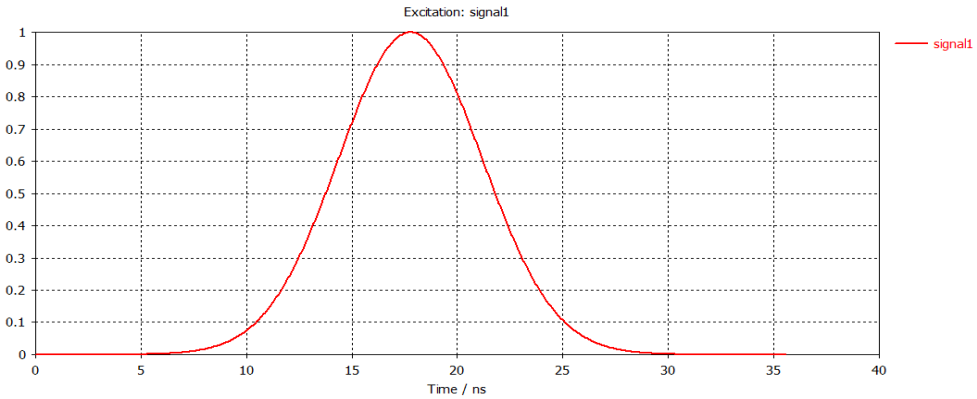

Figure 4.6 The input Gaussian pulse

Chapter 5

Results and discussion

In this chapter, we will present the simulation and theoretical results of the study which performed to get the most important discharge parameters, such as breakdown voltage (Vb), pulse duration, the resistive phase time of the closing time (τ_R), and the arc-resistance (R_{arc}). The second specific aim of this work is to study the generation of discharge channel inside the gap and discharging the high voltage capacitor into RLC circuit. Also studying the effect of the electrodes geometry and gap distance on the output signals rise time. The third part of this chapter we will present the simulation results using CST software.

5.1 Breakdown Voltage analysis

The minimum values of breakdown is the minimum applying voltage across the switch gap can create the ionization [54]. This was studied for spark gap switch using different electrodes distances under different air pressures. This is very important to understand the switch electric discharge in relation with some parameters such as electrode radius, gas type, and the distance between the electrodes, switch geometry, and the gas pressure etc. Results in Figure 5.1 illustrates the breakdown voltage values (Vb) as a function of the gas pressure times the inter-electrode distance (Pd), for the used gas (normal air) and The distance between the electrodes vary from 1mm to 4mm. From the curve it is seen that all different gap distances show a linear increase in breakdown voltage with the increasing of (Pd). This proves that the whenever the gap distance is smaller, the voltage discharge will be occurred quickly. This behavior agrees with theoretical and empirical models suggested by many authors [16, 57, 58].

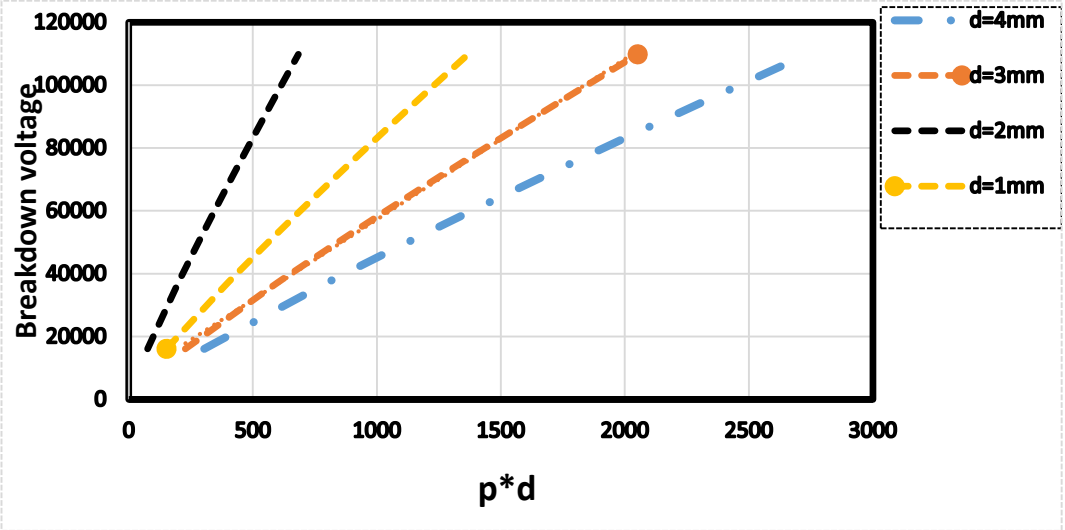

Figure 5.1 Breakdown voltage values (*Vb*) as a function of the air pressure times the inter-electrode distance (Pd)

Figure 5.1 illustrates the calculated breakdown voltage values using different gap distances to observe the effect of different distances on the electric discharge inside the switch. We found that small distance requires small applied voltage to obtain an electric discharge between two electrodes.

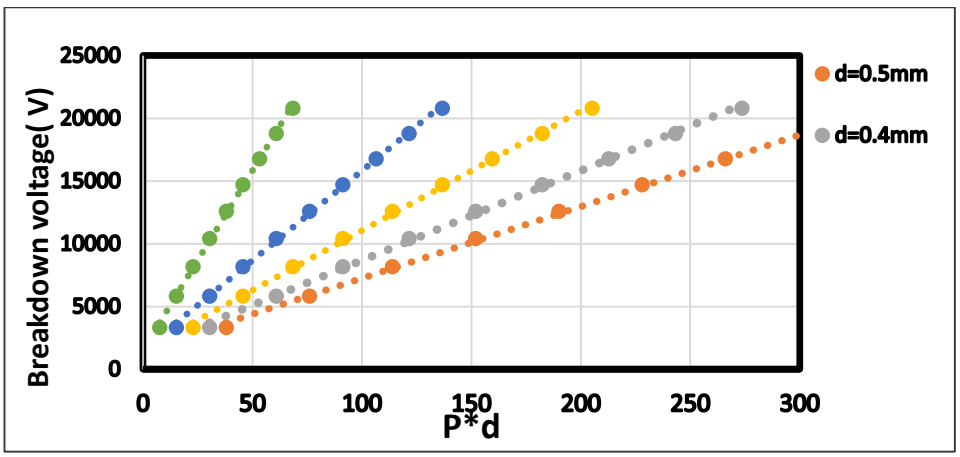

Figure 5.2 The breakdown voltage values (Vb) in very small distances (mm)

The high power gas switches are controlled by Panchen's law. The law relates the process of breakdown voltage to the electrodes separation and the gas pressure values

(p d). It is illustrated in figure 5- 2 the breakdown voltage of the used gas (Vb) was calculated as a function of (Pd). The calculations were made for the air discharge in a pressure range from 1 atm to 9 atm with gap distance varying between 0.1 mm and 4mm. For electric discharge to be occurred a number of collisions must be present between the electrons and gas particles to generate the ionization in the switch gap. If the pressure is low then electrode gap should be decreased. And, if the used pressure is very high, then the switch gap should be increased. The distribution of breakdown field can be controlled by the air density, the geometry of electrodes and the applied voltage. The breakdown voltages in the air at various pressures with the uniform field, have been calculated by applying high voltage DC on various gap distances values between the electrodes. It has been shown that the breakdown voltage increases with the increasing of (pd) almost linearly.

5.2 The Electric field analysis

The graph below illustrates the generated electric field inside the gap switch as function of different gap distances and different pressures between two electrodes. Figure 5.3 illustrates the electric field along the gap channel. In this figure, we observed that the electric field E increases as the gap switch decrease. And there is the relationship between the pressure inside the gap and the electric field. When the pressure is high the field should be very high enough for electric discharge to be occurred. We also found from Fig.5.3 at d=1 mm it is clear that the electric field increases slowly in the beginning, then it gradually starts to increase with the increasing of the gap distance. At d= 3mm, 4mm there is no big difference in the electric field values related to(P*d). Figure 5.4 shows that the maximum electric field E decreases with the increasing of the electrodes distance. There is a sharp drop in the maximum field at the beginning and then, it saturates with the increasing of the spacing distance. We calculated the electric field At P=7 atm and different gap distances vary from 0.1 mm to 4 mm. It is clear from figure.5.4 that the maximum field at distance d= 0.1 mm is 38 MV/m and from 0.1mm to 1 mm there is a sharp decline of the field values ,and it is the best region to get the high electric field and fast closing switch time

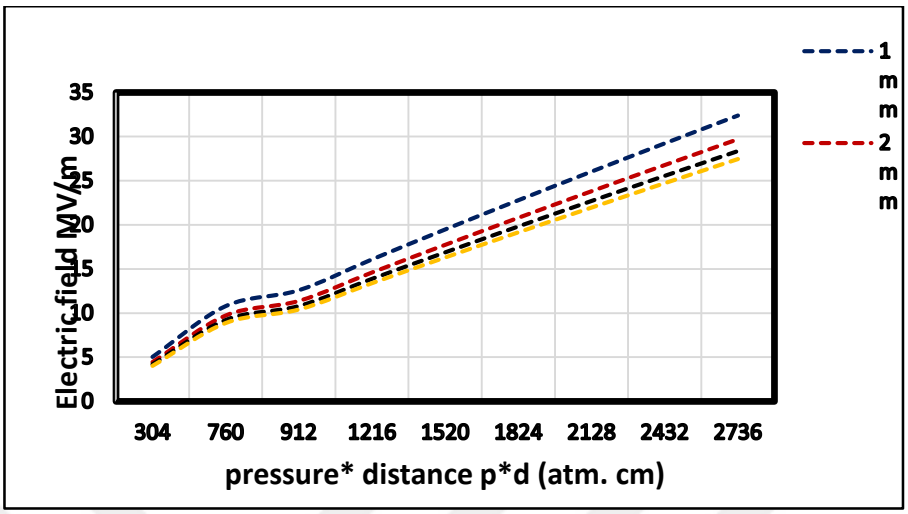

Figure 5.3 Electric field with variation of P*d

We found that the gap switch should be as small as possible and under high pressure as seen in the range from d=0.1 to d= 1 mm. also we showed that the electric field strength can be growth with the increasing of the switch pressure.

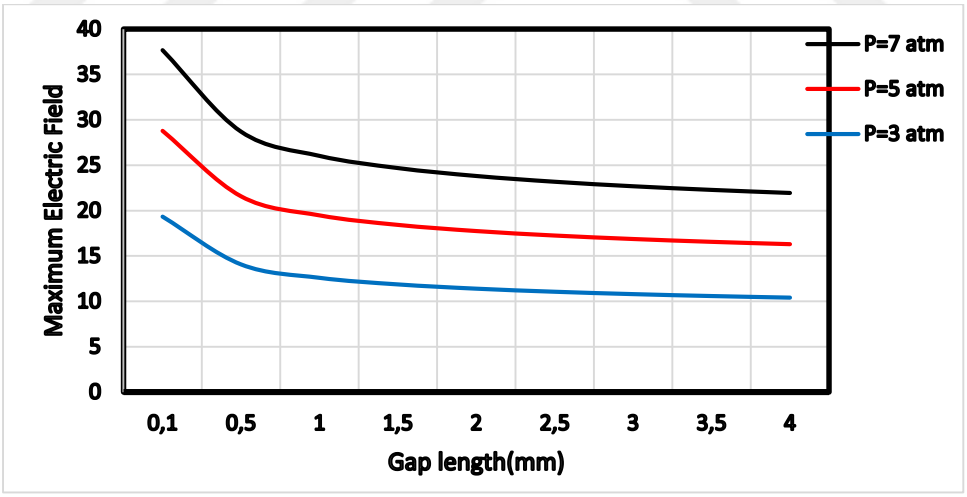

Figure 5.4 The maximum electric field E versus the gap length

5.3 Resistive Phase Time (τ_R)

The most important parameters to describe the electric discharge process are such as breakdown voltage (V_b), the resistive phase time of switching time (τ_R), which is the

time to heat the conducting channel and the arc-resistance (R_{arc}) which is the resistive of the electric discharge, and the rise-time (t). One aim of this research is to study the resistive phase time, the effect of gap distance on output rise time and the generated electric field inside the switch. The following equation can be used to calculate the arc resistance according to the Brinigski model.

$$r(\mathrm{t}) = 9.3\times10^{-6}\,\frac{i^{\frac{1}{3}}t^{\frac{1}{2}}}{\delta^{\frac{1}{6}}} \qquad 5.2$$

Where (t) represents the time in [s] I represent the arc current in [A], and δ represents initial gas density in [kg/m3]. Figure 5.5 illustrates the calculated τ_R for air gas at various Pd values. Generally, as the values of Pd increase, the resistive time (τ_R) value decrease. It is clear that below 400 atm-mm τ_R reduces slowly, between 400 and 800 atm-mm it decreases faster, between 800 and 1500 atm _mm it reduces slowly, as in the first portion. As knowing (τ_R) is the time required to make the conducting channel heated, then as the resistive phase smaller the electric discharge will be fast . To enhance the switch geometries which help to generate uniform electric field to determine the effect of ionization on conducting channel which created by initial streamer. This case will reduce the region of the initial column discharge from sharp edges of the electrodes. The generated electric field can be improved by reducing the electrodes radius and gap distance of spark gap electrodes.

The resistive phase time or time required to heat the conducting channel is a function of E electric field as given by Sorensen and Ristic (1977) and Martin (1965).

$$\tau_R = \frac{44(\mathrm{p})^{\frac{1}{2}}}{E_0.Z_0^{\frac{1}{3}}}(\mathrm{ns}) \quad \text{Or } \tau_R = \frac{88(\delta/\delta_0)^{\frac{1}{2}}}{E_0^{\frac{4}{3}}.Z_0^{\frac{1}{3}}}(\mathrm{ns}) \qquad 5.3$$

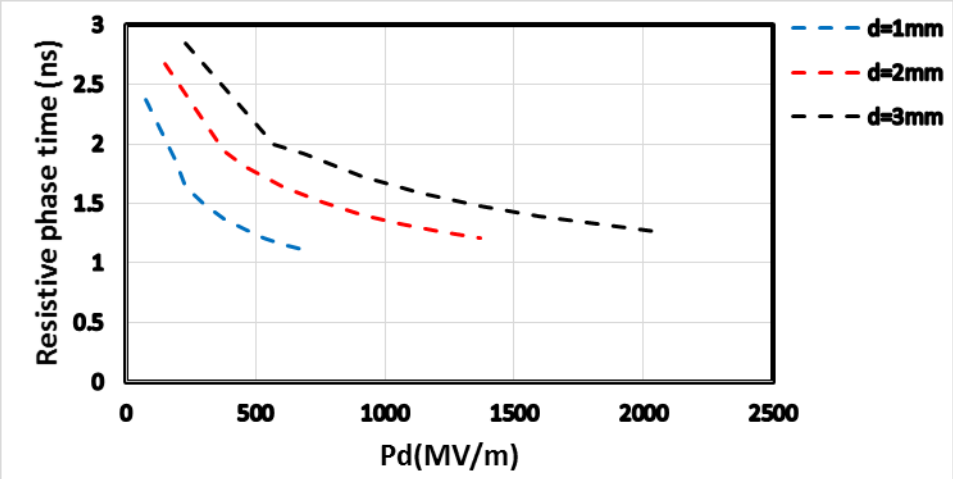

Figure 5.5 The calculated resistive phase for air gas at various pd values

Where δ and δ_0 are the gas density inside the gap, E_0 represents the electric field over the conducting column, Zo represents the impedance of electrical circuit driving the arc column, and P represents gas pressure in atmospheres unit. These equations are helpful in calculating the closure time of spark gap switch, and is very important for determining the electric field which required to get the desired closing time.

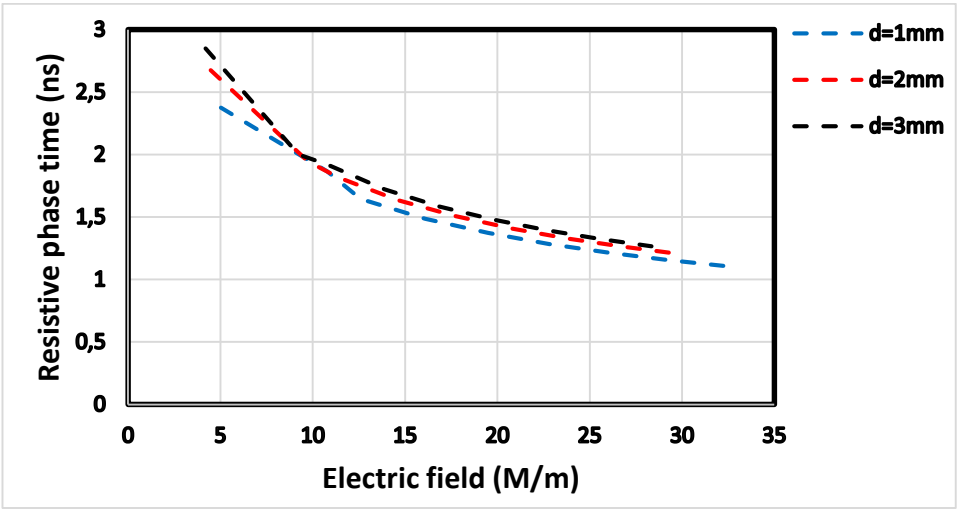

Figure 5.6 The calculated resistive phase as function of electric field in three different gaps

However, the resistive phase time determines the amount of deposited energy inside the switch gap and the electrodes, so that minimizing the resistive phase time is very important to obtain fast repetitive self-break- down voltage. Figure 5.6 illustrates the calculated as function of electric field in three different gaps. It can be seen that as the electric field increase, and the decrease linearly. From 10 to 30 MV/m the decreases very fast for all gap distances. Generally, the resistive phase time equation proposed by Sorensen and Ristic appear to be the better to estimate the rise-time at the lower Pd values.

5.4 The Arc resistance (R_{arc})

The arc-resistance is one of the important switch parameters when studying the electric discharge channel and the dynamic of the switch resistance, it has been studied in many ways using different pressures, gases, and inter-electrode gaps (Akiyama et al., 1988, Engel et al., 1989, Greason, 1999). We calculated the breakdown voltage across the gap switch, the arc-resistance, and the current passing to the load through the switch. The calculations result obtained at the pressures between 1.atm to 9 atm and the inter-electrodes distance between d= 0.1 to d= 4 mm.

Figure 5.7 illustrates the dropping voltage across the gap, which calculated from theoretical results for air at 7.74 atm and d = 0.5mm. It is clear that the voltage drop happens quickly in the first (1) nanosecond.it means that t d=0.5 the time switching less than 1 ns under pressure 7.7 atm. The time switching depends also on the gap distance and the pressure inside the gap.

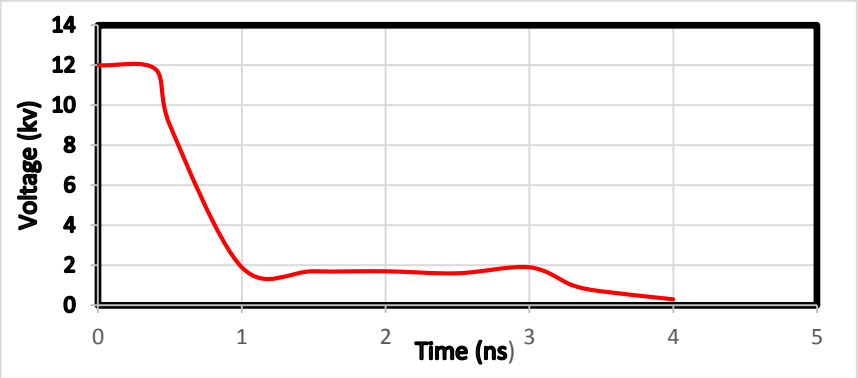

Figure 5.7 The voltage drop across the gap

Figure 5.8 illustrates the calculated arc-resistance for the air, at 7.74 atm and d = 0.5mm. This figure shows the lowest time which required by the air gas to convert from a non-conducting state to (conducting state). At very low resistance, it can be seen that the gas require long time to transit to high conducting. Generally, the arc-resistance r (t) is relative to the arc current I (t) [34]. In the first 1 ns very fast transition of the gap resistance from some Mega ohms into few tens of ohms.

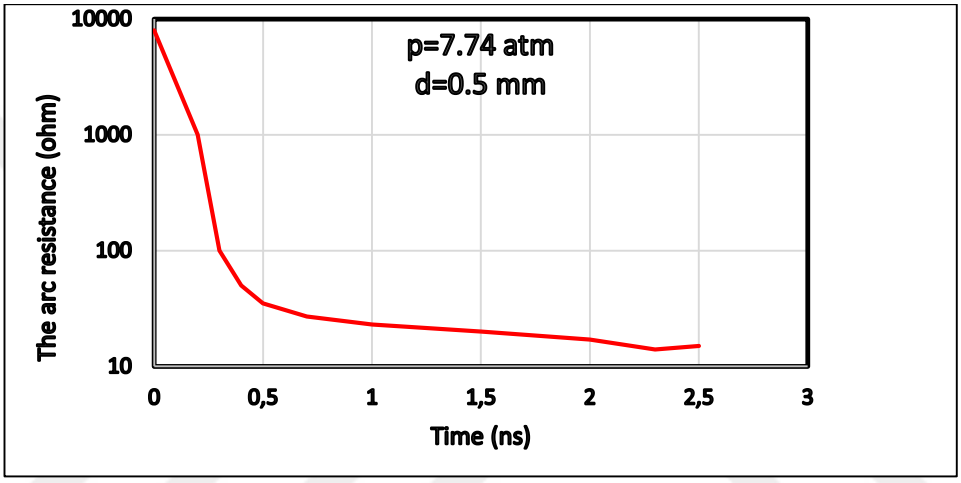

Figure 5.8 The calculated arc-resistance for the air, at 7.74 atm and d = 0.5mm

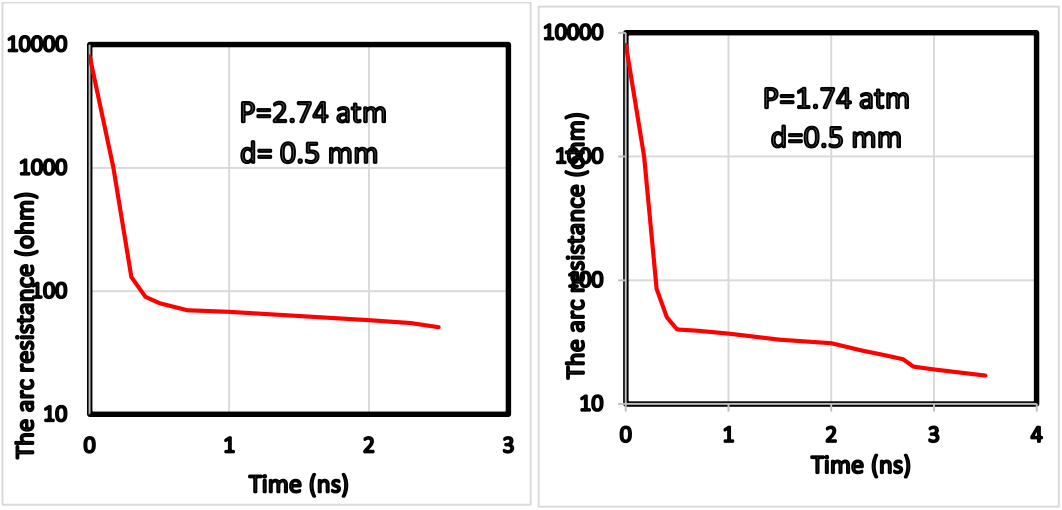

Figure 5.9 The calculated arc-resistance for the three different pressures

Figure 5.9 shows the calculated arc-resistance for the three different pressures between 1.74 atm , 2.74 ,4.74 and 7.74 atm and inter-electrode gap d=0.5 mm. The results show that the transition time from a non-conducting state to the conducting state will be faster at the higher pd-values. It is clear from the curve that the discharge will occur very fast in time less than (1) ns and the gap turned to good conductor in 2 ns.

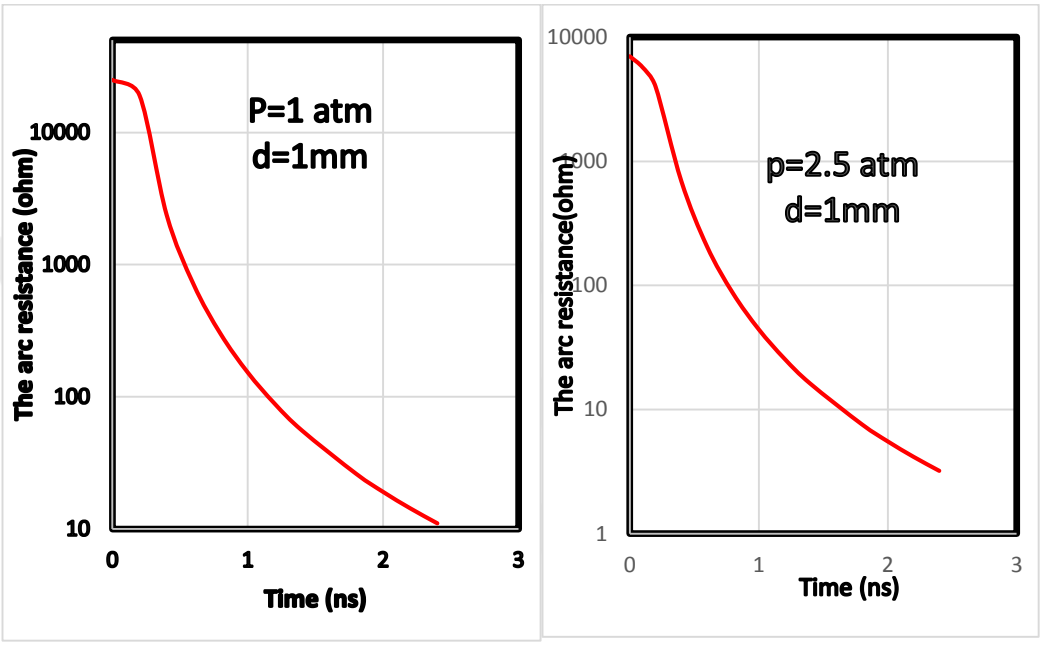

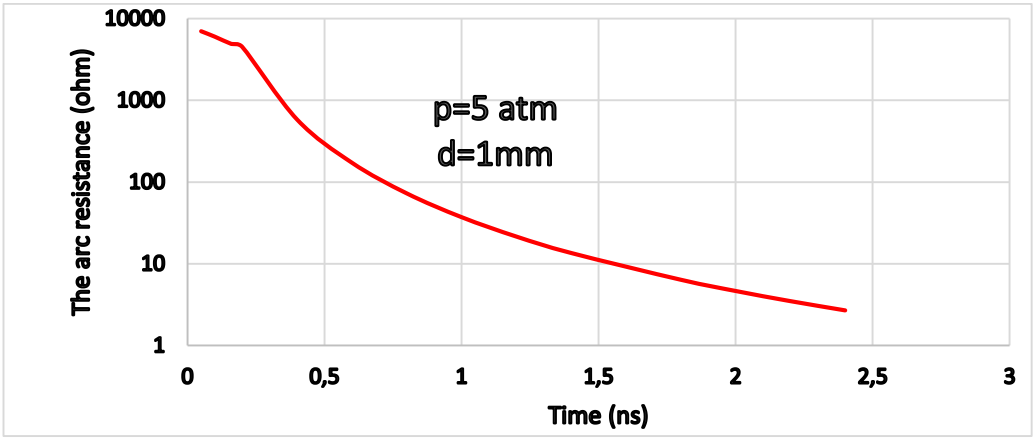

Figure 5.10 The calculated arc-resistance for the three different pressures

In this section, the arc-resistance calculated from the models presented in chapter 4. The arc resistance equations are supposed by the Rompe- Weizel with utilizing another two equations suggested by Sorensen and Ristic. Figure5.10 shows the results for air at 1, 2.5 and 5 atm and d = 2mm. It is clear from the curve if the pressure increases the arc resistance increase and the time will be longer to full discharge occur. Figure 5.11 shows the calculated arc-resistance for the three different pressures between 1 atm, 2.5, and 5 atm , and the inter- electrode distance d= 2mm. it can be seen that there is a proportional relationship between the arc resistance and the inter- electrode distance, as the gap distance increase the arc resistance increase .at p=5 atm the resistance takes longer time than p=2.5 and p= 1 atm to transform the spark gap from the non-conducting state to conducting state.

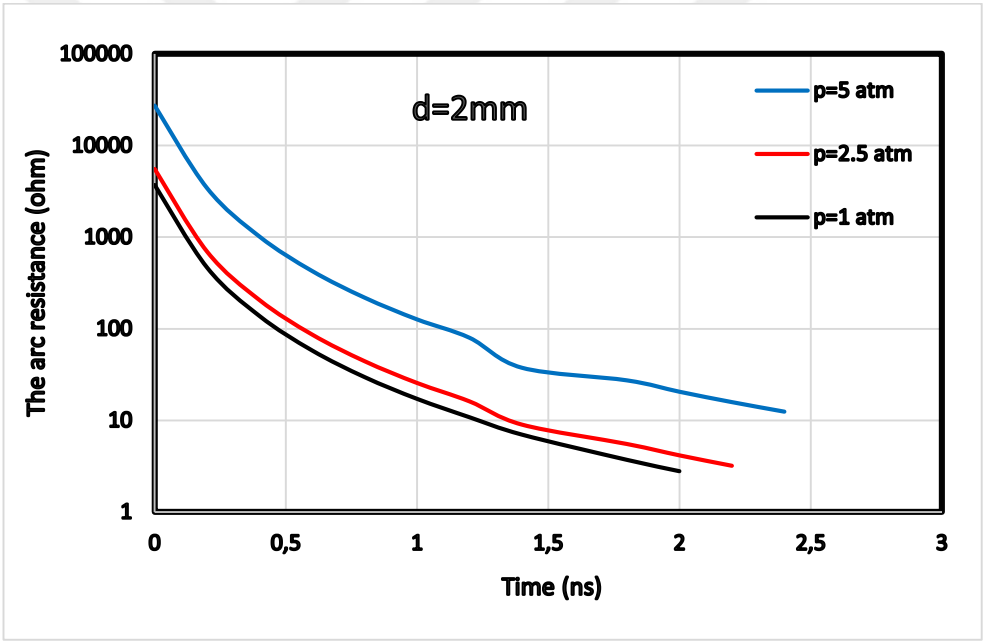

Figure 5.11 The calculated arc-resistance for the three different pressures between 1 atm, 2.5, and 5 atm, and the inter- electrode distance d= 2mm

5.6 Analyzing Spark gap Circuit simulation.

The RLC circuit simulation is carried out under pressure. The switch is modelled as a set of inductor and resistor, in parallel with the capacitor. The input electrode is connected to high voltage capacitor and the output electrode to the load. The inductance of the switch was calculated using equation(2)at different gap distances d= 1mm ,2mm and 4 mm and three different p1= 1 atm , p= 2.5 atm and p= 5 atm .

The results are listed in tables 2, 3 and 4. By starting with inter-electrode distance d= 1mm and p= 5 atm, at the time of switching the value of resistance is and its value is 3Ω [11]. The switch capacitance is 2.78pF and peaking capacitor is 100nF and the calculated switch inductance is 35 n H. The simulation is done using Pspice. The capacitor is charged to 10kVDc, which discharges through spark gap switch to the load. The rise time obtained is 175 ns and peak voltage is 8950kV as shown in figure 5.12.

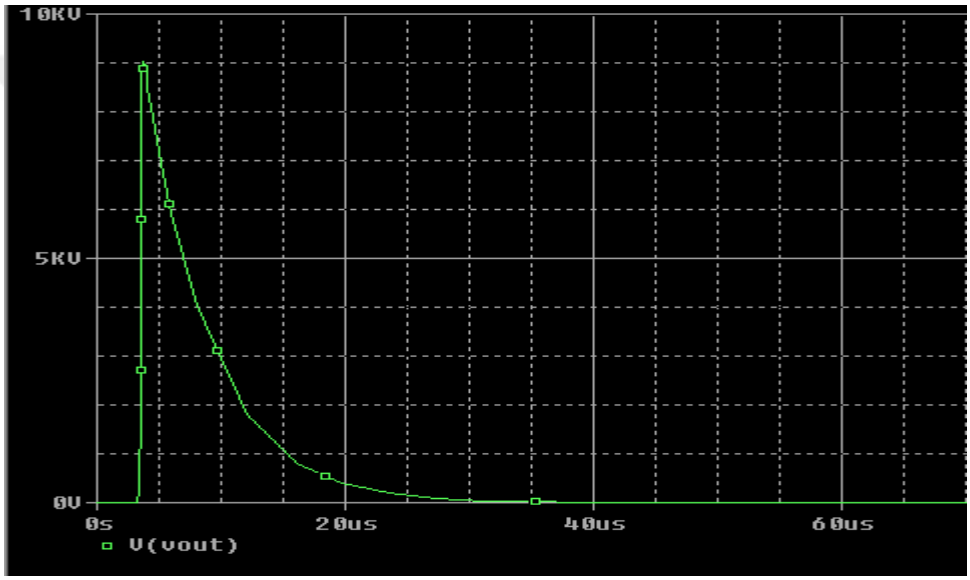

Figure 5.12 The output pulse from the spark gap switch, at p=5atm, d=1mm, r=1cm

The aim of this work ıs to study reducing the output rise time, so it is very ımportant to minimize the arc channel inductance. The switch inductance reduces if the ınter-electrode gap reduces. Once the switch gap distance decreases, the pressure inside the gap should be increased to withstand very high voltage. The results from the simulation are shown in the figure. 5.12 And figure 5.13 which gives the output pulse from the peaking switch with the air as the medium under p=5 atm, d= 1mm and d=2 mm. It is clear that at d= 1mm the output pulse rise time is smaller than the output pulse at d= 2mm. As the inter-electrode distance decreases the output peak voltage also decreases. The dropped voltage at d=1mm is 1000v and at d=2mm is 2000 v this means as the gap distance increase the power losing increases.

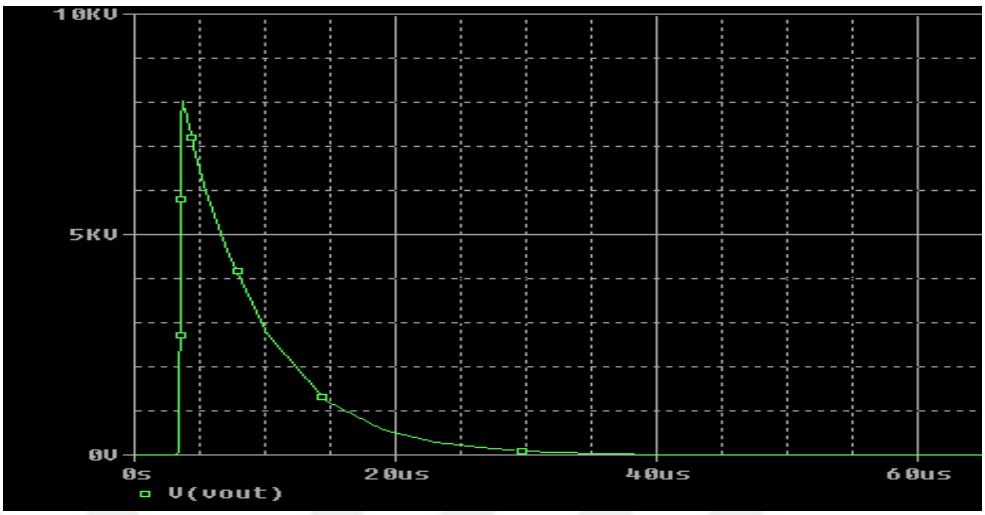

Figure 5.13 The output pulse from the spark gap, at p=5atm, d=2mm. r= 1cm

We found that the influence of the small distance is the most important factor to get the desired signal shape and rise time. The constriction of switch electrodes can be used to control the output signals parameters. We showed that by selecting the correct electrodes geometry and gap distance, we can obtain the best design of spark gap switch which can generate the desired output pulses. However, the highest pressure values with very small gap distances can generates the fastest rise times. The output rise time can be adjusted by varying the gas pressure and the gap distance.

Table 5.1 the values of calculated RLC circuit elements at different inter-electrode distances

gap distance(d)	Gap resistance Ω	Switch inductance(L)	Switch capacitance(c)	The output rise time
1mm	3	35 nH	2.78 PF	175 ns
2mm	2	37 nH	1.3 PF	182 ns
3mm	1.7	40 nH	0.9 PF	183 ns

5.7 The E-Field modeling using CST

In this section, the results of simulation spark gap switch using CST studio are discussed. The switch overview consists of the pulse generator, the input electrode which connects to the gap switch, the output electrode and resistive load, as shown in Figure5 13. 10000-kV was applied to input electrode and zero voltage to another electrode as shown in figure 5.13. In figure5.14 the Electric field is analyzed to observe the influence of the field distribution inside the gap which determine the generation of conducting path.

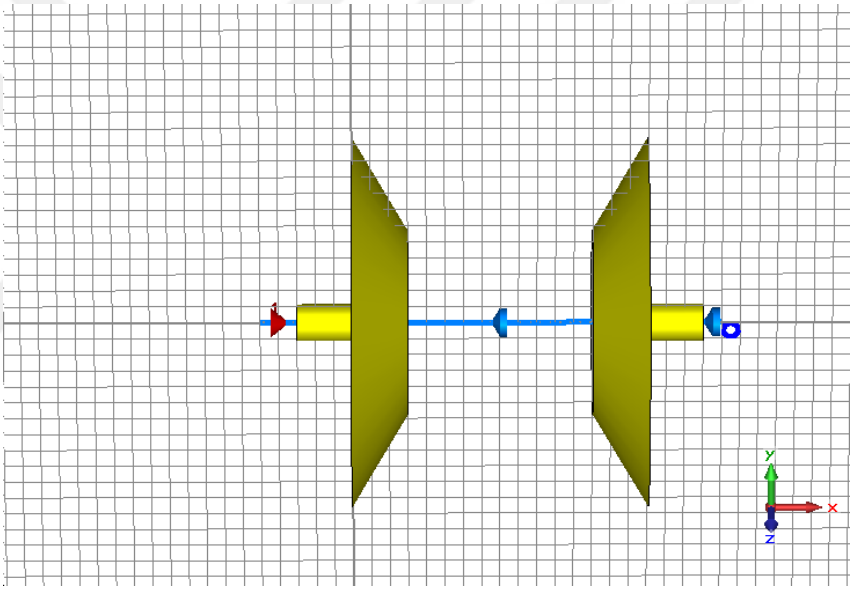

Figure 5.14 The spark gap switch modeled by CST

Static Modeling of the E-Field

In this section, the discharge process in a spark gap is studied when a high-voltage DC is applied. The conducting channel formation is observed by monitoring the electric-field at the input and output electrodes as shown in figure 5.14. The most important factors related to the spark gaps design are the field geometry, dielectric gas and its pressure, gap length, repetition rate requirements, load characteristics, and the applied voltage. The gap switch is made of two aluminum electrodes with cone (diameter =6 mm). From the picture, the maximum value of (E-field) could be seen at the edges of

input and output electrodes. At the hot spots which has the maximum E-field values of 12 MV/m with red color. The yellow portion in Figure 5.14 represents the switch gap region 9.3 MV/m. The simulation proves that the electric field at edges a much larger from the electrode center, and uniform inside the gap. Also we observed that the field distribution is very weak around the electrodes and the discharge will occur inside the gap.

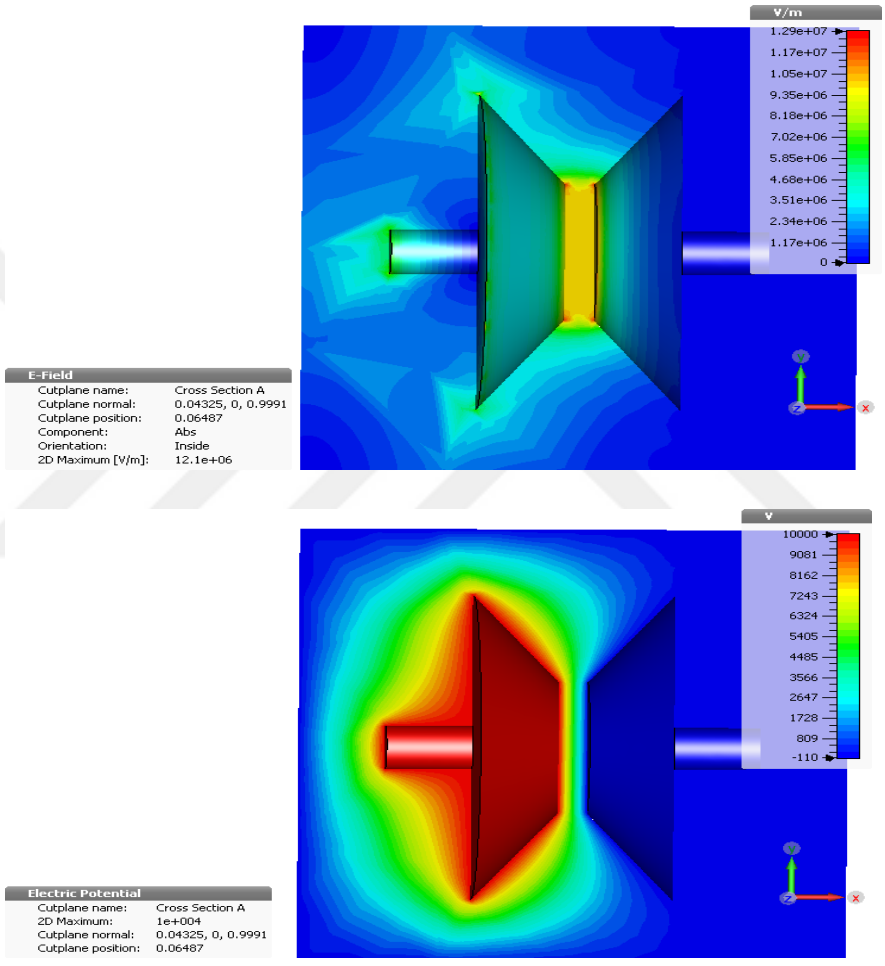

Figure 5.15 The complete electric field distribution inside the gap switch

The influence of gap distance on the rise time

The inter-electrode distance was changed, and its effect on the rise, time output pulse was observed at d= (1 mm, 2mm). The simulation shows that, as the gap distance decreases the pulse rise time decreases this prove that decreasing rise times is associated with decreasing the gap distance, the inductance of the switch and applying

the electric field. Therefore, we proposed a new shape, cone electrodes to minimize the inductance of the switch gap region. A Gaussian signal with rise time =10ns was applied to the switch of inter-electrode distance d= 1mm and 10 mm as shown in figure 5.15. It is shown that the reduction in distance reduces the rise time from 10 ns to 6ns. This can be occurred due to the effects of switch capacitance and inductance.

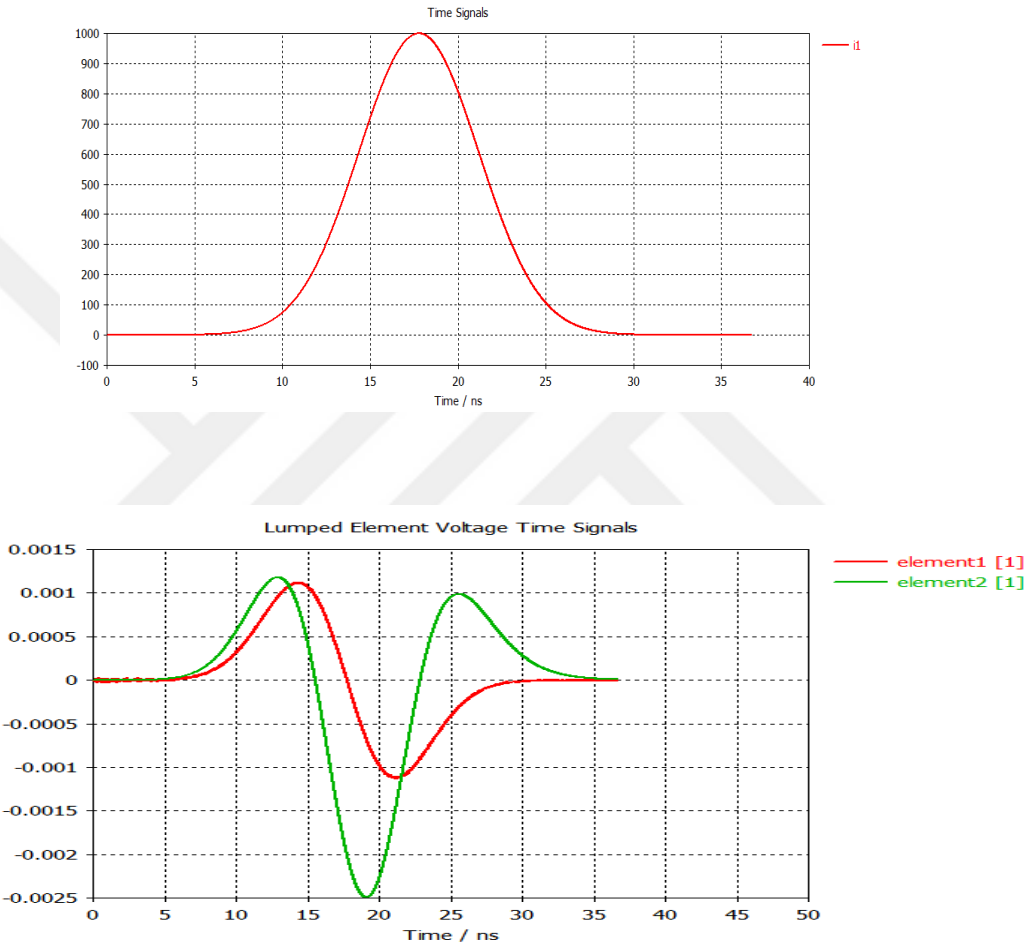

Figure 5.16 The input and output Gaussian signal at d = 1mm and rise time 10 ns

At gap distance d=1cm Gaussian signal was applied again with rise time (10ns) as shown in figure 5.16 to observe the effect of gap spacing on output rise time The output signal gives a rise time of (7 ns).

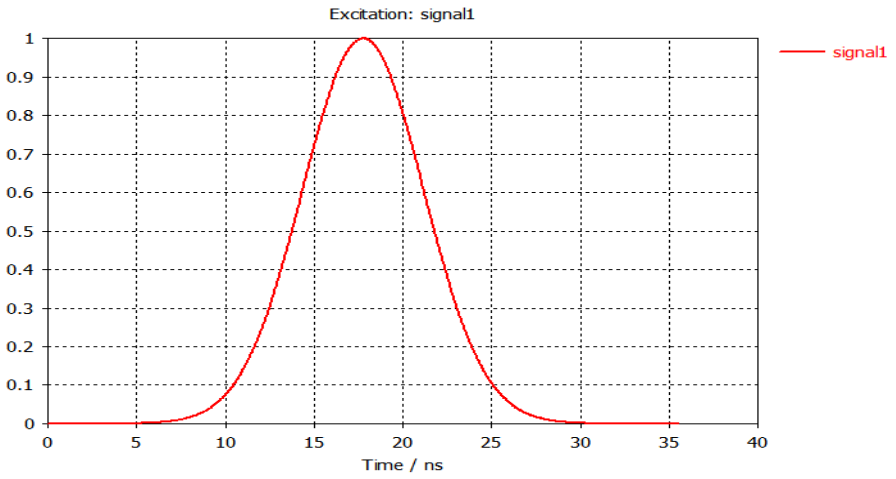

Figure 5.17 The input Gaussian signal at d = 1cm and rise time 10 ns

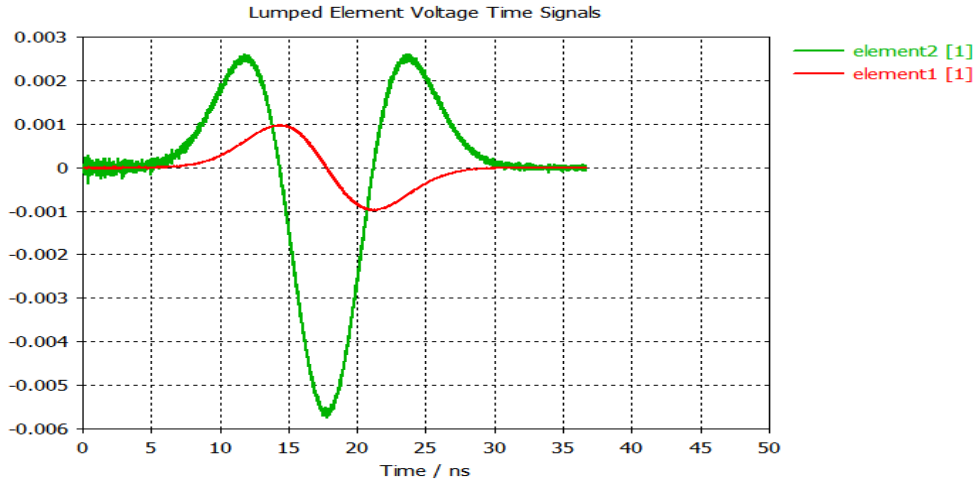

Figure 5.18 Two output Gaussian signals at d = 1cm

A comparison between three different shapes of spark gap switch

We modeled three different electrode shapes of spark gap at the same condition, to study the effect of switch geometry on the electric field and the conducting path inside the gap. The shapes were as following (cone –cone, cylinder- cylinder, spherical-spherical). The results showed there is a small difference in the generated electric field inside the gap.

The conducting path take place in the center of the gap and the field distribution concentrates in the region between the electrodes. The field which obtained by using cylinder shape is the highest value in order of 1.14×10^{7} v/m, the maximum field in the case of spherical shape is 1.11×10^{7} v/m and in the case of cone shape is 1.05×10^{7} v/m. the figure 5.19 and figure 5.20 shows different switch electrodes and the conducting channel inside the gap which responsible to carry the energy through it. The region of the field distribution in the conical shape is larger than the other shapes, so this shape can be used to transfer large amount of energy in very short time. By improving the conical electrode shape to avoid the red spots on the edges, because it can cause pre breakdown voltage which undesirable in our design.

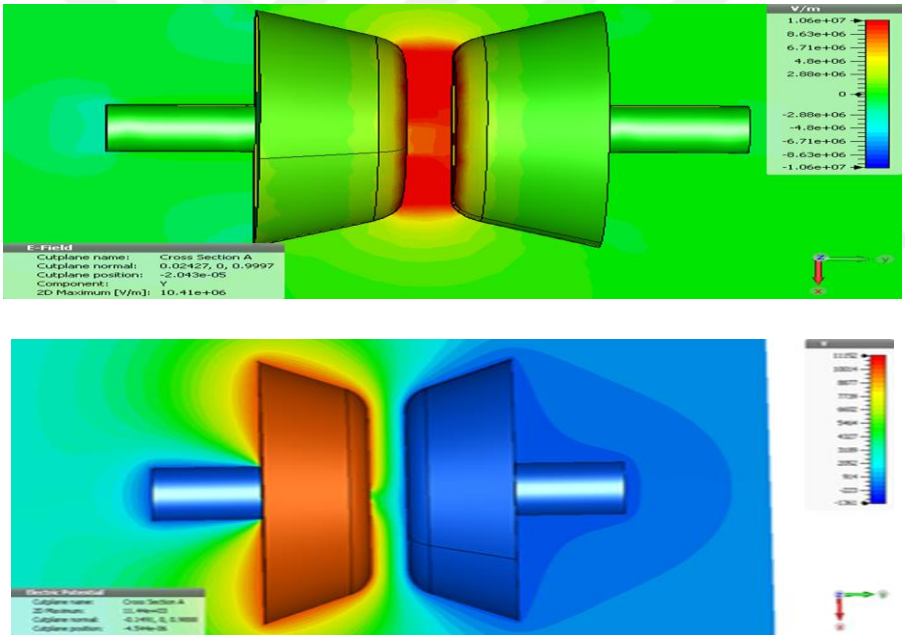

Figure 5.19 The conical shape of spark gap switch

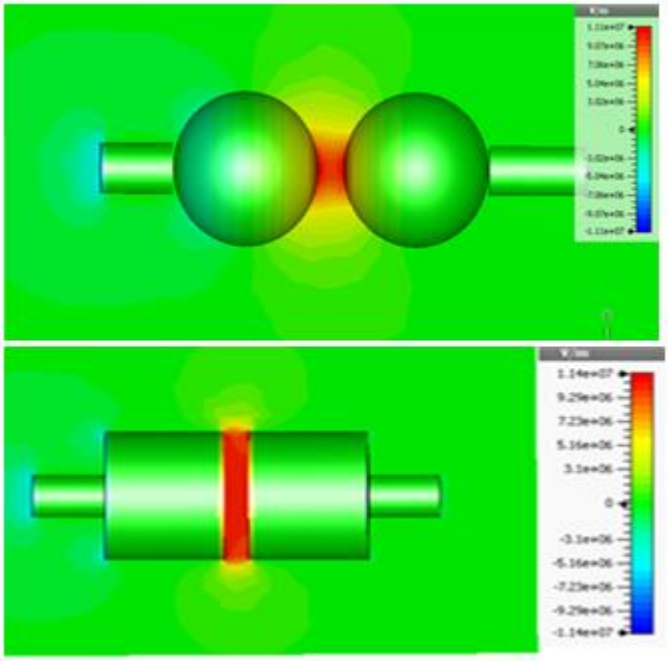

Figure 5.20 The cylinder and spherical shapes of spark gap switch

CHAPTER SIX

6.1 Findings and the summary of work

In previous chapters, we have presented the most important results such as arc discharge, the breakdown voltage of the gap, the resistive phase time and the inductance of the switch. In addition, we also showed the results of the effect of varying distance on the output pulse rise time. The important aim in our research is to drive fast closing discharge with reducing the output rise time. Eventually, we analyzed the electric discharge in the gap depending on the pressure, inter- electrode distance and the applied voltage to the gap, to get the best understanding of different parameters for an optimal switch behavior. In this chapter, we will explain the analysis of numerical modeling and computer simulation.

We studied the breakdown voltages parameters using three theoretical models were supposed by Toepler, Rompe and Weizel [7], and Vlastos [9] to calculate the arc resistance, resistive phase time, the equivalent RLC circuit of the switch, and the switch inductance. Based on switch parameters an electrical circuit was modeled to simulate the discharge process, the circuit of the spark gap was modeled by using (Pspice). The second aim of this work is modeling and simulating of spark gap switch for studying the reducing in rising time for short pulses. The influence of various gap distances and inductance on the output pulses rise time is discussed. The simulation carried out using CST. By using the electrostatic solver, the E-field distribution region can be seen in three dimensions. Two different signals were applied to the first electrode to observe the effect of gap length on output rise time.

6.2 The Most Important Results

The influence of pressure variation on break down voltage

- Based on figure 5.1 the breakdown voltage inside gap switch under various pressures can be occurred as the gas pressure and gap distance were varied. The applied voltage is important to form the conducting channel across the gap. The breakdown voltage increased as the gas pressure increases. The small gap length and high pressure inside the gap can

establish very short arc discharge, which lead to decrease the inductance and resistance of the switch. According to the electric discharge phenomena, we can obtain the critical value of voltage at different values of (pd) by changing the gas pressure (p) and gap distance (d). The calculated breakdown voltage at different distances are shown in table 6.1.

Table 6.1 shows the calculated breakdown voltage at different distances

pd	Vb(Kv) at d= 1 mm	Vb(Kv) at d= 2 mm	Vb(Kv)at d= 3 mm	Vb(Kv)at d= 4 mm
304	5.033813	8.94279	12.59126	16.08809
760	10.79038	19.47987	27.6455	35.50348
912	16.08809	22.7922	32.3899	41.63269
12.59126	19.47987	29.2378	41.63269	53.58237
1520	22.79222	35.50348	50.62793	65.22098
1824	26.04121	41.63269	59.43504	76.62289
2128	29.2378	47.65276	68.09148	87.83506
2432	32.3899	53.58237	76.62289	98.88966
2736	33.456	59.43504	85.04787	109.81

• Based on a figure (5.3) the curve shows the relationship between electric field and Pd (pressure * inter-electrode distance). In different pd ranges, the electric field has been calculated between 4 and 27 MV/m) .it can be seen from the curve that the lowest electric field values (M v/mm) from 1mm to 4 mm take place at the furthest gap distance. At a specific distance from the electrode, the electrons will be accelerated in opposite directions by applying an electric field to separate them and transfer the energy to each electron. It is clear that when the gas pressure increase the field also

increase, and as the gap distance decrease the electric field becomes higher. In this case, the velocity of the electrons is higher than positive ions .by gaining enough energy from the electric field, it will strike another atom, causing ionization and releasing free new electrons, and positive ions. Again, the free electrons will be accelerated and collide with new atoms, creating more electrons/positive-ions. The process helps to build up the conducting path and make the closing very fast. It is clear from the curve the inter-electrode distance from 0.1 to 0.5 mm, the closing switch faster than other distances.

Resistive Phase Time (R)

Based on figure 5.5 the curve illustrates the calculated resistive phase time for air at various Pd values. The switch closure time is the created heating channel during changing the resistance of spark gap from several mega ohms to very small resistance. This resistive phase determines conductivity of the switch. The resistive phase time determines the amount of the deposited energy inside the gap, the switch resistance is a function of several discharges processes. The discharge process is effected by some factors, inclusive the applied electric field (E), the electrodes shape, the electric discharge, and the gas type. can be expended especially in transferring the kinetic energy to electrons and in exciting and ionizing the molecules and atoms of the gas. By consider carefully these effects, we confident that the theory of the spark channel resistance by Rompe–Weizel is the most adequate for the peaking switch.

The arc resistance

The arc resistance is a very important parameter in studying the electric discharge in gasses, it is used to calculate the resistance of discharge channel. Rompe and Weizel supposed an equation to determine the radius of arc channel. By considering the energy balance in the discharge, the equation has an accurate predicting to calculate arc-resistance for the initial step of electric discharge.

Based on Figure 5.9 the curve illustrates the calculated values with respect to time under different pressures and inter-electrode distance. The accuracy of arc-resistance equation supposed by Ristic and Sorensen is high because of the experimental

conditions. For very short time intervals less than 1 ns, the results follow Vlastos' equations. However, the best model for times between 50 PS and 3.5 ns, is observed with the Rompe- Weizel model (Table 4). For the best design the resistance of the switch should be very small to get very high current in the output .so the pressure and the distance between the electrodes should selected to obtain very small resistance during the discharge.

The switch electrodes geometric dependency

A uniform shape of the electrodes can generate breakdown voltages with uniform field. The switch gap length is selected to be very small to reduce the inductance of the switch. The inductance of the arc discharge channel determines the output rise time. The inductance L for switch gap distance d can be calculated as following:

$$L = \delta_{arc} \frac{\mu_0}{2\pi} \ln\left(\frac{r_0}{r_i}\right) \qquad 6.1$$

Where r_0 represents the inner radius of the electrode switch. μ_0 Represents the permeability in free space and r_i is the radius of arc channel.

The inductance of arc discharge can be modeled and calculated based on the switch electrodes dimensions. The used equation works in with the obtained empirical results, and it is also can be used to determine the arc discharge radius. In our work, the Inductance calculations were taken for different values of the pressures, applied voltage and inter-electrode distance in spark gap switch.

Based on figure 4.1 the entire inductance is proportional to the switch parameters such as distance and the gap geometry. For the best design the inductance should be very small to improve the effect on output rise time and output signal shape. In our study we obtained the desired output rise time signals by selecting the best switch inductance values and the results were listed in table 5.1.

The Switch Capacitance

In our study we calculated the switch capacitance (C) depending on the electrodes geometry. For optimal design of the switch the capacitance should be very high to store the energy and send it to the load. The value of the capacitance will affect the generated electric field and the output peak power. By using an equation we calculated three different values of the switch capacitance under different pressures and distances. Table 5.1 shows the calculated switch capacitance.

Equivalent Pspice circuit for spark gap discharge

We presented that by selecting an optimal electrode geometry, we can obtain the best configuration of the switch that can generate the desired output power pulses. Based on Rompe-Weizel model which used to calculate the channel resistance, an equivalent RLC circuit was used to represent the electric discharge inside the gap as shown in figure 6.2.

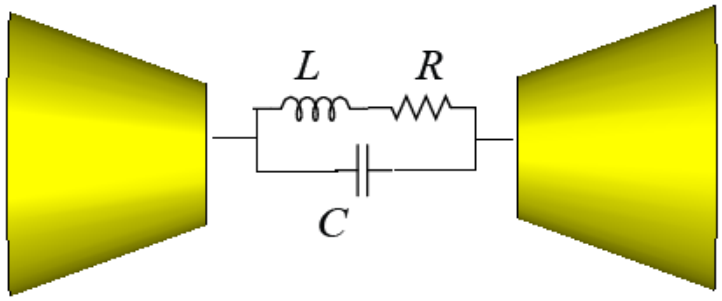

Figure 6.1 Spark gap equivalent RLC circuit

We used Spice program to simulate charging and discharging the high voltage capacitor by spark gap switch. Transient analysis is used to compute the circuit analysis as a function of time as seen in figure 6.3.Voltage monitor is connected to the output signal to measure the rise time.

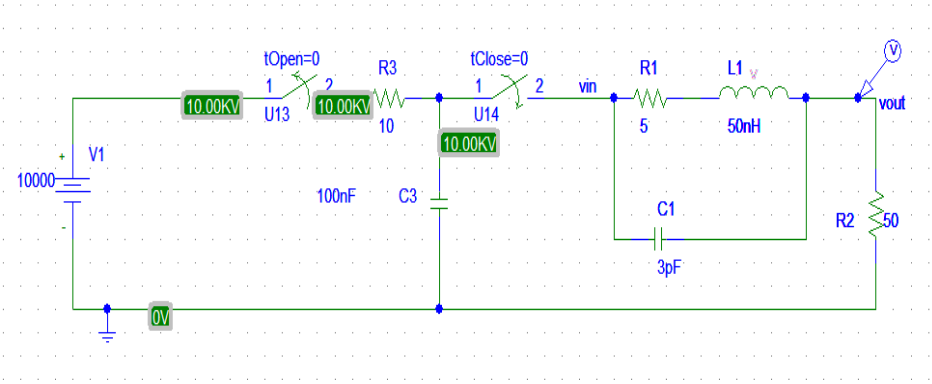

Figure 6.2 The circuit simulation by using Pspice

The representation of circuit diagram of charging and discharging capacitor using the spark gap switch is shown in figure 6- 3. The equivalent RLC circuit connected to the output electrode of the switch to simulate the breakdown voltage of the spark gap. The switch modeling include the breakdown and pre–breakdown phase. Since, all the electric discharge mechanisms cannot considered in the simulation, for this reason we selected simple model of the spark gap switch.

The general model of the spark gap from Pspice models the high-voltage switch only with some parameters of the spark gap such as the inter– electrode distance, breakdown voltages, the output pulse peak power and rise time. A resistance and an inductance are connected in a parallel with capacitance are utilized to model the electric discharge parameters for closing switch. (R2) is estimated from conducting channel of spark discharge. C2 and L1 are the calculated respectively from the switch parameters. The whole switch structure is modeled as transmission lines. In chapter (4) the switch parameters are selected in accurate way to get a good relationship with experimental data. The circuit is useful to study the electric discharge inside the switch and it will help to determine the effect of some physical parameters on the output pulses. The accuracy of the circuit elements depends on the method used to calculate the values of RLC circuit parameters, which estimated from the switch electrode geometry. The switch circuit is supposed to be as coaxial cable which has an arc channel radius much smaller than the electrode radius.

The electric discharge resistance at arcing discharge is very small, and it change from few Mega ohms to f milliohms. The energy is stored in high voltage capacitor before delivering it to the load through the switch. Based on the results from the output signals shown in figure 5.12 and figure 5.13 which gives the output pulse from the peaking spark gap switch with the air as medium under p=5 atm, d= 1mm and d=2 mm. it is clear that at d= 1mm the output pulse rise time is smaller than the output pulse at d= 2mm.

As the inter-electrode distance decreases the output peak voltage also decreases. The dropped voltage at d=1mm is 1000v and at d=2mm is 2000 v this means as the gap distance increases the power losing grows. The obtained rise times at d= 1mm is 175 ns, at d= 2m is 180 ns and at d= 3 mm the output rise time is 183 ns as shown in figure 6.4. Decreasing output rise time can be reached by minimizing the inter electrode distance. From figure 6.4, it is clear that the obtained rise time is reduced to 175 ns seconds and related to the gap distance and gas pressure. Physically, this model is very complex because the gap switch with small inter-electrode gaps can resist high voltage only under the high pressure gas. The problem is that the decreasing in switch gap distance leads to be undesirable pre output pulse at the load. So the optimum design should take care of the switch geometry, gas pressure and inter - electrode distance.

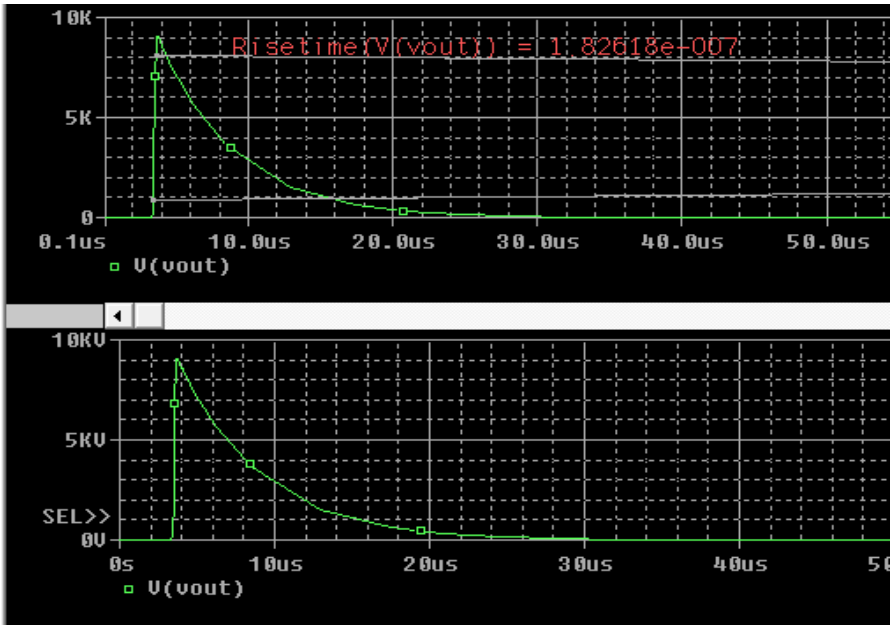

Figure 6.3 The output pulse from the spark gap switch, at p=5atm, d=2mm. r= 1cm

6.3 Recommendation and Future Work

Our work showed the simulation and mathematical methods to model the spark gap switch. , the aim of our research is to design a low cost, minimum weight, and simple design switch. We have shown, in this thesis, that the spark gap can be used to transfer power pulses with reducing output rise time. For future work, we suggest the following: Reduce the capacitive of spark gap.

- Calculate the energy transfer of output pulses.
- Calculate the dissipative energy inside the gap.
- Modeling the switch with different shapes.
- Calculate the passing current through the switch.

6.4 Conclusion

The main objective of this thesis is studying the most important parameters of spark gap switch. We studied breakdown voltages process in electrode gaps from 0.1mm to 4 mm at different ranges of pressures in air. The breakdown voltage depends on many factors such as p d (pressure times gap distance), the applying voltage, the gap distance and the gas pressure inside the gap switch. To analyze the switching discharge process of the switch, the resistive phase time and the arc resistance should be calculated. We observed that the resistive time phase decrease as the (Pd) value increases. We modeled spark gap switch by using CST. The applied voltage on the gap and the field distribution have shown by using EM the static model which gives us a complete idea of the breakdown voltage inside the gap. The static modeling shows the electric field propagation and the influence of electrodes geometry on the generated field. The other aims of the thesis is studying the output rise time of the output pulses with respect to gap distance. We used the equivalent RLC circuit to model the electric discharge presses in the switching time and to study the influence of gap distance and pressure on output rise time.

REFERENCES

[1] F. S. PIEDRAHITA, *EXPERIMENTAL RESEARCH WORK ON A SUB-MILLIMETER SPARK-GAP FOR SUB-NANOSECOND GAS BREAKDOWN*, 2012.

[2] G. Schaefer, M. Kristiansen, and A. H. Guenther, *Gas discharge closing switches* vol. 2: Springer Science & Business Media, 2013.

[3] H. Rahaman, "Investigation of a High-Power, High-Pressure Spark Gap Switch with High Repetition Rate," 2007.

[4] J. Wright, "Theory of the electrical breakdown of gases by intense pulses of light," *Proceedings of the Physical Society,* vol. 84, p. 41, 1964.

[5] S. Bonisch, W. Kalkner, and D. Pommerenke, "Modeling of short-gap ESD under consideration of different discharge mechanisms," *IEEE transactions on plasma science,* vol. 31, pp. 736-744, 2003.

[6] M. Judd, "Contact discharges as a source of sub-nanosecond high voltage pulses," *Journal of Physics D: Applied Physics,* vol. 34, p. 2883, 2001.

[7] K. L. Kaiser, *Electrostatic discharge*: CRC press, 2005.

[8] T. Juestel, P. Huppertz, D. U. Wiechert, W. Mayr, and H. Von Busch, "Dielectric barrier discharge lamp comprising an UV-B phosphor," ed: Google Patents, 2010.

[9] M. Goldman, A. Goldman, and R. Sigmond, "The corona discharge, its properties and specific uses," *Pure and Applied Chemistry,* vol. 57, pp. 1353-1362, 1985.

[10] T. Briels, E. Van Veldhuizen, and U. Ebert, "Positive streamers in air and nitrogen of varying density: experiments on similarity laws," *Journal of Physics D: Applied Physics,* vol. 41, p. 234008, 2008.

[11] L. G. Christophorou, D. L. McCorkle, and S. R. Hunter, "Gas mixtures for spark gap closing switches," ed: Google Patents, 1988.

[12] H. J. Reich, "Theory and applications of electron tubes," 1944.

[13] J. Kuffel and P. Kuffel, *High voltage engineering fundamentals*: Newnes, 2000.

[14] J. P. Dakin and R. G. Brown, *Handbook of Optoelectronics (two-volume set)*: CRC Press, 2006.

[15] S. Y. Moon, W. Choe, and B. Kang, "A uniform glow discharge plasma source at atmospheric pressure," *Applied Physics Letters,* vol. 84, pp. 188-190, 2004.

[16] D. Barnes, R. Nebel, and L. Turner, "Production and application of dense Penning trap plasmas," *Physics of Fluids B: Plasma Physics (1989-1993),* vol. 5, pp. 3651-3660, 1993.

[17] D. R. Reyes, M. M. Ghanem, G. M. Whitesides, and A. Manz, "Glow discharge in microfluidic chips for visible analog computing," *Lab on a Chip,* vol. 2, pp. 113-116, 2002.

[18] J. Meek, "A theory of spark discharge," *Physical Review,* vol. 57, p. 722, 1940.

[19] V. Mehta, *Principles of Electronics*: S. Chand, 2008.

[20] E. B. O. GASES, "JM Meek, JD Craggs," ed: Oxford University Press, London, England, 1953.

[21] Y. P. Raizer and J. E. Allen, *Gas discharge physics* vol. 2: Springer Berlin, 1997.

[22] J. Mankowski and M. Kristiansen, "A review of short pulse generator technology," *IEEE Transactions on Plasma Science,* vol. 28, pp. 102-108, 2000.
[23] H. Bluhm, "Power Systems," 2006.
[24] H. M. Ryan, *High voltage engineering and testing*: Iet, 2001.
[25] T. Kihara, "The mathematical theory of electrical discharges in gases," *Reviews of modern physics,* vol. 24, p. 45, 1952.
[26] J. Lowke, "Theory of electrical breakdown in air-the role of metastable oxygen molecules," *Journal of Physics D: Applied Physics,* vol. 25, p. 202, 1992.
[27] D. Biswas, J. Nilaya, and U. Chatterjee, "On the recovery of a spark gap in a fast discharge circuit," *Review of scientific instruments,* vol. 69, pp. 4242-4244, 1998.
[28] P. Kapitza, "High power electronics," in *Experiment, Theory, Practice*, ed: Springer, 1980, pp. 53-59.
[29] D. J. Biswas and J. P. Nilaya, "Diode-less operation of a resonantly charged repetitive high voltage pulser circuit," *Review of Scientific Instruments,* vol. 72, pp. 2505-2507, 2001.
[30] J. J. Brophy, "Basic electronics for scientists," 1971.
[31] G. N. Glasoe and J. V. Lebacqz, *Pulse generators*: McGraw-Hill, 1948.
[32] G. Schaefer, "Field Distortion Three Electrode Gaps," in *Gas Discharge Closing Switches*, ed: Springer, 1990, pp. 85-123.
[33] A. E. Vlastós, "The resistance of sparks," *Journal of Applied Physics,* vol. 43, pp. 1987-1989, 1972.
[34] T. Engel, A. L. Donaldson, and M. Kristiansen, "The pulsed discharge arc resistance and its functional behavior," *IEEE Transactions on Plasma science,* vol. 17, pp. 323-329, 1989.
[35] J. C. Martin, "Nanosecond pulse techniques," *Proceedings of the IEEE,* vol. 80, pp. 934-945, 1992.
[36] W. Cary and J. A. Mazzie, "Time-resolved resistance during spark gap breakdown," *IEEE Transactions on Electron Devices,* vol. 26, pp. 1422-1427, 1979.
[37] S. Braginskii, "Theory of the development of a spark channel," *SOVIET PHYSICS JETP-USSR,* vol. 7, pp. 1068-1074, 1958.
[38] C. Wadhwa, *High voltage engineering*: New Age International, 2007.
[39] S. Singha and M. J. Thomas, "Toepler's spark law in a GIS with compressed SF 6-N 2 mixture," *IEEE transactions on dielectrics and electrical insulation,* vol. 10, pp. 498-505, 2003.
[40] L. G. Christophorou and J. K. Olthoff, "Electron interactions with SF6," *Journal of Physical and Chemical Reference Data,* vol. 29, pp. 267-330, 2000.
[41] A. E. Vlastós, "Restrike channel resistance of thin exploding wires," *Journal of Applied Physics,* vol. 40, pp. 4752-4760, 1969.
[42] R. Rompe and W. Weizel, "Ueber das toeplersche funkengesetz," *Zeitschrift für Physik,* vol. 122, pp. 636-639, 1944.
[43] T. Hussey, K. Davis, J. Lehr, N. Roderick, R. Pate, and E. Kunhardt, "Dynamics of nanosecond spark-gap channels," in *Pulsed Power Conference, 1999. Digest of Technical Papers. 12th IEEE International*, 1999, pp. 1171-1174.
[44] T. Martin, J. Seamen, and D. Jobe, "Energy losses in switches," Sandia National Labs., Albuquerque, NM (United States)1993.

[45] T. Sorensen and V. Ristic, "Rise time and time-dependent spark-gap resistance in nitrogen and helium," *Journal of Applied Physics,* vol. 48, pp. 114-117, 1977.
[46] H. Akiyama, T. Sakugawa, T. Namihira, K. Takaki, Y. Minamitani, and N. Shimomura, "Industrial applications of pulsed power technology," *IEEE Transactions on Dielectrics and Electrical Insulation,* vol. 14, pp. 1051-1064, 2007.
[47] J. Lehr, C. Baum, W. Prather, and F. Agee, "Aspects of ultrafast spark gap switching UWB HPM generation," in *Pulsed Power Conference, 1997. Digest of Technical Papers. 1997 11th IEEE International*, 1997, pp. 1033-1041.
[48] A. Heylen, "Sparking formulae for very high-voltage Paschen characteristics of gases," *IEEE electrical insulation magazine,* vol. 3, pp. 25-35, 2006.
[49] CST Studio Suit, *CST Version GmbH, CST AG,*: New Age International, 2009.
[50] G. W. Hohmann, "Numerical modeling for electromagnetic methods of geophysics," *Electromagnetic methods in applied geophysics,* vol. 1, pp. 313-363, 1988.
[51] X. Wang, H. Luo, and Y. Hu, "Numerical simulation of the gas discharge in a gas peaking switch," *IEEE transactions on plasma science,* vol. 35, pp. 702-708, 2007.
[52] C. Nunnally, J. Mayes, C. Hatfield, and J. Dowden, "Design and performance of an ultra-compact 1.8-kJ, 600-kV pulsed power system," in *Proceedings of the 17th IEEE International Pulsed Power Conference*, 2009, pp. 930-933.
[53] H. Krompholz, L. L. Hatfield, M. Kristiansen, D. Hemmert, B. Short, J. Mankowski, *et al.*, "Gas breakdown in the subnanosecond regime with voltages below 15 kV," *IEEE transactions on plasma science,* vol. 30, pp. 1916-1921, 2002.
[54] M. M. Pejovic and C. S. Milosavljevic, "The estimation of static breakdown voltage for gas-filled tubes at low pressures using dynamic method," *IEEE transactions on plasma science,* vol. 31, pp. 776-781, 2003.